2(mix)

(NASA-CR-124232) METHODS FOR STRUCTURAL DESIGN AT ELEVATED TEMPERATURES Final Report (Lockheed Missiles and Space Co.) 189 p HC CSCL 13M

N73-22851

PRICES SUBJECT TO CHANGE

G3/32 Unclas 17623

Lockheed

HUNTSVILLE RESEARCH & ENGINEERING CENTER

LOCKHEED MISSILES & SPACE COMPANY, INC.
A SUBSIDIARY OF LOCKHEED AIRCRAFT CORPORATION

HUNTSVILLE, ALABAMA

N73-22851

HREC-8170-1
LMSC-HREC TR D306579

LOCKHEED MISSILES & SPACE COMPANY, INC.

HUNTSVILLE RESEARCH & ENGINEERING CENTER

HUNTSVILLE RESEARCH PARK

4800 BRADFORD DRIVE, HUNTSVILLE, ALABAMA

METHODS FOR STRUCTURAL DESIGN AT ELEVATED TEMPERATURES

FINAL REPORT

April 1973

Contract NAS8-28170

Prepared for National Aeronautics and Space Administration
Marshall Space Flight Center, Alabama 35812

by

A.M. Ellison
W.E. Jones, Jr.
K.R. Leimbach

APPROVED: J.S. Farrior

J.S. Farrior
Resident Director

PRECEDING PAGE BLANK NOT FILMED

FOREWORD

This report presents results of work performed by Lockheed's Huntsville Research & Engineering Center for the NASA-Marshall Space Flight Center under Contract NAS8-28170, "Methods for Structural Design at Elevated Temperature".

The NASA-MSFC technical monitor for this contract is Mr. John E. Key of the Analytical Mechanics Division, Astronautics Laboratory.

Preceding page blank

SUMMARY

The factor of safety used to compute the ultimate load from the limit load is a factor to account for uncertainties both in the strength and stiffness of the structure and in the applied loads. This uncertainty is twofold; first, in the physical reality and second, in the mathematical description.

The objective of this study is to define a procedure which can be used to design elevated temperature structures. The desired goal is to have the same confidence in the structural integrity at elevated temperature as the factor of safety gives on mechanical loads at room temperature.

Methods of design and analysis for creep, creep rupture, and creep buckling are presented in Section 2. Example problems are included to illustrate the analytical methods. Creep data for some common structural materials are presented in Appendix A. Appendix B is description, user's manual, and listing for the Creep Analysis Program developed on the contract. The program predicts time to a given creep or to creep rupture for a material subjected to a specified stress-temperature-time spectrum.

Fatigue at elevated temperature is discussed in Section 3. Methods of analysis for high stress-low cycle fatigue, fatigue below the creep range, and fatigue in the creep range are discussed. The interaction of thermal fatigue and mechanical loads is considered, and a detailed approach to fatigue analysis is given for structures operating below the creep range.

Section 4 is a brief discussion of structural analysis at elevated temperature. Limitations of linear, elastic analyses and the desirability of developing efficient nonlinear analytical tools are pointed out.

Design methods for elevated temperature structures are recommended in Section 5. Both ultimate load failure (fracture) and functional failure from excessive permanent deformations are considered as design criteria. The recommended approach to elevated temperature design consists of applying a factor of safety to the mechanical loads, a life factor to the service life, and a factor to the design heating rates or temperatures. The rationale for applying the factors is explained based on reliability principles. The design load, temperature, and life factors assure that the design conditions (load, temperature and time) have a safe margin when compared to the allowable (failure or deformation) envelope.

CONTENTS

CONTENTS (Continued)

Section 1
INTRODUCTION

In their simplest form, the criteria for designing room temperature structures are:

1. The limit load is defined as the maximum load expected to act on a structure;
2. The limit load is multiplied by a factor of safety to obtain the ultimate load;
3. The structure must possess adequate strength and stiffness to withstand limit load without yielding; and
4. The structure must withstand ultimate load without failure.

The factor of safety used to compute the ultimate load from the limit load is a factor to account for uncertainties both in the strength and stiffness of the structure and in the applied loads. This uncertainty is twofold; first, in the physical reality and second, in the mathematical description. Strength will vary with material properties, manufacturing tolerances, and fabrication techniques. The applied loads vary with trajectory perturbations, wind gusts, maneuver loads, atmospheric conditions, and numerous other random phenomena encountered during service.

Due to scatter in measured material properties and the randomness of the loads, which are highly probabilistic in magnitude and frequency of occurrence, it has been logically hypothesized that the factors of safety should be determined from a statistical analysis of the basic factors which affect the strength and the loads. Unfortunately, a statistical analysis is usually not possible in an early design stage and also it is too time-consuming to be performed in every step of a structural design. Therefore, design criteria are desirable which convert the probabilistic properties of the design variables into deterministic ones. This leads to the factor of safety, which has been used as an effective design tool for a long time.

Although the factor of safety approach to designing reliable structures has served well, the high temperatures to which space shuttle structures will be exposed require a generalization of this approach to a wider range of application. At elevated temperatures the uncertainties of the design variables are greater and call for larger factors of safety as compared to room temperature. In addition, the factors of safety should be functions of the design variables rather than a constant. The latter aspect is emphasized by the large percentage of vehicle weight incorporated in elevated temperature structures. Excessive conservatism as a result of an insensitive factor of safety would buy structural reliability at the expense of high weight penalties.

The objective of this study is to define a procedure which can be used to design elevated temperature structures. The desired goal is to have the same confidence in the structural integrity at elevated temperature as the factor of safety gives on mechanical loads at room temperature.

The problem of design of elevated temperature structures is to attain a safe, reliable structure for combined load-temperature-time environments. Elevated temperature design differs from "room temperature" design only when the combined environments and material properties interact to produce changes in the strength or deformation characteristics of the structure as the load or temperature cycles are repeated. That is, the time becomes a major parameter in the design of elevated temperature structures.

The following sections of this report discuss methods for structural design and analysis which are peculiar to elevated temperature structures: creep, creep rupture, thermal and mechanical fatigue, and thermal stresses. The interaction of the thermal and mechanical loads to produce accumulated damage and permanent deformations with service lifetime are considered. An approach to design of elevated temperatures is proposed.

Section 2
CREEP

This section presents a summary of the phenomenon of creep and its effects on the design of a structural component at elevated temperatures. Creep is one of the major drivers in elevated temperature design, especially in flight structures where permanent deformations are undesirable from an aerodynamic standpoint. This section covers the mathematical theories of creep from the aspect of material laws and description of the creep behavior of structural components. Questions of creep rupture and creep buckling are discussed. Finally, a computer program is described which implements three popular creep theories used in studying the effects of a time-temperature-load history on a structural component.

2.1 CREEP LAWS

The mechanisms of deformation and failure of metallic materials at elevated temperature, that is, at temperatures above approximately one-third of the melting temperature measured on an absolute scale, are traditionally studied on two levels, the crystal lattice and the continuum (Ref. 2-1).

On the crystal lattice level there are two softening mechanisms, cross slip and the temperature-sensitive dislocation climb. If the stress is kept constant the hardening effect decreases while the softening increases rapidly as the temperature is raised. The strain rate, $d\epsilon/dt$, can be expressed in terms of the stress, σ, as

$$\frac{d\epsilon}{dt} = C\,\sigma^n\,e^{-\frac{Q}{RT}} \qquad (2.1)$$

where Q is the activation energy for self diffusion, R is the gas constant, and T is the absolute temperature. There are several empirical methods to relate σ, T and time, t, at rupture or at a given strain. A frequently used parameter is the one by Larson and Miller (Ref. 2-2), where

$$P(\sigma) = T\,(C + \log t) \quad . \tag{2.2}$$

A list of parameters is given on page 200 of Ref. 2-3, and methods are described for extrapolating creep and creep rupture data. Typically the data are in the form of "master curves" (Fig. 2-1) from which individual creep curves of creep strain versus time at constant temperature with parametric variation of stress (Fig. 2-2a) or creep strain versus time at constant stress with parametric variation of temperature (Fig. 2-2b) can be constructed. In Appendix A the sources of material data and creep curves for a number of metallic materials are presented.

The material behavior shown on Fig. 2-2 can be described approximately by

$$\epsilon = \left(\frac{\sigma}{\sigma_o}\right)^{n_o} + \int_0^t \left(\frac{\sigma}{\sigma_c}\right)^{n} dt \quad . \tag{2.3}$$

as shown on Fig. 2-3.

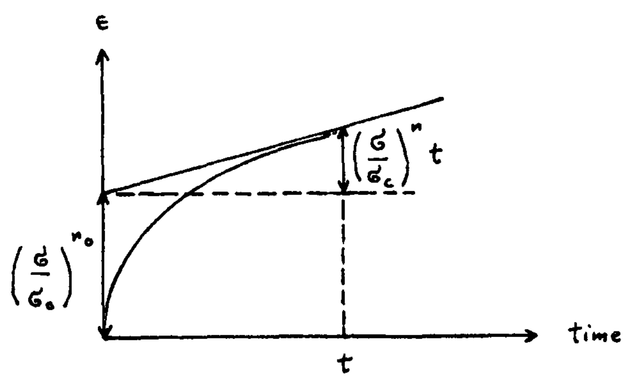

Fig. 2-3 - Approximation of Creep Curve

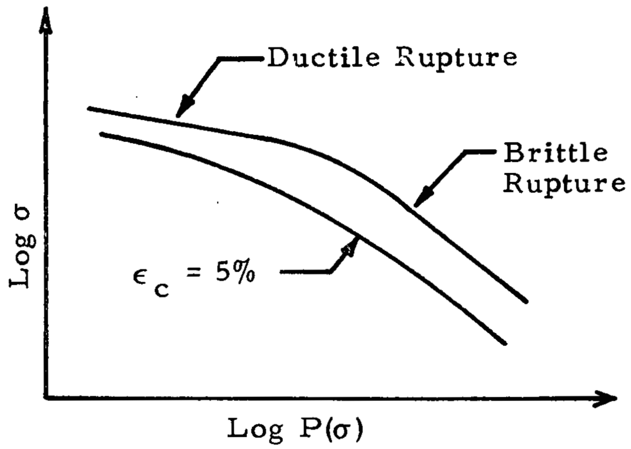

Fig. 2-1 - Creep and Creep Rupture Master Curves

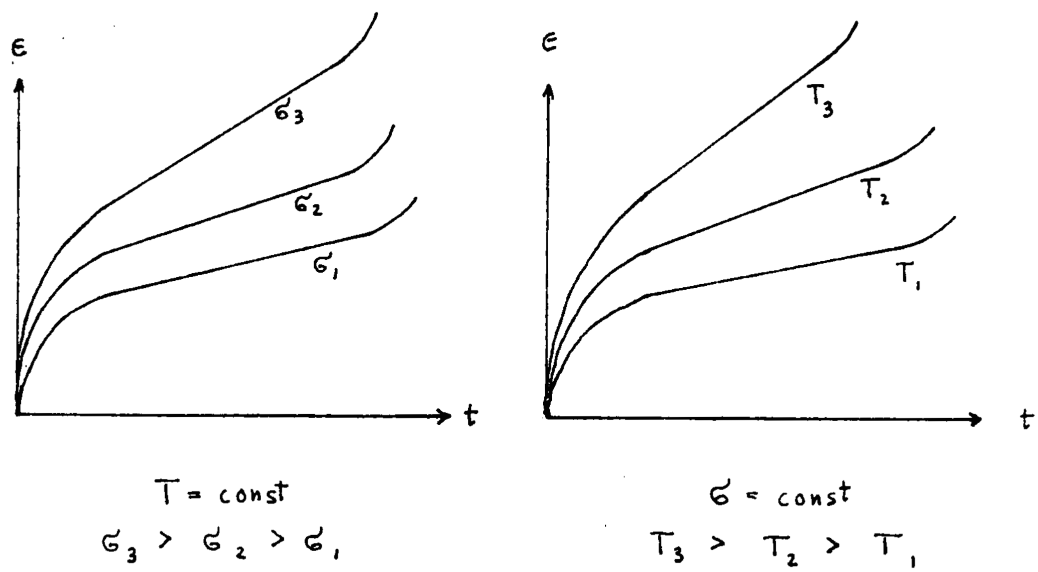

Fig. 2-2 - Constant Stress, Constant Temperature Creep Curves

The term

$$\epsilon_o = \left(\frac{\sigma}{\sigma_o}\right)^{n_o} \tag{2.4}$$

(Norton) describes the plastic strain with strain hardening, while

$$\frac{d\epsilon_c}{dt} = \left(\frac{\sigma}{\sigma_c}\right)^{n} \tag{2.5}$$

represents the viscous flow under constant stress. The elastic strain

$$\epsilon_e = \frac{\sigma}{E} \tag{2.6}$$

has been neglected in Eq. (2.3).

Before the mathematical implications of Eq. (2.3) are pursued any further it may be of interest to explore alternate formulations. Generally all strain theories can be written as

$$\epsilon = f_1(\sigma)\, f_2(t)\, f_3(T) \tag{2.7}$$

in a multiplicative form of functions of stress, σ, time, t, and temperature, T. Particular "rules" are the time hardening,

$$\frac{d\epsilon}{dt} = f_1(\sigma)\, \frac{d\, f_2(t)}{dt}\, f_3(T) \tag{2.8}$$

strain hardening,

$$\frac{d\epsilon}{dt} = g_1(\sigma)\, g_2(\epsilon)\, g_3(T) \tag{2.9}$$

or a combined theory as

$$\frac{d\epsilon}{dt} = C\,\sigma^{\alpha}\,\epsilon^{\beta}\,t^{\gamma} \qquad (2.10)$$

Other material laws are expressed as

$$\frac{d\epsilon}{dt} = C\,\frac{\sigma^{p}}{\epsilon^{q}} \quad \text{(Nadai)} \qquad (2.11)$$

and,

$$\frac{d\epsilon}{dt} = (C_1\,q\,e^{-qt} + C_2)\,\sigma^{\alpha} \quad \text{(Marin).} \qquad (2.12)$$

The material law of Eq. (2.3) has advantages for steady state problems (secondary creep) while for transient problems (primary creep) the material laws of Eqs. (2.7) through (2.12) have to be considered.

To complete the catalog of material laws Eq. (2.3) is generalized to loading and unloading problems, including recovery effects (Ref. 2-4). During loading

$$\frac{d\epsilon}{dt} = \frac{d}{dt}\left[\frac{\sigma}{E} + \left(\frac{\sigma}{\sigma_o}\right)^{n_o}\right] + \left(\frac{\sigma}{\sigma_c}\right)^{n} \qquad (2.13)$$

while during unloading

$$\frac{d\epsilon}{dt} = \frac{d}{dt}\left[\frac{\sigma}{E} + \left(\frac{\sigma}{\sigma_1}\right)^{n_1}\right] + \left(\frac{\sigma}{\sigma_c}\right)^{n} \qquad (2.14)$$

This creep law is illustrated on Fig. 2-4.

2.2 CREEP RUPTURE LAWS

Creep rupture is a failure condition which is associated with a particular stress temperature and rupture time. Since Hencky's notable paper of 1925 (Ref. 2-5) a number of theories to predict rupture times have appeared (Refs. 2-6 through 2-9). These papers are briefly summarized on Fig. 2-5, on which the following notation is used:

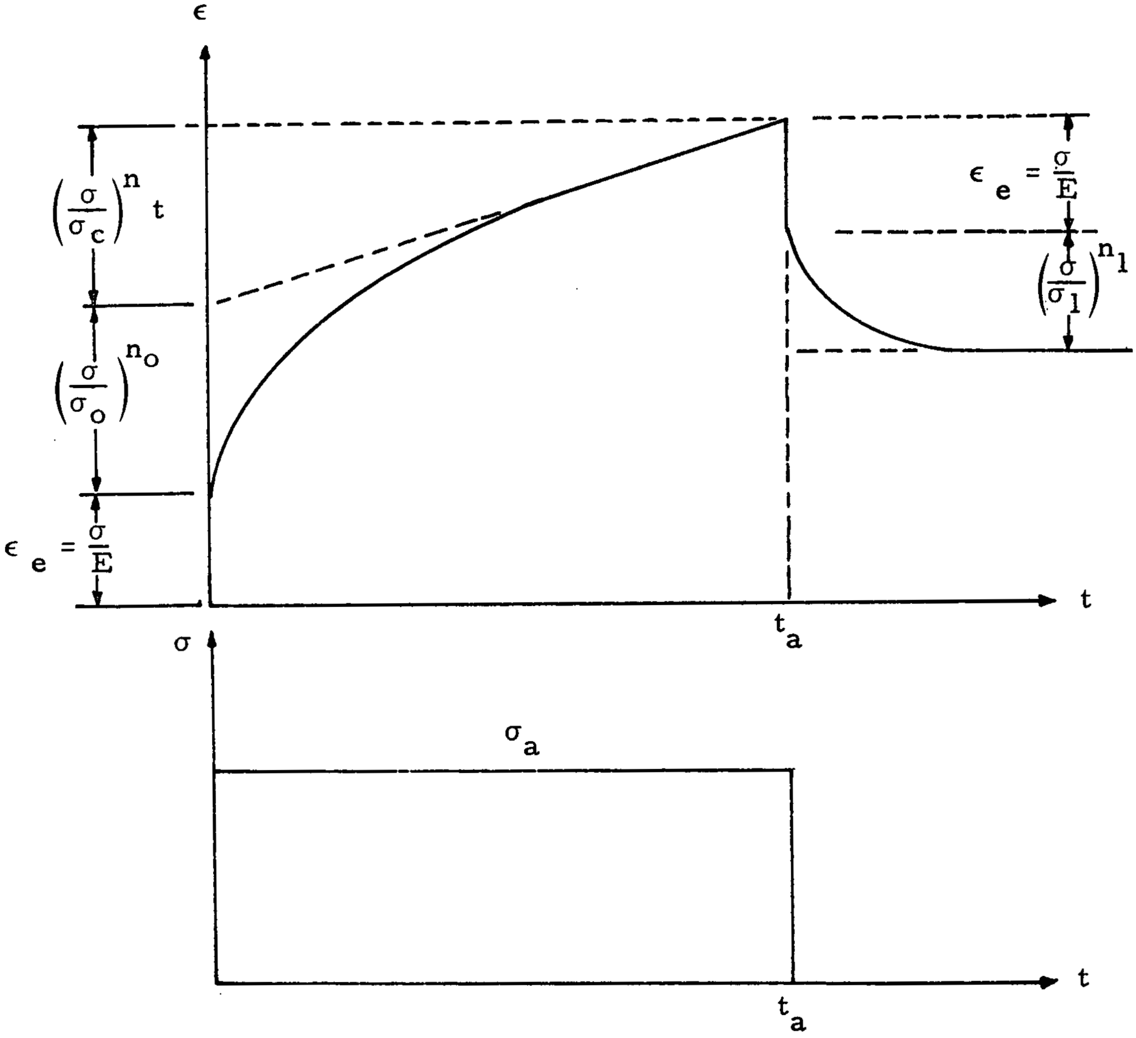

Fig. 2-4 - Loading and Unloading with Recovery

Name	Material Law	Time to Ductile Rupture	Time to Brittle Rupture
1. Hencky 1925	$\sigma_y = \sigma_{yo} + 3K\dot{\epsilon}$	$t_R = \frac{3K}{\sigma_{yo}} \ln \frac{\sigma_o}{\sigma_o - \sigma_{yo}}$	
2. Odqvist 1933	$\sigma_y = \sigma_{yo} + 3K\dot{\epsilon} + K\epsilon$	$t_R = \frac{3K}{\sigma_{yo} - K} \ln \frac{\sigma_o - K}{\sigma_o - \sigma_{yo}}$	
3. Robinson 1952	$\sigma_K = f(T_K, t_K)$ Larson-Miller Manson-Haferd	$\int_0^{t_R} \frac{dt}{t_K} = 1$	
4. Hoff 1953	$\dot{\epsilon} = \left(\frac{\sigma}{\sigma_c}\right)^n$	$t_R = \frac{1}{n}\left(\frac{\sigma_c}{\sigma_o}\right)^n$	
5. Hoff with primary creep	$\dot{\epsilon} = \left(\frac{\dot{\sigma}}{\sigma_i}\right)^m + \left(\frac{\sigma}{\sigma_c}\right)^n$	$t_R = \frac{1}{n}\left(\frac{\sigma_c}{\sigma_o}\right)^n \left[1 - \frac{nm}{n-m}\left(\frac{\sigma_o}{\sigma_i}\right)^m\right]$	
6. Kachanov 1958	$C\sigma_K^r t_K = \frac{1}{r+1}$	$\int_0^{t_R} \left(\frac{\sigma}{\sigma_K}\right)^r dt = t_K$	

Fig. 2-5 - Creep Rupture Laws

σ_y = yield stress
σ_{yo} = initial yield stress
k = "viscosity"
σ_o = initial stress (at t=0)
σ_i, m = material constants for incipient creep
σ_c, n = material constants for steady state creep
σ_k, r, t_k = material constants for creep rupture
t_R = rupture time.

Robinson's theory is very useful in predicting rupture times for complicated temperature-stress histories since it applies the law of linear cumulative damage to creep rupture. To compute the expended lifetime to rupture the material data from a "master curve" such as the Larson-Miller curve are evaluated and the contributions of the individual phases of the temperature-stress history are summed.

Kachanov's theory can be combined with the theories of ductile rupture in lines (4) and (5) of Fig. 2-5 so that a prediction of both ductile and brittle rupture is possible. The terms ductile and brittle refer to the amount of cross-sectional necking. When the cross-section shrinks to zero at rupture, it is called ductile. Kachanov's theory can be used to calculate rupture times for multiaxial states of stress in which either the maximum tensile stress or, as may be the case in some materials, the equivalent stress σ_e is used. In the case of non-homogeneous stresses the travel of a rupture surface through a structural member can be treated using Kachanov's theory.

Another form of presenting Kachanov's theory is as follows

$$\frac{dD}{dt} = C\left(\frac{\sigma}{1-D}\right)^n \tag{2.15}$$

where

$$D = \frac{A - A_{red}}{A} \tag{2.16}$$

is the "damage factor" which approaches 1 when the reduced cross-sectional area A_{red} approaches zero.

2.3 EVALUATION OF MATERIAL CONSTANTS

The material law given by Eq. (2.3) is written in a slightly different form as

$$\epsilon = C_1 \sigma^m + C_2 \sigma^n t \tag{2.17}$$

The material constants C_1 and m are associated with the incipient (or intercept) strain ϵ_i and C_2 and n with the steady state creep strain ϵ_c (Fig. 2-6)

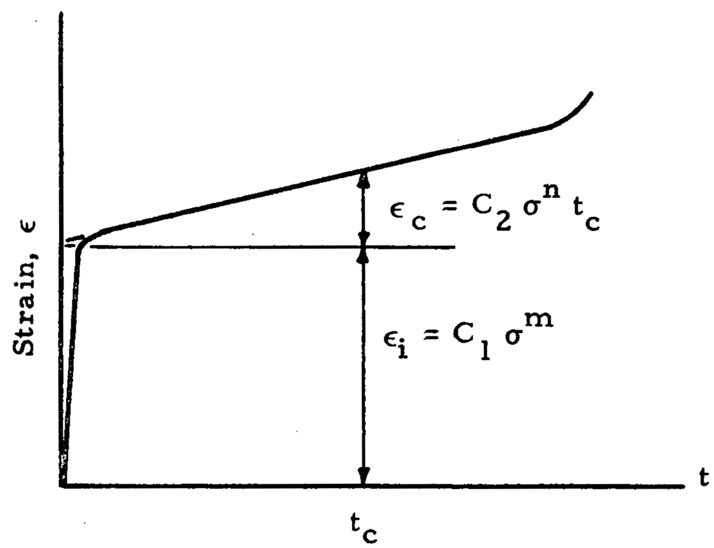

Fig. 2-6 - Simplified Creep Law

The intercept strain data are presented in the form of Fig. 2-7, where the actual curve is approximately a straight line with the slope m. Then

$$\frac{\epsilon_{i_1}}{\epsilon_{i_2}} = \left(\frac{\sigma_1}{\sigma_2}\right)^m \tag{2.18}$$

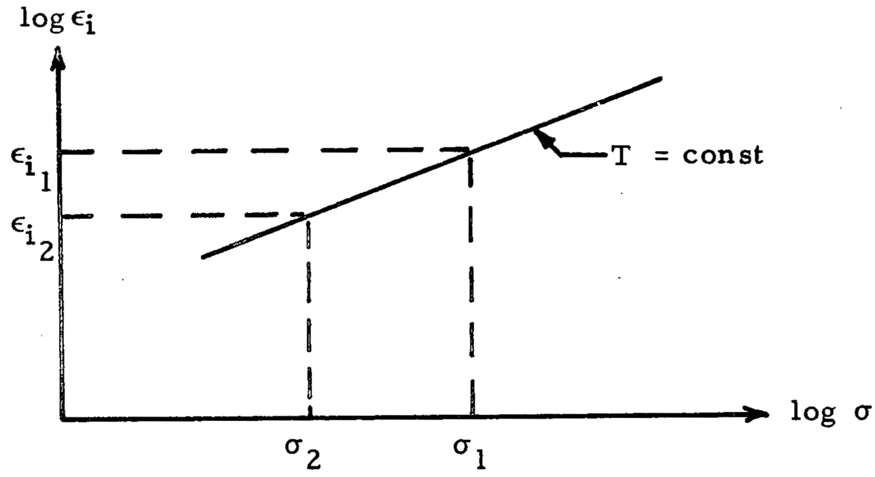

Fig. 2-7 - Intercept Strain ϵ_i vs Stress σ

from which

$$m = \ell n\left(\frac{\epsilon_{i_1}}{\epsilon_{i_2}}\right) \Big/ \ell n\left(\frac{\sigma_1}{\sigma_2}\right) \quad . \tag{2.19}$$

The constant C_1 is found from

$$C_1 = \epsilon_{i_1}/\sigma_1^m \tag{2.20}$$

The steady state creep data follow from "master curves" such as the ones in Fig. 2-8 as follows.

The creep rate $\dot{\epsilon}_1$ at stress level σ_1 is

$$\dot{\epsilon}_1 = \frac{\epsilon_1}{t_c} \tag{2.21}$$

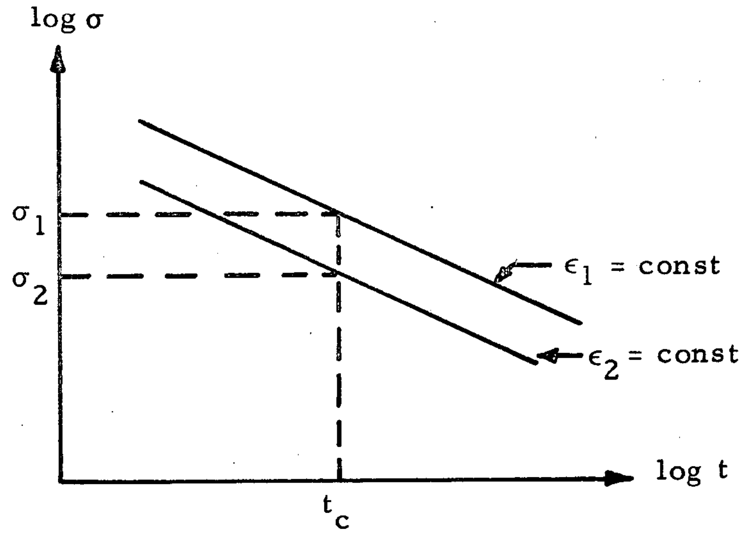

Fig. 2-8 - Master Creep Curves

and at stress level σ_2

$$\dot{\epsilon}_2 = \frac{\epsilon_2}{t_c} \tag{2.22}$$

To find n and C_2 the relation

$$\left(\frac{\dot{\epsilon}_1}{\dot{\epsilon}_2}\right) = \left(\frac{\sigma_1}{\sigma_2}\right)^n \tag{2.23}$$

is used so that

$$n = \ell n\,(\dot{\epsilon}_1/\dot{\epsilon}_2)/\ell n\,(\sigma_1/\sigma_2) \tag{2.24}$$

and

$$C_2 = \dot{\epsilon}_1/\sigma_1^n \tag{2.25}$$

2.4 LIFETIME CALCULATION IN A RANDOM TEMPERATURE FIELD

In the following the creep law is considered in the form (Ref. 2-10)

$$\frac{d\epsilon}{dt} = K\,\sigma^n \tag{2.26}$$

where for moderate temperature variations

$$K = c\,e^{\beta T(t)} \tag{2.27}$$

This is the "viscosity factor" with c and β being material constants.

When the temperature is subject to temperature fluctuations

$$T(t) = T_m(t) + \theta\,(t) \tag{2.28}$$

where T_m is a mean temperature and θ is the random fluctuation, then the viscosity constant becomes sensitive to these fluctuations

$$K = c\,e^{\beta\,(T_m(t)\,+\,\theta\,(t))} = K_m\,e^{\beta\,\theta\,(t)} \tag{2.29}$$

where

$$K_m = c\,e^{\beta\,T_m(t)} \tag{2.30}$$

If the probability density function $p(\theta)$ of the temperature fluctuation is known, the expected (mean) value of the viscosity constant is

$$K = K_m \int_{-\infty}^{+\infty} e^{\beta\theta(t)} p(\theta)\,d\theta = K_m \mu\,(t) \tag{2.31}$$

For a normal distribution

$$\mu(t) = e^{\frac{\beta^2 \tau^2}{2}} \tag{2.32}$$

where τ^2 is the variance of the distribution.

This formulation can be used to find the reduction of lifetime of structures subjected to temperature fluctuations in the high temperature range.

Consider a bar under constant load P. The necking of the bar expressed as

$$\zeta = \frac{A(t)}{A_o} \tag{2.33}$$

where A_o is the original cross-sectional area, is a measure of the lifetime

$$1 \geq \zeta \geq 0 \, . \tag{2.34}$$

It is assumed that the life is up when $\zeta = 0$.

The natural strain is

$$\epsilon = - \ln \zeta \tag{2.35}$$

and the strain rate

$$\dot{\epsilon} = - \frac{\dot{\zeta}}{\zeta} \tag{2.36}$$

while the stress is

$$\sigma = \frac{1}{\zeta} \sigma_o \tag{2.37}$$

where $\sigma_o = \frac{P}{A_o}$.

Using Norton's law in the form of Eq. (2.26) the following differential equation is arrived at

$$\dot{\zeta} + c\,\sigma_o^n\, e^{\beta T(t)}\, \zeta^{1-n} = 0 \tag{2.38}$$

which leads to the integrals

$$\int_{\zeta(o)}^{\zeta(t)} \zeta^{n-1}\, d\zeta = -c\,\sigma_o^n \int_o^t e^{\beta T(t)}\, dt \tag{2.39}$$

Taking expectations on both sides of Eq. (2.36) and setting the expected value of ζ at lifetime to be zero the following result is obtained

$$\int_o^{t_\ell} \mu(t)\, K_m(t)\, dt = \frac{1}{n\sigma_o^n} \ . \tag{2.40}$$

For stationary conditions the lifetime can be explicitly expressed from Eq. (2.40) by

$$t_\ell = \frac{1}{n\sigma_o^n\, \mu\, K_m} \tag{2.41}$$

2.5 VARIATIONS IN STRESS AND TEMPERATURE

It is instructive to qualitatively examine the behavior of a constrained bar with various material laws involving creep effects, when it is subjected to temperature cycles (Refs. 2-11 and 2-12). Figure 2-9 is an extension of the case of elastic-plastic material with constant yield stress and of elastic-linear work hardening with various types of yield strength (temperature dependent, unstable, etc.) involving the accumulation of stress (residual stress). The establishment of various cyclic patterns according to heating and cooling rates is evident, Fig. 2-10.

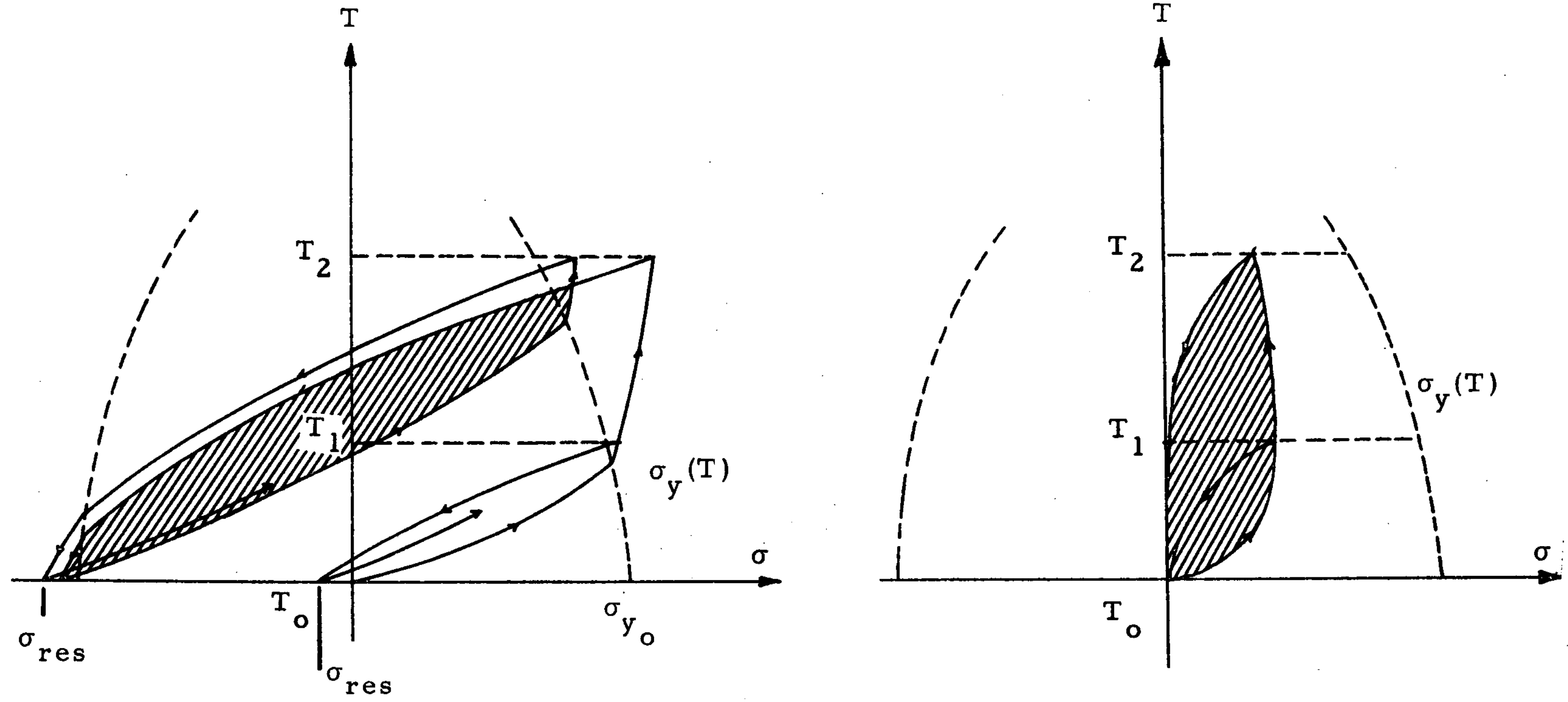

(a) Viscoelastic-Viscoplastic

$$\dot{\epsilon} = \frac{\dot{\sigma}}{E} + \frac{\sigma}{C_1} + \frac{\sigma - \sigma_y(T)}{C_2}$$

(b) Slow Heating and Slow Cooling

$$\dot{\epsilon} = \frac{\dot{\sigma}}{E} + \frac{\sigma}{C_1}$$

Fig. 2-9 - Thermo-Cycling of a Clamped Bar

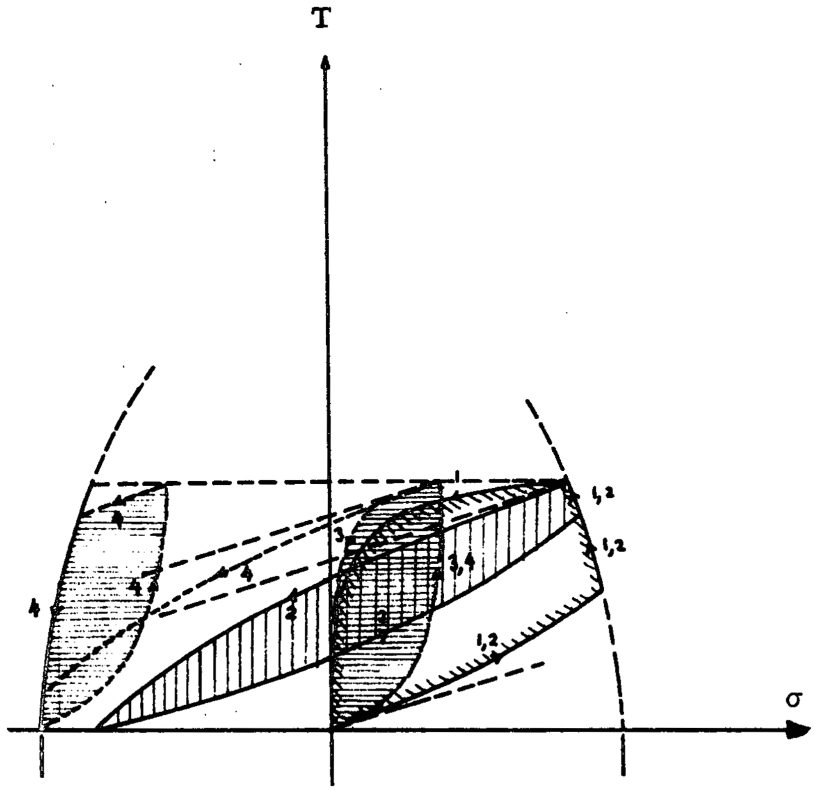

	Heating	Cooling
1	Rapid	Slow
2	Rapid	Rapid
3	Slow	Slow
4	Slow	Rapid

Fig. 2-10 - Viscoelastic-Plastic Bar Subjected to Various Heating and Cooling Rates

The case of variable stress at constant temperatures is illustrated on Fig. 2-11. The accumulation of creep strain when calculated with some of the theories discussed earlier, Eqs. (2.7 through 2.12) is depicted. In Ref. 2-3 a number of stress histories and their effect on the strain accumulation are discussed.

2.6 MATHEMATICAL THEORIES FOR ANALYSIS OF STRUCTURAL COMPONENTS SUBJECTED TO CREEP

Consider the tensor of deviator stresses S_{ij}, where i, j = 1, 2, 3 refer to a rectangular Cartesian coordinate system. For isotropic materials an equivalent stress σ_e is defined by

$$\sigma_e^2 = \frac{3}{2} S_{ij} S_{ij} \quad . \tag{2.42}$$

The summation convention of repeated indices is used. Similarly an equivalent strain ϵ_e is

$$\epsilon_e^2 = \frac{2}{3} \epsilon_{ij} \epsilon_{ij} \tag{2.43}$$

and an equivalent strain rate v_e is

$$v_e^2 = \frac{2}{3} v_{ij} v_{ij} \tag{2.44}$$

where

$$v_{ij} = \frac{d\epsilon_{ij}}{dt} \tag{2.45}$$

It is assumed that the material law of Eq. (2.3) is used. Then

$$\epsilon_e = \left(\frac{\sigma_e}{\sigma_o} \right)^{n_o} \tag{2.46}$$

and

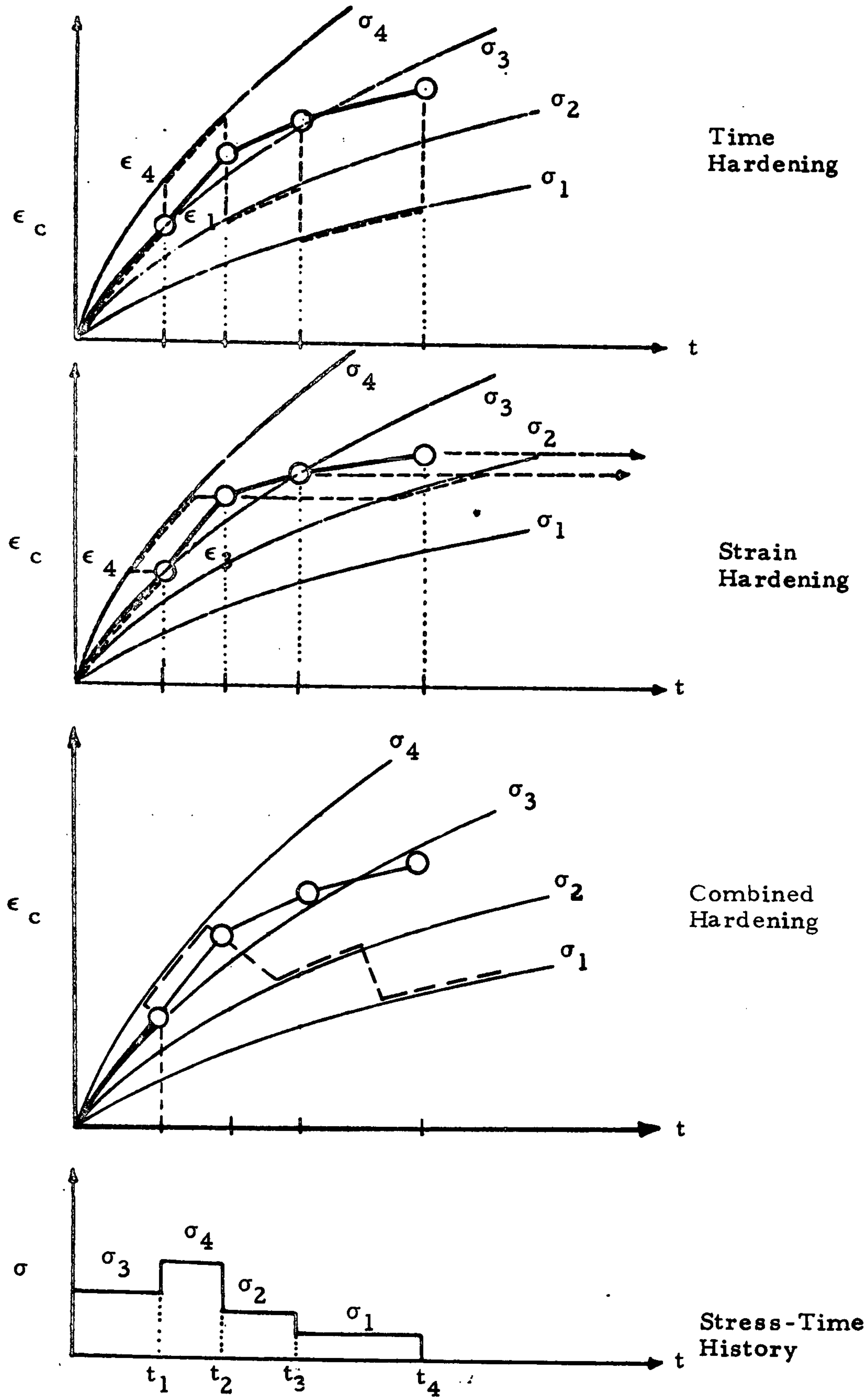

Fig. 2-11 - Strain Accumulation at Variable Stress But Constant Temperatures

$$v_e = \frac{d\epsilon_e}{dt} = \left(\frac{\sigma_e}{\sigma_c}\right)^n \tag{2.47}$$

The corresponding tensor relations are

$$\epsilon_{ij}^{(o)} = \frac{3}{2}\left(\frac{\sigma_e}{\sigma_o}\right)^{n_o - 1} \frac{S_{ij}}{\sigma_o} \tag{2.48}$$

and

$$v_{ij} = \frac{3}{2}\left(\frac{\sigma_e}{\sigma_c}\right)^{n-1} \frac{S_{ij}}{\sigma_c} \tag{2.49}$$

The bending of a beam following the material law of Eq. (2.47) can be described in a similar fashion as an elastic beam. This has been called the elastic analog (Ref. 2-4). The strain rate is

$$v = -z \frac{\partial^3 w}{\partial x^2 \partial t} = -z \dot{w}'' \tag{2.50}$$

Rewriting the material law as

$$v = \left|\frac{\sigma}{\sigma_c}\right| \operatorname{sgn} \sigma \tag{2.51}$$

and solving for σ gives

$$\sigma = \sigma_c |v|^{\frac{1}{n}} \operatorname{sgn} v \tag{2.52}$$

Let a bending moment M and an axial force N act on the cross section (Fig. 2-12). Then the stress resultants in terms of the stress are

$$\int_{-e_1 + d}^{e_2 + d} \sigma \, dA = N \tag{2.53}$$

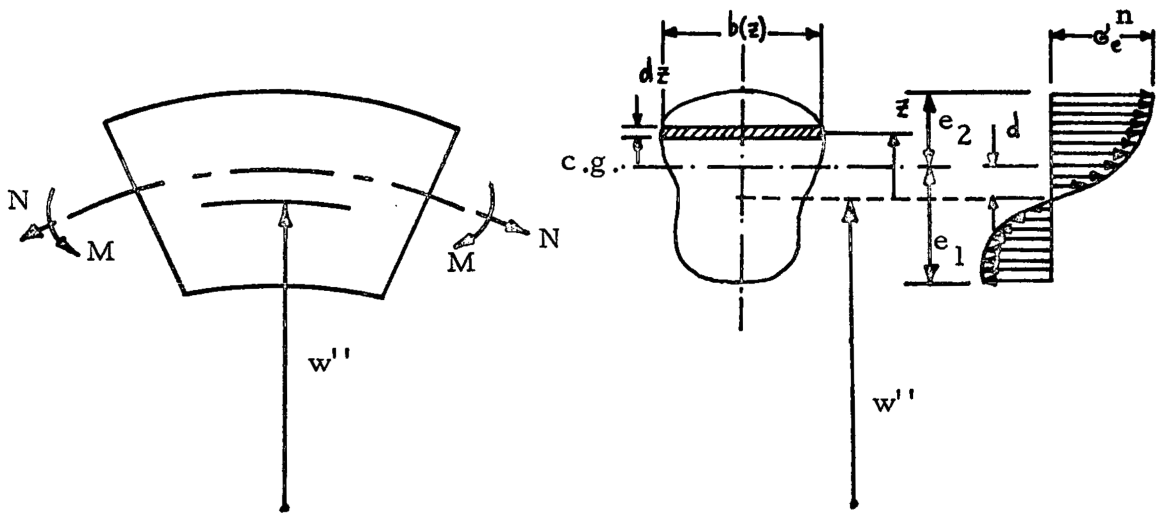

Fig. 2-12 - Beam Cross Section

$$\int_{-e_1 + d}^{e_2 + d} \sigma\,(z-d)\,dA = M \tag{2.54}$$

which can be rewritten with Eqs. (2.50) and (2.51) as

$$\sigma_c \left|v\right|^{\frac{1}{n}} \operatorname{sgn} v\, S_n = N \tag{2.55}$$

$$\sigma_c \left|v\right|^{\frac{1}{n}} \operatorname{sgn} v\, I_n = M + dN \tag{2.56}$$

The area integrals are

$$S_n = \int_{-e_1 + d}^{e_2 + d} |z|^{\frac{1}{n}} \operatorname{sgn} z \; b(z)\, dz \tag{2.57}$$

$$I_n = \int_{-e_1 + d}^{e_2 + d} |z|^{1 + \frac{1}{n}} b(z)\, dz \tag{2.58}$$

On Fig. 2-13 the area integrals for a few cross sections are given.

The material law of Eqs. (2.46) and (2.47) also lends itself to deriving a beam theory, as well as plate and shell theories. A beam equation similar to Bernoulli's equation for elastic beams can be visualized from Eq. (2.56). For example a cantilever beam with a tip load P has a bending moment

$$M(x) = P\, x \tag{2.59}$$

if the x-axis runs from the tip.

From Eq. (2.56) it follows that

$$v = -\dot{w}'' = \left(\frac{P}{\sigma_c I_n}\right)^n x^n \tag{2.60}$$

It is a simple matter to derive beam solutions for a variety of boundary conditions (Fig. 2-14).

Using the foregoing the lifetime of a cantilever beam with a tip load, subjected to the temperature fluctuation of Eq. (2.28) would be computed from

Shape	I_n	S_n
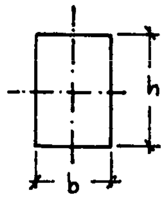	$\frac{2n}{2n+1}\,\frac{bh^2}{4}\left(\frac{h}{2}\right)^{\frac{1}{n}}$	$\frac{n}{n+1}\,bh\left(\frac{h}{2}\right)^{\frac{1}{n}}$
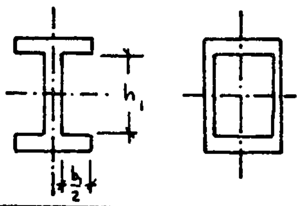	$\frac{2n}{2n+1}\left[\frac{bh^2}{4}\left(\frac{h}{2}\right)^{\frac{1}{n}}-\frac{b_1h_1^2}{4}\left(\frac{h_1}{2}\right)^{\frac{1}{n}}\right]$	$\frac{n}{n+1}\left[bh\left(\frac{h}{2}\right)^{\frac{1}{n}}-b_1h_1\left(\frac{h_1}{2}\right)^{\frac{1}{n}}\right]$
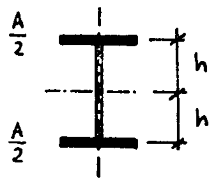	$A\,h^{1+\frac{1}{n}}$	$A\,h^{\frac{1}{n}}$
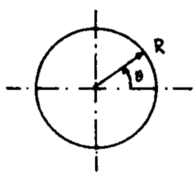	$\int_0^{2\pi}\int_0^{R} r^{2+\frac{1}{n}}\sin^{1+\frac{1}{n}}\theta\,d\theta\,dr$	$\int_0^{2\pi}\int_0^{R} r^{1+\frac{1}{n}}\sin^{\frac{1}{n}}\theta\,d\theta\,dr$

Fig. 2-13 - Area Integrals for Beam Cross Sections for Elastic Analog

Case	$\dot{w}(x)$	$\dot{\delta}$
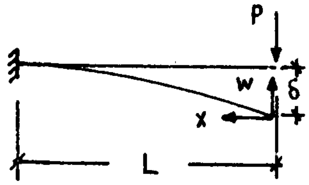	$\left(\frac{PL}{\sigma_c I_n}\right)^n \frac{L}{n+1}\left[x - \frac{x^{n+2}}{(n+2)L^{n+1}}\right]$	$\left(\frac{PL}{\sigma_c I_n}\right)^n \frac{L^2}{n+2}$
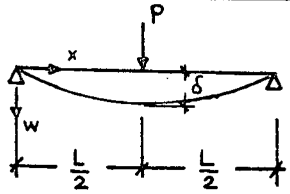	$\left(\frac{PL}{\sigma_c I_n}\right)^n \frac{L}{2^{2n+1}(n+1)}\left[x - \frac{x^{n+2}\,2^{n+1}}{(n+2)L^{n+1}}\right]$	$\left(\frac{PL}{\sigma_c I_n}\right)^n \frac{L^2}{(n+2)\,2^{2(n+1)}}$
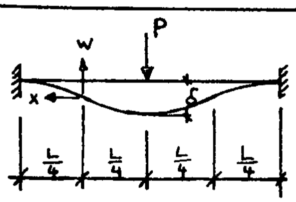	$\left(\frac{PL}{\sigma_c I_n}\right)^n \frac{L}{2^{3n+2}(n+1)}\left[x - \frac{x^{n+2}\,2^{2n+2}}{(n+2)L^{n+1}}\right]$	$\left(\frac{PL}{\sigma_c I_n}\right)^n \frac{L^2}{(n+2)\,2^{3(n+1)}}$
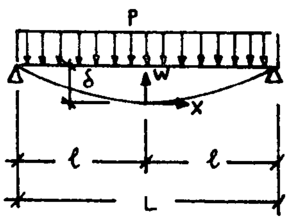	$\xi = \frac{x}{\ell}$ n = 1 $-\left(\frac{p\ell^2}{2\sigma_c I}\right)\frac{\ell^2\xi^2}{2}\left(1 - \frac{\xi^2}{6}\right)$ n = 3 $-\left(\frac{p\ell^2}{2\sigma_c I_3}\right)^3\frac{\ell^2\xi^2}{2}\left(1 - \frac{\xi^2}{2} + \frac{\xi^4}{5} - \frac{\xi^6}{28}\right)$ n = 5 $-\left(\frac{p\ell^2}{2\sigma_c I_5}\right)^5\frac{\ell^2\xi^2}{2}\left(1 - \frac{5}{6}\xi^2 + \frac{2}{3}\xi^4 - \frac{5}{14}\xi^6 + \frac{\xi^8}{9} - \frac{\xi^{10}}{66}\right)$	$\left(\frac{pL^2}{\sigma_c I_n}\right)^n \frac{L^2}{2^{3n+2}}\, C^{(n)}$ $C^{(1)} = .4166 = \frac{5}{12}$ $C^{(3)} = .3321 = \frac{93}{280}$ $C^{(5)} = .2860 = \frac{793}{2772}$
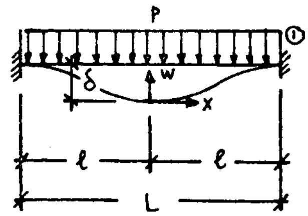	$\xi = \frac{x}{\ell}$ $m = 1 + \frac{2M_①}{p\ell^2}$ $n = 1,\ m = \frac{1}{3}$ $-\left(\frac{p\ell^2}{2\sigma_c I}\right)\frac{\ell^2\xi^2}{2}\left(m - \frac{\xi^2}{6}\right)$ $n = 3,\ m = .3959$ $-\left(\frac{p\ell^2}{2\sigma_c I_3}\right)^3\frac{\ell^2\xi^2}{2}\left(m^3 - \frac{m^2\xi^2}{2} + \frac{m\xi^4}{5} - \frac{\xi^6}{28}\right)$ $n = 5,\ m = .4225$ $-\left(\frac{p\ell^2}{2\sigma_c I_5}\right)^5\frac{\ell^2\xi^2}{2}\left(m^5 - \frac{5}{6}m^4\xi^2 - \frac{2}{3}m^3\xi^4 - \frac{5}{14}m^2\xi^6 + \ldots\right)$ see above	$\left(\frac{pL^2}{\sigma_c I_n}\right)^n \frac{L^2}{2^{3n+2}}\, C^{(n)}$ $C^{(1)} = .08333 = \frac{1}{12}$ $C^{(3)} = .01357$ $C^{(5)} = .00262$

Fig. 2-14 - Deflection Rate for Beams with Various Boundary Conditions

$$\delta(t) = \frac{PL^3}{3EI} + \left(\frac{PL}{I_n}\right)^n \frac{L^2}{n+2} \mu K_m t \tag{2.61}$$

when a deflection limitation is given.

Another application is the development of design charts for combined loads. The largest effective stress for a non-linear structure subjected to r loads $L_1, L_2, \ldots, L_r$ acting simultaneously,

$$\sigma_e^{(n)} = f_n (L_1, L_2, \ldots, L_r) \tag{2.62}$$

or with

$$\alpha_i = \frac{L_i}{L_1} \quad i = 2, 3, \ldots, r \tag{2.63}$$

$$\sigma_e^{(n)} = L_1 f_n (1, \alpha_2, \alpha_3, \ldots, \alpha_r) \tag{2.64}$$

can be compared to the effective stress for an equivalent linear structure

$$\sigma_e^{(1)} = L_1 f_1 (1, \alpha_2, \alpha_3, \ldots, \alpha_4) \tag{2.65}$$

by introducing (Ref. 2-13)

$$\theta = \frac{\sigma_e^{(n)}}{\sigma_e^{(1)}} \ . \tag{2.66}$$

If tables or charts of θ are available, then by simply computing σ_e^1 with standard handbooks method and looking up θ the equivalent stress of the nonlinear structure is

$$\sigma_e^{(n)} = \theta \ \sigma_e^{(1)} \tag{2.67}$$

For a beam subjected to an axial force N and a bending moment M, i.e., with r=2, simple graphs result for θ for various values of n and ratios $\frac{M}{N}$ can be obtained. This is accomplished by using

$$\frac{M}{N} = \frac{I_n}{S_n} - d \tag{2.68}$$

and finding

$$\theta = \frac{\sigma_e^{(n)}}{\sigma_e^{(1)}} = \frac{M + dN}{M + d^*N} \left|\frac{Z_{max}}{Z^*_{max}}\right|^{\frac{1}{n}} \frac{I_1}{I_n} \tag{2.69}$$

The starred quantities refer to n=1. These examples are given on Figs. 2-15 through 2-17.

To complete the applications of the mathematical theory of the elastic analog for non-linear structures some solutions for cases involving rotational symmetry (ring, plate, shell of revolution, rotating disk) are tabulated in Tables 2-1 through 2-4. In these tables σ_t is the tangential (circumferential) stress, σ_x the axial stress and σ_r the radial stress. The same indices are used for the strain rates $\dot{\epsilon}$.

2.7 CREEP BUCKLING

Design for creep buckling requires that the usual concept of a critical (or buckling) load is replaced by the concept of critical lifetimes. The critical lifetime is the time necessary for collapse under constant load and temperature. The criterion of elastic stability

$$\frac{d\delta}{dP} \Rightarrow \infty \tag{2.70}$$

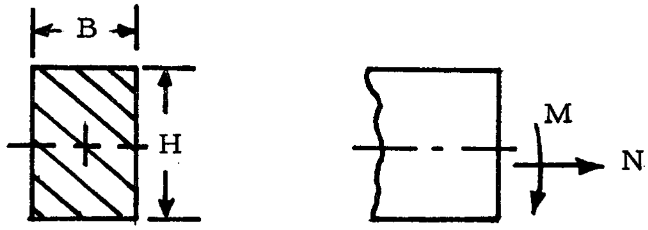

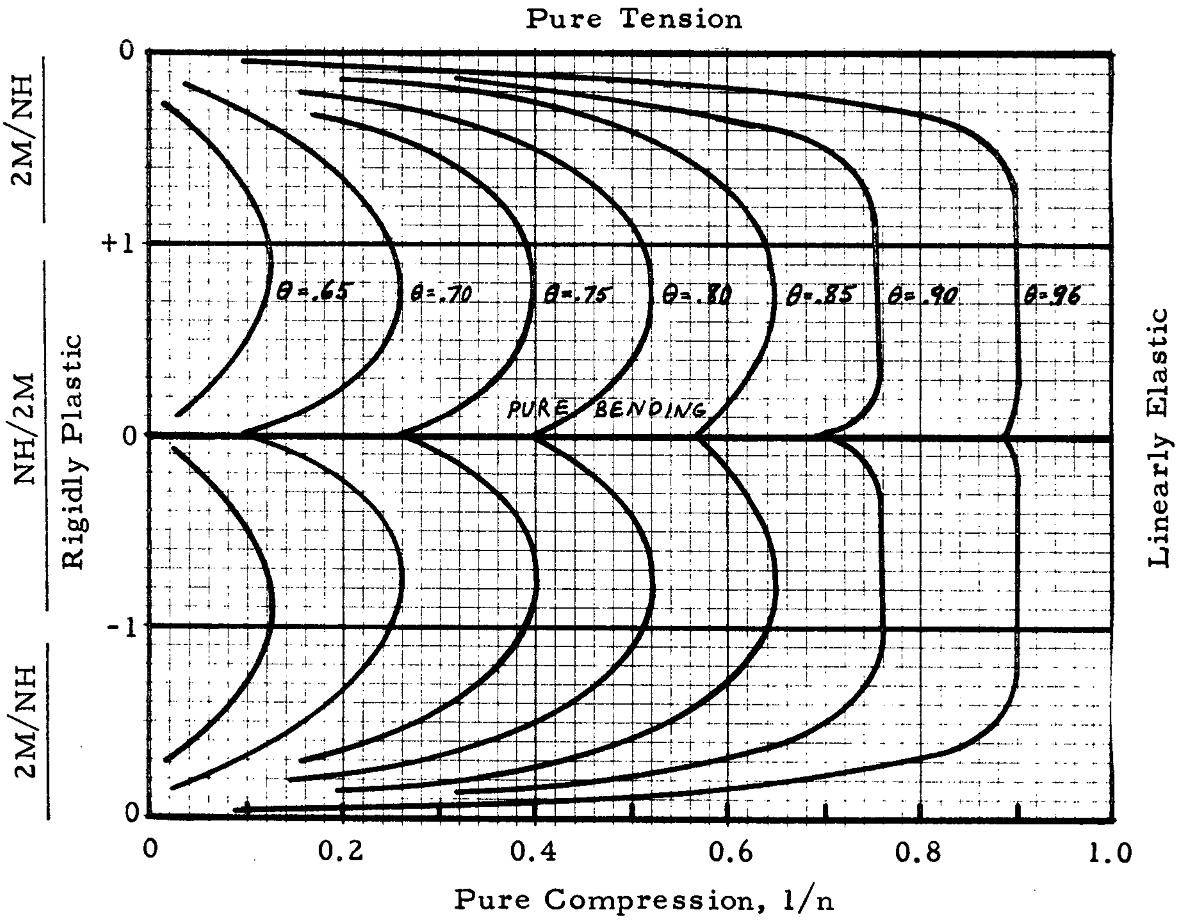

Fig. 2-15 - Design Chart for Bending of Rectangular Section, B/H = 0.5

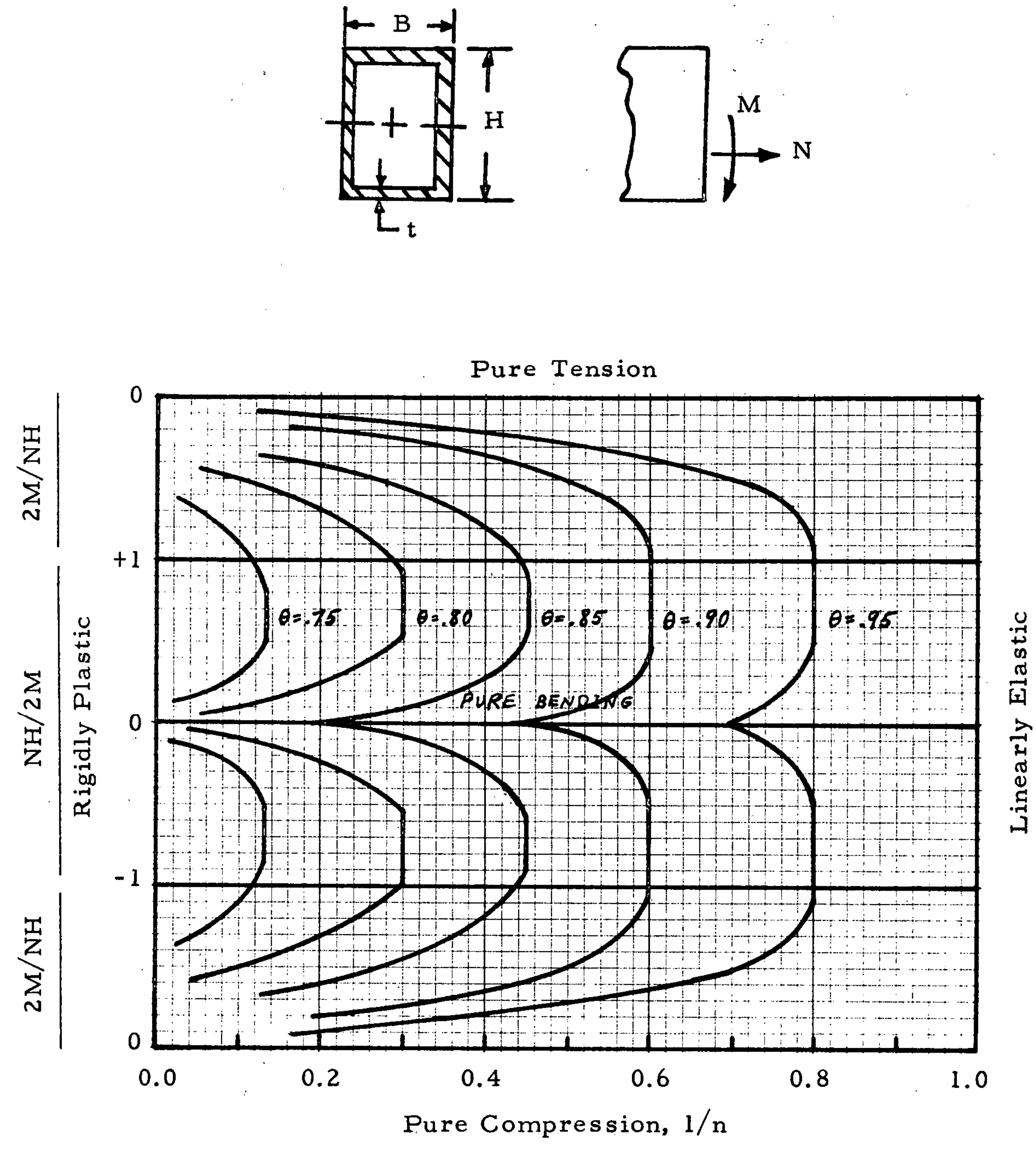

Fig. 2-16 - Design Chart for Bending of Rectangular Tube, B/H = 0.5, t/H = 0.025

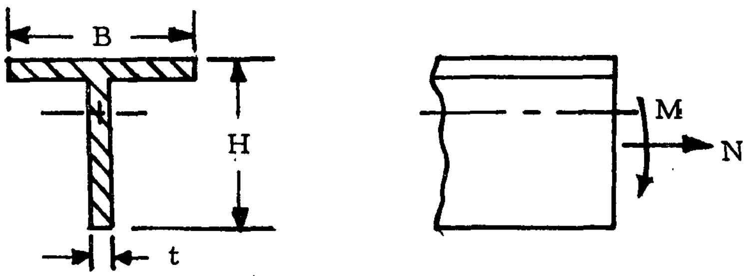

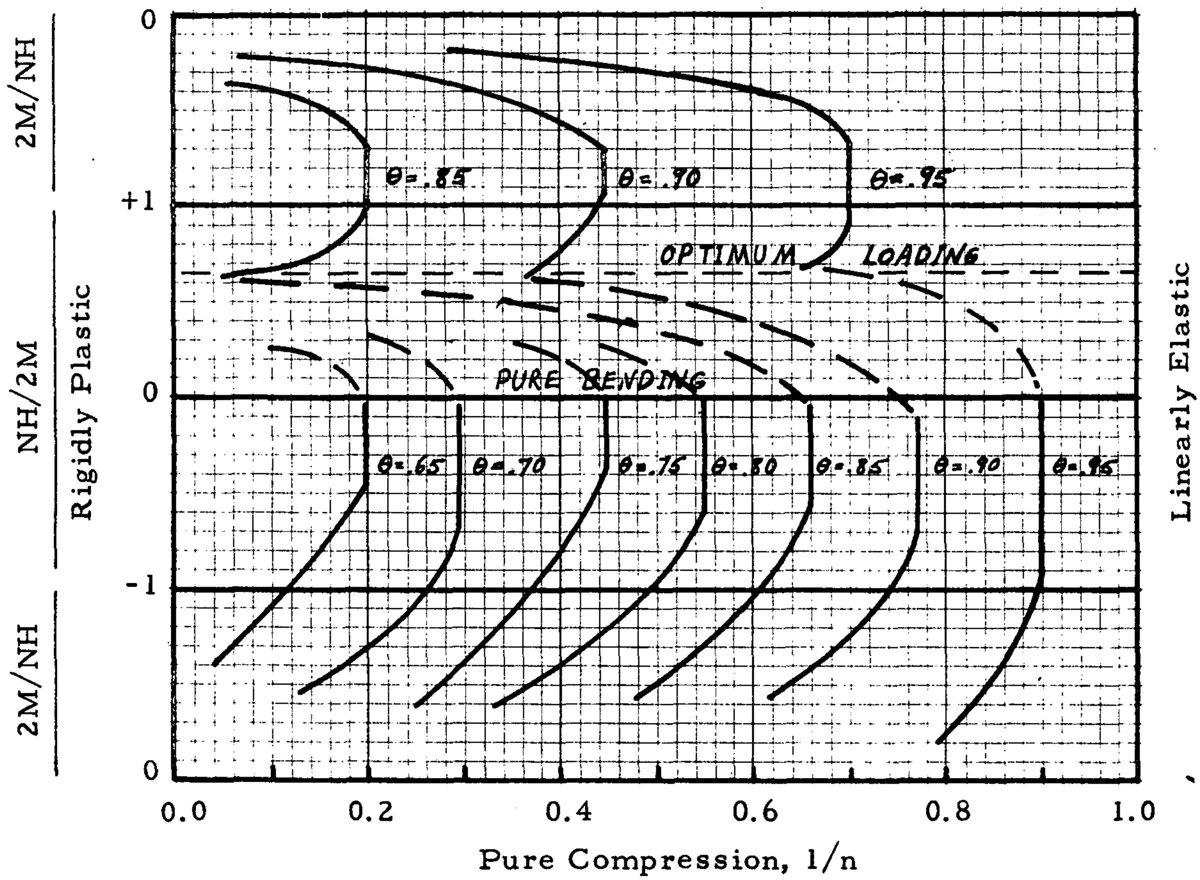

Fig. 2-17- Design Chart for Bending of T-Section, B/H = 0.5, t/H = 0.025

Table 2-1

CIRCULAR RING WITH RECTANGULAR CROSS SECTION (Ref. 2-14)

	Stress	Rotation
Circular Ring of Rectangular Cross Section Subjected to Uniform Moments 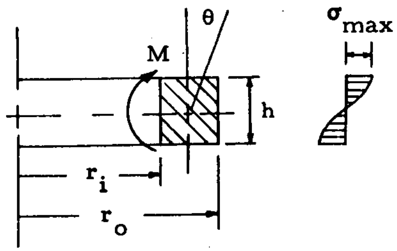	$\sigma_{max} = \left(\frac{h}{2 r_i}\right)^{\frac{1}{n}} \left(\frac{M}{2\pi}\right) \left[\frac{\left(2^{1+\frac{1}{n}}\right)\left(1-\frac{1}{n}\right)\left(2+\frac{1}{n}\right)}{\left(r_o^{1-\frac{1}{n}} - r_i^{1-\frac{1}{n}}\right) h^{2+\frac{1}{n}}}\right]$	$\theta = \left[\left(\frac{M}{2\pi}\right) \frac{\left(2^{1+\frac{1}{n}}\right)\left(1-\frac{1}{n}\right)\left(2+\frac{1}{n}\right)}{\left(r_o^{1-\frac{1}{n}} - r_i^{1-\frac{1}{n}}\right) h^{2+\frac{1}{n}}}\right]^n Bt$ where B and n are used in $\dot{\epsilon} = B\sigma^n$

Table 2-2

FORMULAS FOR STRESSES AND CREEP RATES IN PLATES (REF. 2-15)

	Stresses	Deflection Rate
Case a Simply Support-Distributed Load $W = p\pi R_o^2$ 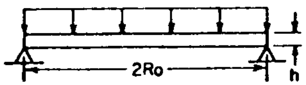 	$\sigma_r = -\frac{3W}{8\pi mh^2}\left[(3m+1)\left(1-\frac{r^2}{R_o^2}\right)\right]$ $\sigma_t = -\frac{3W}{8\pi mh^2}\left[(3m+1)-(m+3)\frac{r^2}{a^2}\right]$ where $m = \frac{1}{\nu}$	$\dot{W}_{max} = \frac{11B}{4}\left(\frac{5}{8}\frac{p}{J}\right)^n \frac{3^{(n+1)/2}(2n+1)^n R_o^{2(n+1)}}{n^n h^{2n+1}}$ W_{max} = normal deflection at center
Case b Clamped-Distributed Load $W = p\pi R_o^2$ 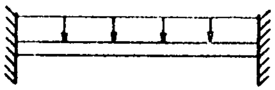	$\sigma_r = \frac{3W}{8\pi mh^2}\left[(3m+1)\frac{r^2}{R_o^2} - (m+1)\right]$ $\sigma_t = \frac{3W}{8\pi mh^2}\left[(m+3)\frac{r^2}{R_o^2} - (m+1)\right]$	$\dot{W}_{max} = \frac{B}{4}\left(\frac{p}{24J}\right)^n \frac{3^{(n+1)/2}(2n+1)^n R_o^{2(n+1)}}{n^n h^{2n+1}}$
Case c Simply Supported-Point Load 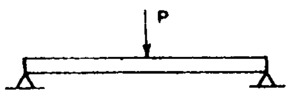 		$\dot{W}_{max} = \frac{7B}{12}\left(\frac{7P}{24\pi J}\right)^n \frac{3^{(n+1)/2}(2n+1)^n R_o^2}{n^n h^{2n+1}}$

Table 2-2 (Continued)

	Stresses	Deflection Rate
Case d Clamped-Point Load 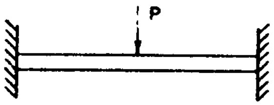		$\dot{W}_{max} = \frac{B}{4}\left(\frac{P}{8\pi J}\right)^n \frac{3^{(n+1)/2}(2n+1)^n R_o^2}{n^n h^{2n+1}}$

Values of J for Cases a to d

n	*J*			
	a	*b*	*c*	*d*
∞	3.65	0.534	0.647	0.429
5	5.51	0.552	0.707	0.429
2.5	8.36	0.574	0.782	0.432
1.667	12.8	0.600	0.877	0.442
1.25	19.5	0.631	0.997	0.459
1.0	30.0	0.667	1.17	0.500

Table 2-3

FORMULAS FOR STRESSES AND CREEP RATES IN PRESSURE VESSELS (REFS. 2-15 AND 2-16)

	Stress	Creep Rates
Thin-Walled Tubes with Internal Pressure and Bending	$\sigma_t = pr/t$ $\sigma_x = \frac{pr}{2t} + \frac{M \cdot y}{\pi r^3 t}$ $\sigma_r = 0$	$\dot{\epsilon}_x = B(\sigma_t^2 - \sigma_x \sigma_t + \sigma_x^2)^{\frac{(n-1)}{2}} (\sigma_x - \sigma_{t/2})$ $\dot{\epsilon}_t = (\sqrt{3/2})^{n+1} B(pr/t)^n$
Thin-Walled Tubes with Internal Pressure and Axial Load	$\sigma_t = pr/t$ $\sigma_x = pr/2t + P/A$	Same as above
Thin-Walled Tubes with Internal Pressure and Torsion	Principal stresses can be determined by Mohr's circle $\sigma_1, \sigma_2 = \frac{\sigma_t + \sigma_x}{2} \pm \left[\left(\frac{\sigma_t - \sigma_x}{2}\right)^2 + \tau^2\right]^{\frac{1}{2}}$	Principal strain rates can be determined and then the strain rates in the axial and tangential direction obtained.
Thick-Walled Cylinder with Internal Pressure	$\sigma_t = p \frac{R_i^2}{R_o^2 - R_i^2}\left(1 + \frac{R_o^2}{r^2}\right)$ $\sigma_x = p \frac{R_i^2}{R_o^2 - R_i^2}$ $\sigma_r = p \frac{R_i^2}{R_o^2 - R_i^2}\left(1 - \frac{R_o^2}{r^2}\right)$	$\dot{\epsilon}_t = B(\frac{3}{4})^{\frac{(n+1)}{2}} \left[\frac{p}{(R_o/R_i)^{2/n} - 1} (\frac{2}{n})\right]^n \left(\frac{R_o}{r}\right)^2$ $\dot{\epsilon}_x = 0$ $\dot{\epsilon}_r = -\dot{\epsilon}_t$

Table 2-3 (Continued)

	Stress	Creep Rates
Thick-Walled Sphere with Internal Pressure (Ref. 2-15)	$\sigma_t = \frac{p R_i^3}{R_o^3 - R_i^3}\left(1 + \frac{R_o^3}{2r^3}\right)$ $\sigma_r = \frac{p R_i^3}{R_o^3 - R_i^3}\left(1 - \frac{R_o^3}{r^3}\right)$	$\dot{\epsilon}_t = \frac{B}{2}(\sigma_t - \sigma_r)^n$ $\dot{\epsilon}_r = -2\dot{\epsilon}_t$
Thin-Walled Cylinders Internal Pressure (Ref. 2-16)	$\sigma_\theta = pr/t$ $\sigma_x = pr/2t$ $\sigma_r = 0$ Effective Stress $S = \frac{\sqrt{3}}{2}\ \frac{pr}{t}$	$\dot{\epsilon}_\theta = (\sqrt{3/2})^{n+1}(B)(pr/t)^n$ $\dot{\epsilon}_x = 0$ $\dot{\epsilon}_r = -(\sqrt{3/2})^{n+1}(B)(pr/t)^n$
Thin-Walled Hemisphere Internal Pressure (Ref. 2-16) 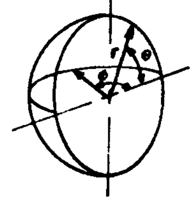	$\sigma_\theta = pr/2t$ $\sigma_\phi = pr/2t$ $\sigma_r = 0$ Effective Stress $S = pr/2t$	$\dot{\epsilon}_\theta = \frac{1}{2}B\left(\frac{pr}{2t}\right)^n$ $\dot{\epsilon}_\phi = \frac{1}{2}B\left(\frac{pr}{2t}\right)^n$ $\dot{\epsilon}_r = -B\left(\frac{pr}{2t}\right)^n$

Table 2-3 (Continued)

	Stress	Creep Rates
Thin-Walled Ellipsoidal Heads – Internal Pressure (Ref. 2-16) 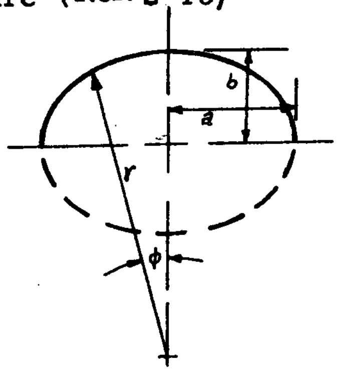	$\sigma_\phi = (pa^2/2t)\left(\frac{1}{F}\right)$ $\sigma_\theta = \frac{pa^2}{2t}\left(\frac{2b^2 - F^2}{b^2 F}\right)$ Effective Stress $\sigma_e = \frac{pa}{2tb^2}\left(3b^4 - 3a^2b^2 + a^4\right)^{\frac{1}{2}}$ where $F = \left(a^2 \sin^2\phi + b^2 \cos^2\phi\right)^{\frac{1}{2}}$	$\dot{\epsilon}_\phi = \left(\frac{pa}{2tb^2}\right) B \frac{a^2}{2}\left(3b^4 - 3a^2b^2 + a^4\right)^{n-\frac{1}{2}}$ $\dot{\epsilon}_\theta = \left(\frac{pa}{2tb^2}\right)^n B\left(\frac{3}{2}b^2 - a^2\right)\left(3b^4 - 3a^2b^2 + a^4\right)^{n-\frac{1}{2}}$ $\dot{\epsilon}_r = -\left(\frac{pa}{2tb^2}\right)^n B\left(\frac{3}{2}b^2 - \frac{1}{2}a^2\right)$ $\left(3b^4 - 3a^2b^2 + a^4\right)^{n-\frac{1}{2}}$

Table 2-4

FORMULAS FOR STRESSES AND CREEP RATES FOR ROTATING DISKS (REF. 2-15)

	Stresses	Deflection Rates
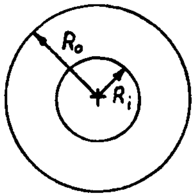 ρ = mass density Ω = angular velocity	$\sigma_t = \frac{n-1}{n}\left[\frac{\rho\Omega^2(R_o^3-R_i^3)}{3} + R_o\,\sigma_{R_o}\right]$ $\frac{r^{-1/n}}{R_o^{(n-1)/n} - R_i^{(n-1)/n}}$ $\sigma_r = \frac{1}{r}\left[\frac{\rho\Omega^2(R_o^3 - R_i^3)}{3} + R_o\,\sigma_{R_o}\right]$ $\left[\frac{r^{(n-1)/n} - R_i^{(n-1)/n}}{R_o^{(n-1)/n} - R_i^{(n-1)/n}}\right]$ $- \frac{\rho\Omega^2(r^3 - R_i^3)}{3r}$	$\dot{\epsilon}_t = B\left(\sigma_t^2 - \sigma_t\,\sigma_r + \sigma_r^2\right)^{(n-1)/2}\left(\sigma_t - \frac{\sigma_r}{2}\right)$ $\dot{\epsilon}_r = B\left(\sigma_t^2 - \sigma_t\,\sigma_r + \sigma_r^2\right)^{(n-1)/2}\left(\sigma_r - \frac{\sigma_t}{2}\right)$ $\dot{\epsilon}_a = -(\dot{\epsilon}_r + \dot{\epsilon}_t)$

in which the lateral displacement δ begins to grow without an increase in load P, is augmented by the criterion

$$\frac{d\delta}{dt} \Rightarrow \infty \tag{2.71}$$

in which the lateral velocity becomes infinite.

Numerous creep buckling theories have been devised based on these two criteria. They allow the critical lifetime to be computed as a function of load, slenderness ratio, initial eccentricity and mechanical properties of the material (Refs. 2-17 and 2-18).

A simple example to illustrate the concept of creep buckling is that of the frame shown on Fig. 2-18 in which the concept of a creep hinge described by

$$\dot{\theta} = \left(\frac{M}{M_c}\right)^n \tag{2.72}$$

is used.

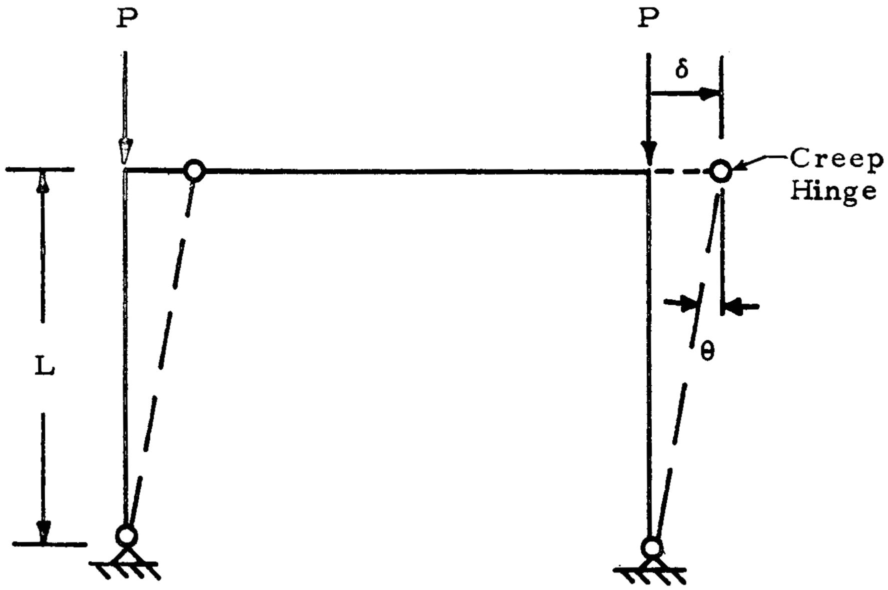

Fig. 2-18 - Frame with Creep Hinge

The lateral velocity is

$$\dot{\delta} = \dot{\theta} L \tag{2.73}$$

The bending moment in the creep hinge is

$$M = P \delta \tag{2.74}$$

The differential equation for $\dot{\delta}$ is given by substituting Eqs. (2.73) and (2.74) into Eq. (2.72),

$$\frac{\dot{\delta}}{L} = \left(\frac{P\delta}{M_c}\right)^n \tag{2.75}$$

With the initial condition

$$\delta\Big|_{t=0} = \delta_0 \tag{2.76}$$

the solution is given by

$$\frac{1}{\delta_o^{n-1}} - \frac{1}{\delta_n^{n-1}} = (n-1) L \left(\frac{P}{M_c}\right)^n t \tag{2.77}$$

The critical time is reached with δ becomes infinite

$$t_{cr} = \frac{\delta_o}{(n-1)L} \left(\frac{M_c}{P\delta_o}\right)^n \tag{2.78}$$

Results for the creep buckling of two other structural systems are given in Tables 2-5a and 2-5b.

The creep buckling of idealized columns assuming an H-section and pin-ended boundaries has been the subject of a number of investigations (Refs. 2-22 through 2-26 and 2-4). The most popular approach is to assume an initial imperfection in sinusoidal form and expand the deformation as Fourier series.

Table 2-5a

CREEP BUCKLING OF BAR WITH "CREEP HINGE" (REF. 2-20)

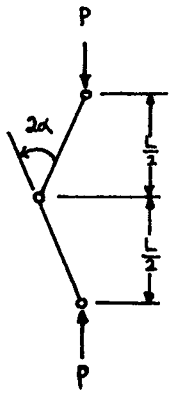	CREEP HINGE 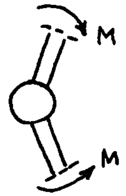
INITIAL DEVIATION FROM STRAIGHT LINE DEFLECTION AT $t = 0$ DEFLECTION AT t	$\phi = 2\alpha_0$ $\phi^{(i)} = 2\alpha_i - 2\alpha_0$ $\qquad \alpha_i = \dfrac{\alpha_0}{1 - \frac{P}{P_E}}$ $\phi^{(c)} = 2\alpha - 2\alpha_0$
DEFINITIONS: EULER BUCKLING LOAD STRAIN RATE ELASTIC STRAIN	$P_E = \dfrac{4 M_e}{L}$ $\dot{\phi}_n = (M/M_n)^n$ $\phi_e = M/M_e$
DIFFERENTIAL EQUATION FOR $\alpha(t)$ $\dfrac{d\alpha}{dt}\left[2 - \dfrac{PL}{2M_e}\cos\alpha\right] = \left(\dfrac{PL}{2M_n}\right)^n \sin^n\alpha$	
CRITICAL TIME WHEN α APPROACHES INFINITY $t_c = 2\left(\dfrac{2M_n}{PL}\right)^n \dfrac{1 - \frac{P}{P_E}}{n-1}\,\alpha_i^{1-n}$	

Table 2-5b

CREEP BUCKLING OF A SIMPLY SUPPORTED RECTANGULAR PLATE (REF. 2-21)

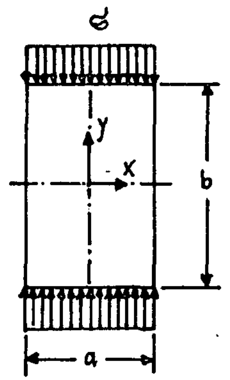

REAL PLATE — EQUIVALENT SANDWICH PLATE

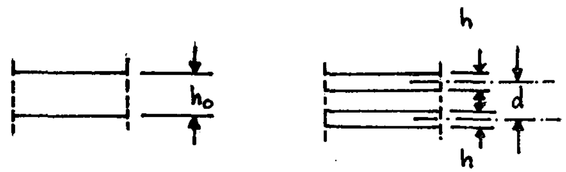

$$d = \frac{h_o}{\sqrt{3}} \quad \text{for } n = 1 \qquad d = \left(\frac{n}{2n+1}\right)^{\frac{n}{n+1}} h_o$$

INITIAL DEVIATION FROM PLANE $\quad w = w^{(o)} \cos\alpha \cos\beta \qquad \alpha = \frac{\pi x}{a}, \; \beta = \frac{\pi y}{b}$

DEFLECTION AT $t=0 \quad w(t=0) = w^{(i)} \cos\alpha \cos\beta \qquad w^{(i)} = w^{(o)} \frac{\sigma_E}{\sigma_E - \sigma}$

DEFLECTION AT $t \quad w(t) = w^{(c)}(t) \cos\alpha \cos\beta$

DEFINITIONS:

EULER BUCKLING STRESS	$\sigma_E \approx 3.6\, E\left(\frac{h_o}{a}\right)^2$	
STRAIN RATE	$\dot{\epsilon}_n = k\,\sigma^n$	n, k = material constants
EULER STRAIN	$\epsilon_E = \sigma_E / E$	
EULER TIME	$t_E = \epsilon_E / \dot{\epsilon}_n$	

DIFFERENTIAL EQUATION FOR $w(t)$ HAS SOLUTION

$$\frac{t}{t_E}\,\frac{\sigma_E}{\sigma_E - \sigma} = c_1 \ln \frac{\bar{w}^{(c)2}\left(c_2 + \bar{w}^{(i)2}\right)}{\bar{w}^{(i)2}\left(c_2 + \bar{w}^{(c)2}\right)} \qquad \bar{w}^{(i)} = \frac{w^{(i)}}{d} \qquad \bar{w}^{(c)} = \frac{w^{(c)}}{d}$$

CRITICAL TIME, WHEN w APPROACHES INFINITY

$$\frac{t_{crit}}{t_E}\,\frac{\sigma_E}{\sigma_E - \sigma} = c_1 \ln\left[1 + c_3\left(\frac{h_o}{w^{(i)}}\right)^{n-1}\right]$$

n	c_1	c_2	c_3
3	.366	1.69	.564
3 *)	.368	1.26	.420
5	.172	1.67	.185
7	.111	1.38	.0511

*) including the effect of shearing stress

This approach leads to values for t_{cr} if certain assumptions for n (i.e., n=3, 5, 7, etc.) are made. No closed form solutions for other than n=odd integers have been obtained.

2.8 NUMERICAL EXAMPLES

Several numerical examples are presented to demonstrate some of the principles discussed in the previous sections.

Example 1: Determine the total strain over a period of time for Rene' 41 at 1500°F, using the material law of Eq. (2.17). Given are the intercept strains as shown on Table 2-6.

Table 2-6
INTERCEPT STRAINS (REF. 2-27)

Stress (psi)	ϵ_o (in./in.)
35,000	.00175
39,500	.0020
55,000	.0030
55,000	.0040
60,000	.0045

These strain values include the elastic component. From these data Fig. 2-19 is constructed.

The parameters in Eq. (2.17) follow from Eq. (2.18) through (2.20)

$$\left(\frac{.78 \times 10^{-3}}{.3 \times 10^{-3}}\right) = \left(\frac{20 \times 10^{3}}{10 \times 10^{3}}\right)^{m}$$

$$m = \frac{\ln 2.6}{\ln 2.0} = \frac{.955}{.693} = 1.38$$

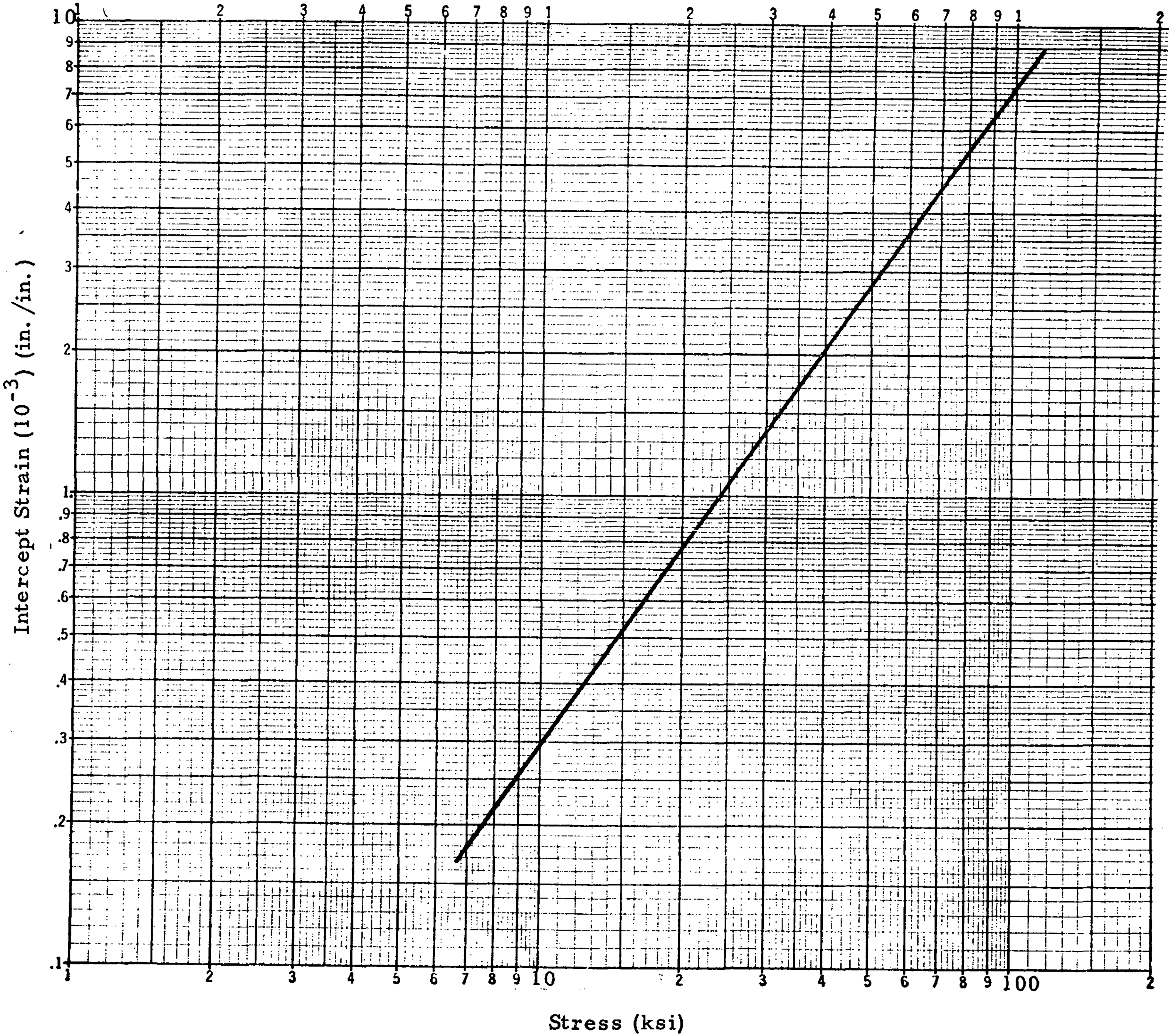

Fig. 2-19 - Intercept Strain - Rene' 41 at 1500°F

$$C_1 = \frac{\epsilon_o}{\sigma^m} = \frac{.3 \times 10^{-3}}{(10{,}000)^{1.38}} = \frac{.3 \times 10^{-3}}{3.35 \times 10^5} = 8.95 \times 10^{-10}$$

The other two constants are determined from a Larson-Miller master creep curve, where the parameter P according to Eq. (2.2) is

$$P = (T + 460)\ (20 + \log t) \times 10^{-3}$$

In Table 2-7 these data for ϵ = 0.2% creep at T = 1500°F are given for various stress levels.

Table 2-7
CREEP DATA FROM MASTER CURVE (REF. 2-27)

σ (psi)	P	log t	t (hr)	$\dot{\epsilon}$ =.2%/t (in./in./hr)
40,000	42	1.430	26.95	7.4×10^{-5}
30,000	43	1.940	87.20	2.3×10^{-5}
20,000	45	2.960	913.0	2.2×10^{-6}
15,000	45.5	3.220	1662.0	1.2×10^{-6}
10,000	46.0	3.465	2920.0	6.85×10^{-7}

Using Eqs. (2.23) through (2.25) the parameters are

$$\left(\frac{7.4 \times 10^{-5}}{2.2 \times 10^{-6}}\right) = \left(\frac{40{,}000}{20{,}000}\right)^n$$

$$n = \frac{\ln 33.6}{\ln 2} = \frac{3.515}{.694} = 5.07$$

$$C_2 = \frac{7.4 \times 10^{-5}}{(40{,}000)^{5.07}} = \frac{7.4 \times 10^{-5}}{2.24 \times 10^{23}} = 3.3 \times 10^{-28}$$

The equation for the strain at any time t for Rene' 41 at 1500°F is

$$\epsilon = 8.95 \times 10^{-10} \sigma^{1.38} + 3.3 \times 10^{-28} \sigma^{5.07} t \qquad (2.79)$$

Equation (2.79) is evaluated on Fig. 2-20 below for σ=35 ksi.

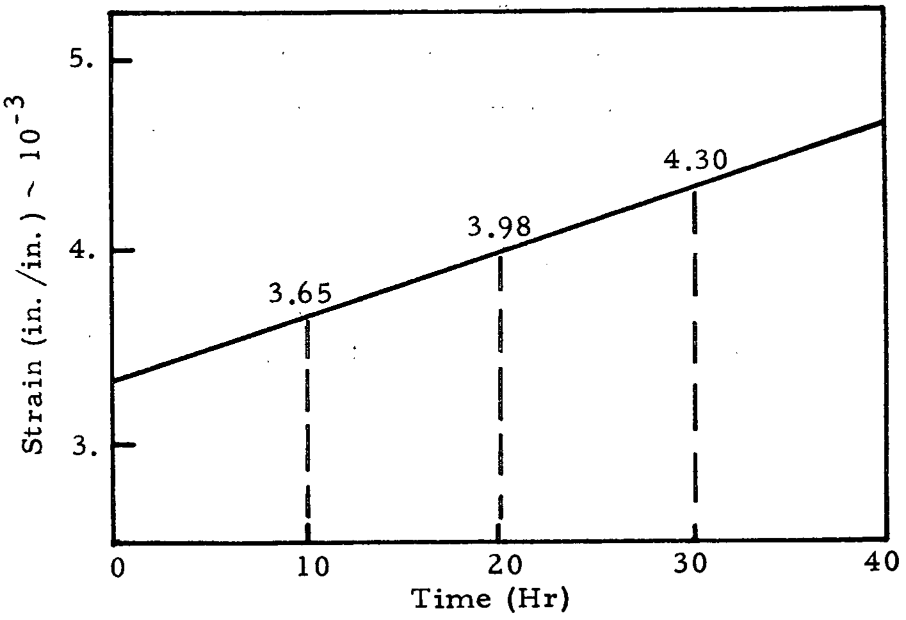

Fig. 2-20 - Rene' 41 at T = 1500°F and σ = 35 ksi

Example 2: Determine the creep parameters for Ti-6Aℓ-4V, using Eqs. (2.24) and (2.25). Data from Ref. 2-28 show the creep curves given in Fig. 2-21. From this figure the following values can be extracted:

at

$$T = 750^{\circ}F, \quad \sigma = 65{,}000 \text{ psi},$$

$$\dot{\epsilon}_1 = \frac{\Delta\epsilon_1}{\Delta t_1} = \frac{.05\%}{80} = 6.25 \times 10^{-6}/\text{hr}, \quad \text{and}$$

at

$$T = 750^{\circ}F, \quad \sigma = 50{,}000 \text{ psi},$$

$$\dot{\epsilon}_2 = \frac{\Delta\epsilon_2}{\Delta t_2} = \frac{.05\%}{130} = 3.85 \times 10^{-6}/\text{hr} \quad .$$

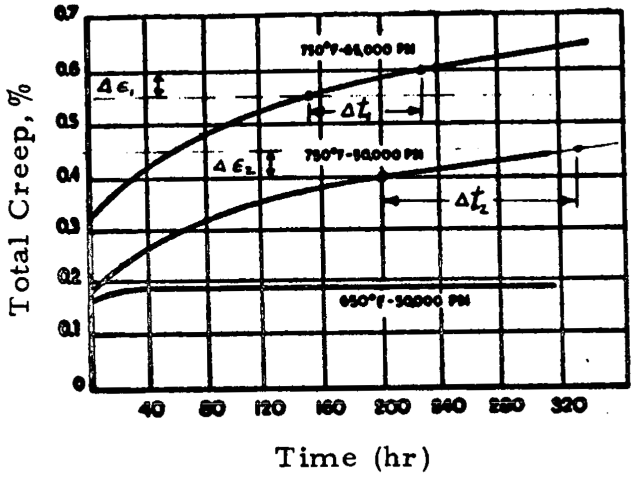

Fig. 2-21 - Creep Curves of Annealed MST 6Aℓ-4V

The parameters of Eq. (2.26) are then

$$\frac{\dot{\epsilon}_1}{\dot{\epsilon}_2} = \left(\frac{\sigma_1}{\sigma_2}\right)^n$$

$$n = \frac{\ln\left(\frac{\dot{\epsilon}_1}{\dot{\epsilon}_2}\right)}{\ln\left(\frac{\sigma_1}{\sigma_2}\right)} = \frac{\ln\left(\frac{6.25}{3.85}\right)}{\ln\left(\frac{65}{50}\right)} = \frac{.483}{.262} = 1.84 \approx 2$$

$$K = \frac{\dot{\epsilon}}{\sigma^n} = \frac{3.85 \times 10^{-6}}{(5.10^4)^2} = 1.5 \times 10^{-15}$$

To determine β in Eq. (2.27) one other data point is needed:

at $T = 800^\circ F\ (426^\circ C)$, $\sigma = 50{,}000$ psi,

$$\dot{\epsilon}_1 = \frac{(.50 - .26)\%}{40} = \frac{.24\%}{40} = 6. \times 10^{-5}/\text{hr}$$

Then β is computed from

$$\beta = \frac{\ell n\left(\frac{\dot{\epsilon}_1}{\dot{\epsilon}_2}\right)}{T_1 - T_2} = \frac{\ell n\left(\frac{6 \times 10^{-5}}{3.85 \times 10^{-6}}\right)}{(426^{\circ}C - 398^{\circ}C)} = \frac{\ell n\ 15.6}{28} = .0983/^{\circ}C$$

Example 3: Determine the service life of a Ti-6Aℓ-4V bar with axial tension load, $\sigma = 50$ ksi, at elevated temperature, $T = 750^{\circ}F$ ($398^{\circ}C$).

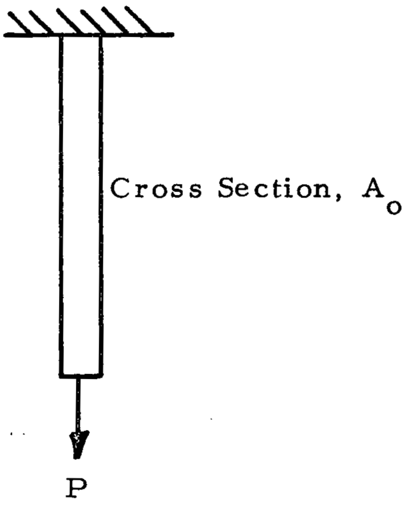

Fig. 2-22 - Axial Bar

From Eq. (2.41) it follows for $\mu = 1.0$ that the lifetime is

$$t_\ell = \frac{1}{2 \times (5 \times 10^4)^2 (1.5 \times 10^{-15})} = 133{,}300 \text{ hr} .$$

This service life is large due to the assumption that $A/A_o = 0$ at $t = t_\ell$. Actually, $A/A_o \approx .95$ would be a minimum.

Example 4: Determine the service life of the bar in Example 3 when σ = 50 ksi, but T = 750°F ±25°F, considering a normal distribution of the temperature fluctuations. Then

$$\Delta T = 50^{\circ}F\ (28^{\circ}C)$$

and the deviation is

$$t = \frac{\Delta T}{2} = \frac{28}{2} = 14^{\circ}C$$

and μ(t) according to Eq. (2.32) is

$$\mu = e^{\frac{(0.0983)^2 (14)^2}{2}} = e^{0.954} = 2.6$$

The lifetime is

$$t_{\ell} = \frac{133,300}{2.6} = 51,300 \text{ hr} .$$

This is considerably less than at constant temperatures.

Example 5: Determine the time to creep so that the total tip deflection of a tip-loaded cantilever beam is twice the elastic tip deflection. The material is Ti-6Aℓ-4V.

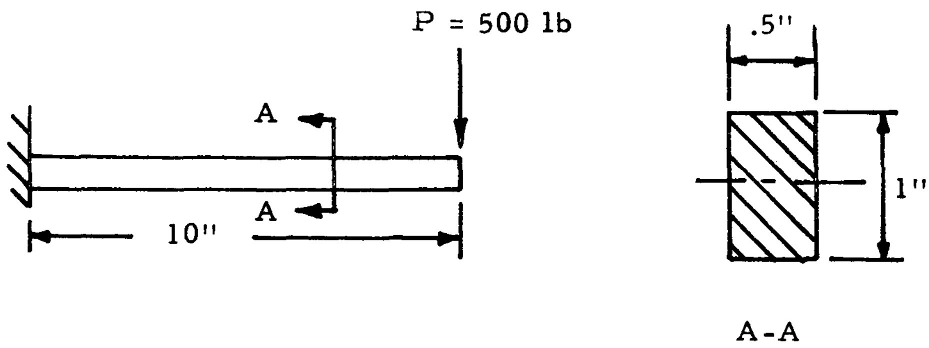

Fig. 2-23 - Cantilever Beam

Further data are: $T = 750^\circ F$ ($398^\circ C$), $E_T = .76E = .76\ (16 \times 10^6) = 12.16 \times 10^6$ psi, and $I = .5 \times 1^3/12 = .0417$ in.^{4}. The elastic tip deflection is from Eq. (2.61)

$$\delta_e = \frac{500 \times 10^3}{3 \times (12.16 \times 10^6)\ (.0417)} = .3285 \text{ in.}$$

From Fig. 2-13

$$I_n = \frac{2(2)}{2(2)+1} \quad \frac{.5(1)^2}{4} \quad \left(\tfrac{1}{2}\right)^{\frac{1}{2}} = .0707 \ .$$

With the creep deflection given, Eq. (2.61) can be solved for the lifetime t_ℓ,

$$t_\ell = \frac{\delta_c}{\left(\frac{PL}{I_n}\right)^n \frac{L^2}{n+2}\ \mu\ K_m} \tag{2.80}$$

For $\mu = 1.0$ (no temperature variation) the lifetime is

$$t_\ell = \frac{.3285}{\left(\frac{5 \times 10^3}{.0707}\right)^2 \frac{10^2}{4}\ (1.5 \times 10^{-15})} = 1{,}750 \text{ hr}$$

For $\mu = 2.6$ (a temperature variation of $\pm 25^\circ F$)

$$t_\ell = \frac{1750}{2.6} = 673 \text{ hr} \ .$$

2.9 CREEP ANALYSIS PROGRAM

The Creep Analysis program is a digital computer program which is designed to determine the creep damage for a variable uniaxial loading condition. The program will determine the time to rupture, fracture of life expended, creep rate, creep strain and total creep strain based on the given material data. Three theories of creep deformation are included to predict the total creep strain for the load-temperature-time history. These are:

- Time Hardening Theory (Eq. (2.8))
- Strain Hardening Theory (Eq. (2.9)), and
- Pao-Marin Theory (Eq. (2.12)).

Plots of creep strain versus time are constructed for these three methods of analysis. The program is written in FORTRAN V language and configured for execution on the Univac 1108, (see listing in Appendix B).

The primary difference between the time hardening and the strain hardening theories is the method used for strain accumulation. For the analysis of the transient creep range the plots of creep strain versus time are input in table form for each stress-temperature level. Interpolation is used to trace the strain plot over the time period, Δt. Both theories sum the change in strain values during the time intervals at the various stress levels to arrive at the total creep strain value

$$\epsilon = \sum_{i=1}^{n} \Delta\epsilon_i \quad \text{at} \quad \Delta t_i, \ \sigma_i \ .$$

In the change from one stress level to another the time-hardening method starts the new time interval at the ending time values of the preceding stress level. The strain hardening starts the time interval at the same strain level that was reached at the end of the preceding stress level. These two methods were illustrated in Fig. 2-11.

The Pao-Marin theory is an analytical representation of the creep strain-time curve by determining parameters based on the material data. Parameters are computed for both the transient and minimum rate creep strain regions. The strain-hardening method of strain accumulation is used.

The other required material input data consist of master creep curves such as the Larson-Miller or Manson-Haferd parameters. If both creep rupture and percent creep strain curves are input, the service life expended and total creep strain are computed. The rupture data are required for the service life analysis and the percent creep strain data are required for the creep strain calculations. If only one set of data is required or available, the specific analysis will be performed and the other bypassed. A maximum allowable strain value can also be specified that will terminate the program when the total creep strain exceeds this value. This is useful in certain cases where excessive deformation may be more critical than rupture time predictions.

The creep parameter data, both rupture and percent creep, are described by inputting specific stress values and their corresponding parameter value in table form, starting with the maximum stress value. The program will interpolate between these values in subroutine GIR1 to determine the appropriate parameter for the given stresses.

As shown in Fig. 2-24 the stress values $\sigma_1, \sigma_2, \sigma_3$, etc., and their corresponding parameter values P_1, P_2, P_3, etc. would be input. For a specified stress value f the program interpolates logarithmicly to determine P. Using P, the time to rupture or time to creep to a given percent strain can be determined. For the creep parameter data the appropriate percent creep strain, such as 0.2, 0.5, 1.0% creep, must also be specified for the creep rate computations. The Larson-Miller master creep curve for 0.2% creep strain for Rene' 41 was input in the sample problem in Appendix B.

The appropriate master parameter curve equation must also be in the program for the correct solution. These expressions and their location in the program are noted by comment cards, (see program listing in Appendix B). If different parameters are used as input data the correct parameter equation must be input into the program deck. The original deck is set up with the Manson-Succop parameter for the creep rupture data and the Larson-Miller parameter for 0.2% creep strain for Rene' 41 data. These parameter expressions are noted in the program deck.

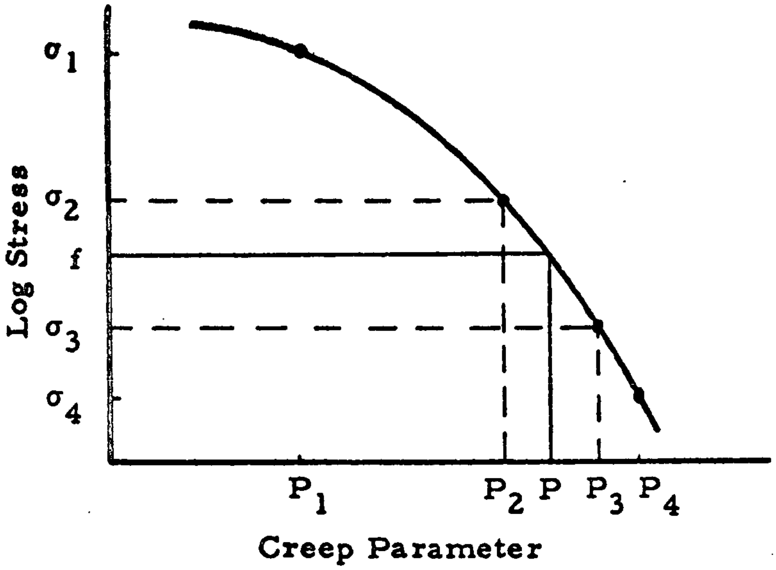

Fig. 2-24 - Master Creep Curve

A stress level, temperature and time period make up a load case. A series of these is constructed to represent the load history of the structure to be analyzed. The stress-temperature-time history is idealized as shown in Fig. 2-25.

The time to rupture, fraction of life expended, creep rate and creep strain are determined for each of the load conditions. If the stress level falls outside the range of stress values given for the parameters a message is printed and the program continues to the next load condition. A running sum of the life expended and the total creep strain is determined. If the creep strain sum exceeds the maximum strain specified, the program terminates. A service life margin is computed based on the sum of the fraction parts

$$\text{Margin} = \frac{1}{\sum (t/t_r)} - 1$$

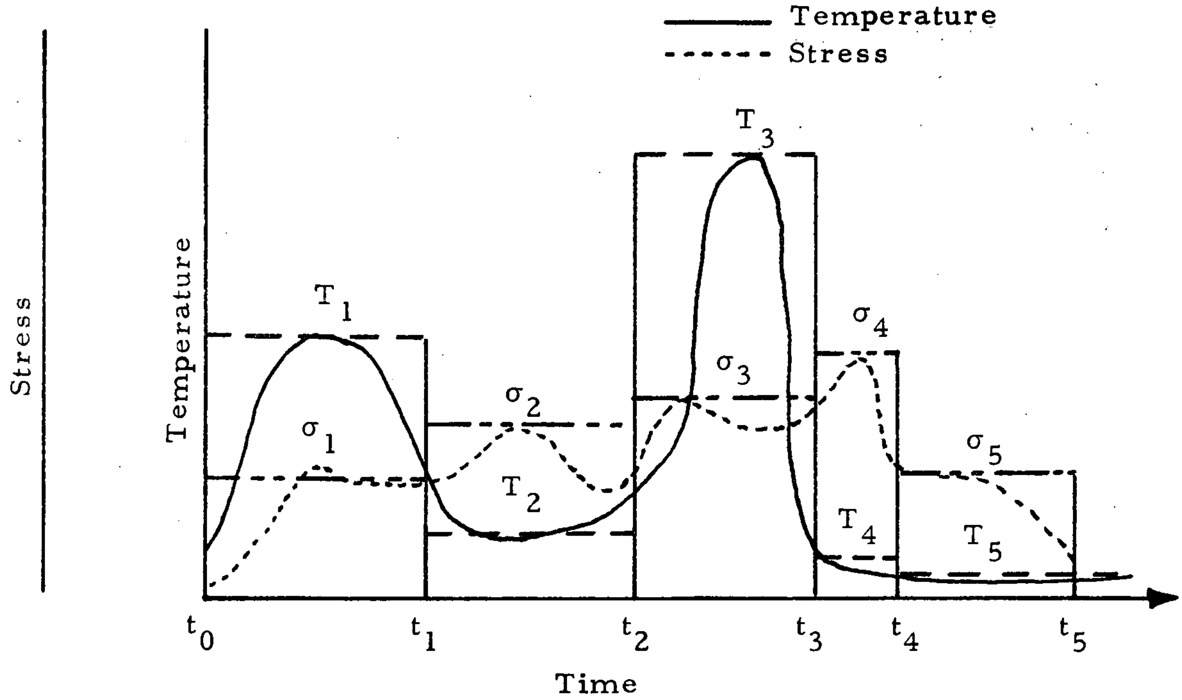

Fig. 2-25 - Idealized Stress-Temperature-Time History

where t is the time period and t_r is the time to rupture at σ. If a negative margin occurs the program will terminate. Full output up to the point of termination is given if the program is stopped before all load conditions have been processed.

The program solution is carried out in two main DO loops. The first loop (DO 131 L=1, 3), specifies the theory to be used.

L = 1 Time Hardening Theory
L = 2 Strain Hardening Theory
L = 3 Pao-Marin Theory

The second primary DO loop (DO 130 I=1, NS), is inside the first loop and controls the calculations for all of the specified NS load-temperature-time conditions.

The program output is given for a sample problem in Appendix B and should be self-explanatory with the proper headings. The life expected value that is calculated is based on cycling the prescribed load condition and may not be appropriate for each problem. The corresponding factor of safety should also be used with discretion. It is based on the specified life required and the fractional part of the life that is used up and the maximum temperature that occurs in the load history.

The program listing and a sample problem using Rene' 41 data are given in Appendix B. Plots of creep strain versus time are generated for each of the three strain theories. In the final plot all three theories are compared. The time hardening, strain hardening and Pao-Marin plots are denoted by the plotting symbols T, S and P, respectively.

2.10 REFERENCES

2-1. Van Vlack, Materials Science for Engineers, New York, 1970.

2-2. Larson, F. R., and J. Miller, Trans. ASME, 174, July 1952.

2-3. Penny, R. K., and D. L. Marriott, Design for Creep, McGraw-Hill, London, 1972.

2-4. Odqvist, F. K. G., Mathematical Theory of Creep, Oxford Press, 1966.

2-5. Hencky, H., Z. angew. Math. Mech. 5, 115, 1925.

2-6. Odqvist, F. K. G., Z. agnew. Math. Mech. 13, 360, 1933.

2-7. Robinson, E. L., Trans. ASME, 74, 777, 1952.

2-8. Hoff, N. J., J. Appl. Mech., 20, 105, 1953.

2-9. Kachanov, L. M., Izv. Akad. Nauk, USSR, 8, 26, 1958.

2-10. Parkus, H., Recent Progress in Applied Mechanics, Wiley, New York, 1967, p. 391.

2-11. Freudenthal, A. M., Trans. New York Academy of Science, 19, (4), 1957.

2-12. Freudenthal, A. M., J. Appl. Phys., 25 (9), 1954.

2-13. Hult, J., and U. Edstam, Advances in Creep Design, Wiley, New York, 1971.

2-14. Marin, J., J. Franklin Institute, 226, 1938, pp. 645-657.

2-15. Finnie, I., and W. R. Heller, Creep in Engineering Materials, McGraw-Hill, New York, 1959.

2-16. Marin, J. (Editor), Materials Engineering Design for High Temperatures, Pennsylvania State University, July 1958.

2-17. DeVeubeke, B. F., High Temperature Effects in Aircraft Structures, AGARDograph No. 28, Pergamon Press, New York, 1958.

2-18. Hoff, N. J., J. Roy. Aero. Soc., 58, (517), 1954, p. 1.

2-19. Shanley, F. R., Weight-Strength Analysis of Aircraft Structures, Dover, New York, 1960.

2-20. Hult, J. A. H., Creep in Engineering Structures, Blaisdell, Waltham, Mass., 1966.

2-21. Hoff, N. J., et al., Advances in Creep Design, Wiley, New York, 1971.

2-22. Flügge, W., Viscoelasticity, Blaisdell, Waltham, Mass., 1967.

2-23. deVenbeke, F. B., High Temperature Effects in Aircraft Structures, Pergamon Press, London, 1958.

2-24. Carlson, R. L., and W. W. Breindel, Creep in Structures, Springer, Berlin, 1962, p.274.

2-25. Lempiere, B. M., Creep in Structures, Springer, Berlin, 1962, p. 291.

2-26. Zyczkowski, M., Creep in Structures, Springer, Berlin, 1962. p. 307.

2-27. Gluck, J. V., and J. W. Freeman, "Effect of Creep-Exposure on Mechanical Properties of Rene' 41," ASD TR 61-73, August 1961.

2-28. Metallic Materials and Elements for Aerospace Vehicle Structures, MIL-HDBK-5B, Department of Defense, Washington, D. C., September 1971.

Section 3
FATIGUE

Fatigue analyses must be performed when a structural design includes a requirement for a reusable structure with a long lifetime or for a structure which must survive a significant number of fluctuating load cycles. While the life characteristics of fatigue sensitive structures should be verified by tests, it is also necessary to have the capability to predict the service life with reasonable accuracy during the design phase. Elevated temperature with the associated problems of creep, thermal stresses, temperature and time dependent material properties, only complicate the lifetime predictions.

The elevated temperature fatigue problem can be approached in a number of different ways depending on the magnitude of the loads, the temperature range, and the number of load cycles. Three of the more important approaches to fatigue analysis are:

- Low-cycle fatigue analysis
- Fatigue in the creep range
- Fatigue below the creep range

Each of these approaches is discussed in the following paragraphs preceded by comments on applying factors of safety to fatigue design.

3.1 FATIGUE – FACTOR OF SAFETY

It is well known that the fatigue strength of materials exhibits considerable scatter and can best be characterized in statistical terms. Unfortunately, few materials have been subjected to the vast amount of testing required to quantify the statistical properties of the fatigue strength. The engineer is left with a need for design criteria which will result in a reliable, fatigue-resistant structure without explicitly knowing the statistical characteristics of the material properties.

Static strength of materials as given in MIL-HDBK-5B have a probabilistic basis:

> A basis — The A value is the value above which at least 99% of the population is expected to fall, with a confidence of 95%.
>
> B basis — The B value is the value above which at least 90% of the population is expected to fall, with 95% confidence.

Fatigue data presented in MIL-HDBK-5 are not considered design allowables. Instead, fatigue data are presented as typical properties of the material. Two kinds of figures are used: (1) individual S-N curve, and (2) constant-life diagrams that can be constructed from a family of S-N curves. These data are, therefore, not suitable for estimating survival probability. Other means are needed to establish a factor of safety (FS) or probability value to associate with lifetime predicted from the curves.

Inspection of typical S-N curves which show data points or scatter band indicate that for a given stress level the spread in the lifetime can be quite large, whereas for a given lifetime, the spread in stress is much smaller. Figure 1 of Ref. 3-5 shows a set of probability S-N curves for 7075-T6 aluminum. This curve is reproduced here as Fig. 3-1. At an alternating stress of 30 ksi and a probability of failure of 0.01, the value of N is 1.5×10^6; for a probability of failure of 0.99, N is 1.5×10^8. The above represents a life factor of 100. Between the 0.01 and the 0.50 probability curves there is a life factor of 10. These large values of the life factor occur at a low stress level near the endurance limit. At 50 ksi alternating stress, the life factor is only 1.7 between the 0.01 and the 0.50 probability curves.

Inspection of the probability curves reveals that at a specified lifetime, the spread in the fatigue strength is significantly less. At 1.5×10^7 cycles the ratio between the 0.50 probability fatigue strength and the 0.01 probability strength is 1.25, and at 3×10^5 cycles the ratio is about 1.1.

Results from fatigue tests of aircraft components are similar to the results for fatigue specimens, except that the scatter is even larger for the

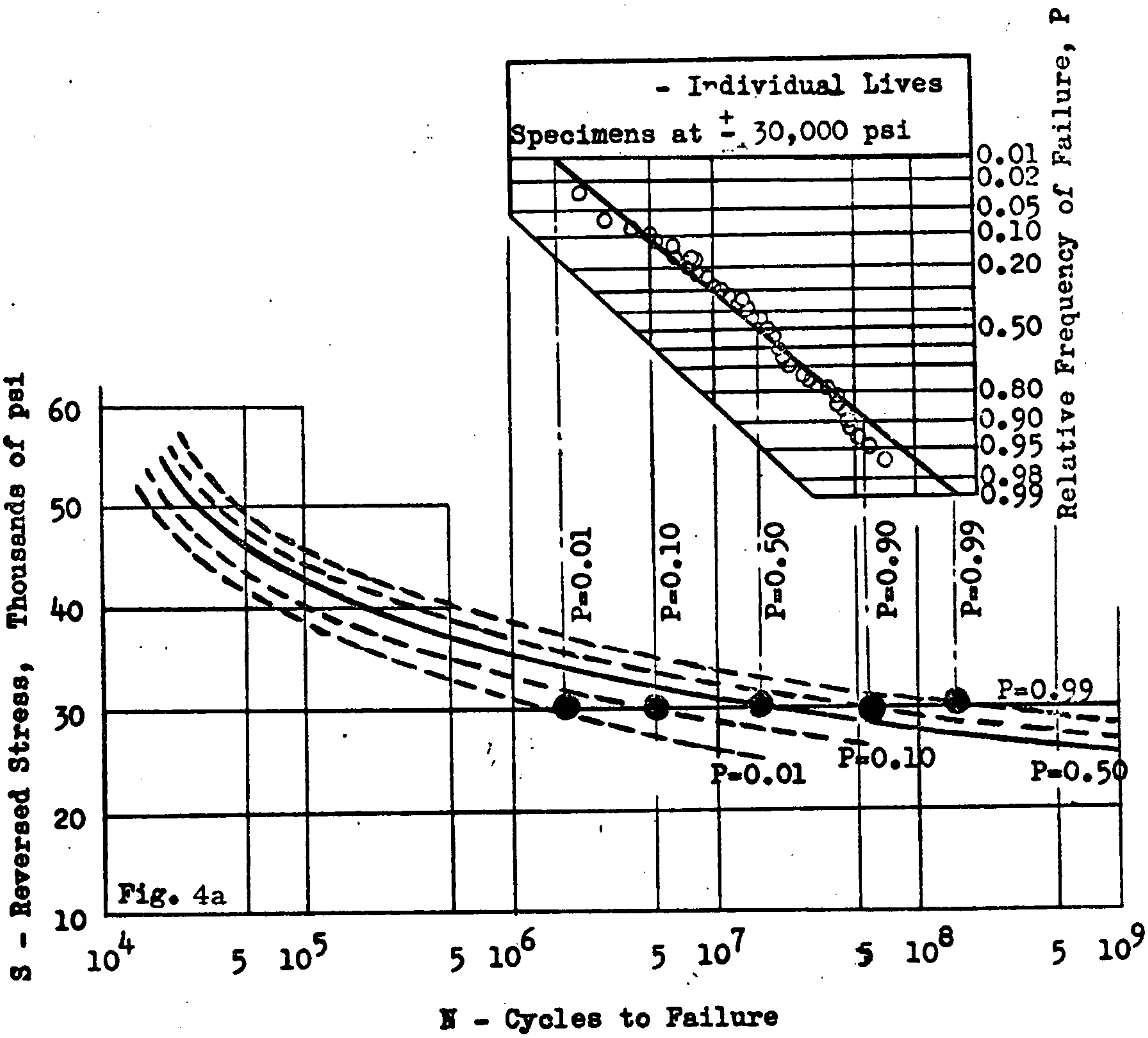

Fig. 3-1 - S-N Fatigue and Probability Curves for 7075 Aluminum Alloy (Ref. 3-5) component tests. Figure 3-2 (Ref. 3-7) is based on a large number of component tests from many aircraft programs. Figure 3-2 can be used for preliminary estimates of the maximum allowable ultimate design tension stress for typical aircraft structures made from aluminum, steel, and titanium alloys. The curves indicate the scatter in spectrum fatigue tests and constant amplitude fatigue tests of aircraft components. The 50% probability curve is based on achieving a fatigue quality comparable to previous aircraft such as the P3V, Electra, F104, and Model 286 helicopter. The use of design stresses higher than the 50% probability design curve must be accompanied by an improvement in fatigue quality. Fatigue problems are less likely to occur if design stresses below the 50% probability design curve are used.

The maximum allowable ultimate design tension stress (mean plus alternating) is expressed as a percentage of the ultimate strength of the material. The 50% probability design curve is considered to provide a best estimate of the allowable stresses that can be used for the required number of flights or cycles.

Since the S-N curves of Figs. 3-1 and 3-2 are typical of the majority of metallic materials, the following conclusions can be drawn:

1. Fatigue strength data are subject to a large scatter band even neglecting complicating factors such as temperature, stress concentrations, random loads, etc.
2. The variability in the fatigue life at a specified stress level is much larger than the variability in the fatigue failure stress at a given lifetime.
3. The scatter in the predicted service life will increase as the applied stress becomes smaller; the scatter becomes extremely large as the applied stress approaches the endurance limit.
4. Additional data are required for most materials before an FS can be based on the statistical scatter of the fatigue strength.

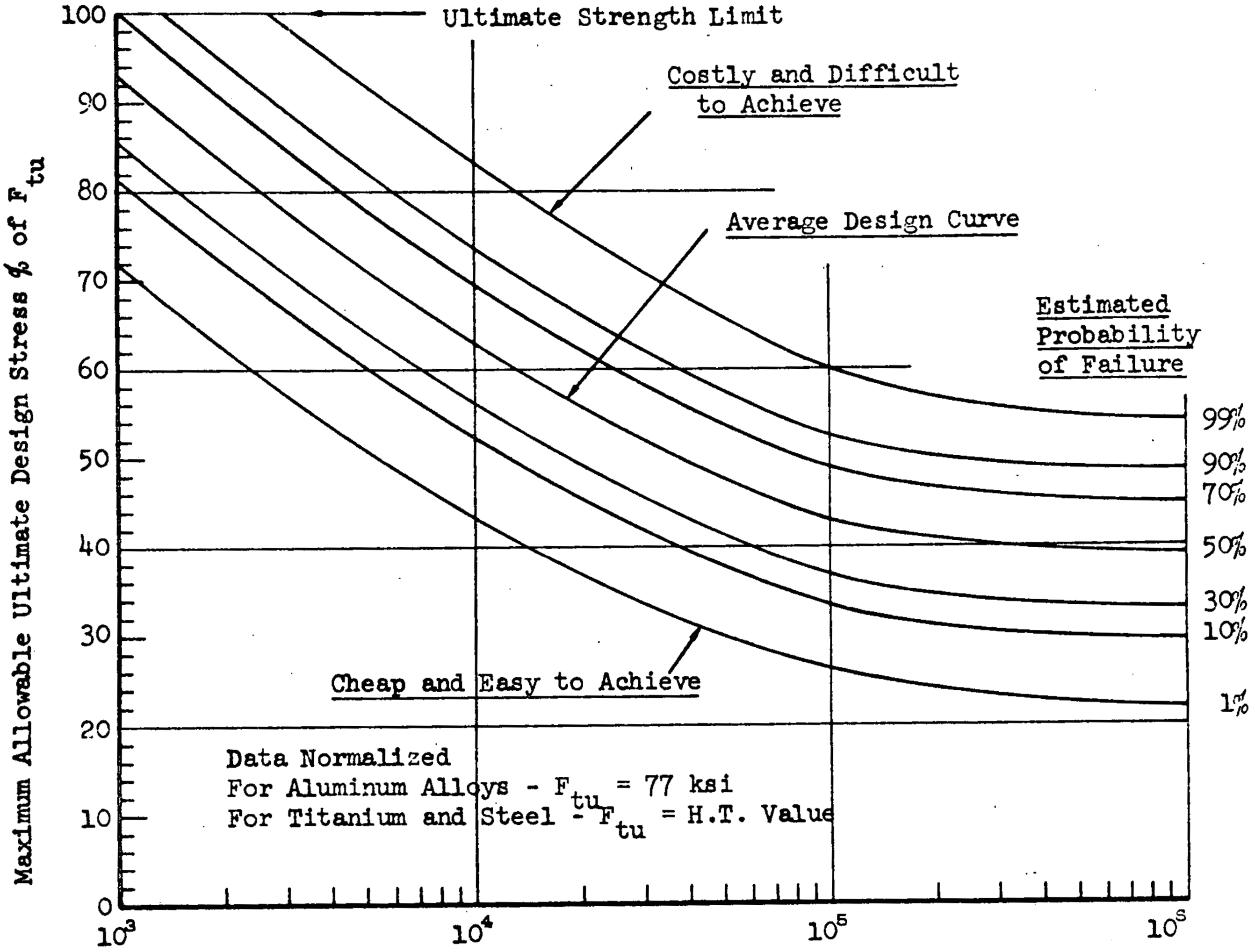

Fig. 3-2 - Flights or Cycles to Failure

3.2 LOW-CYCLE FATIGUE

When parts are subjected to frequent applications of near-limit loads during the service life of a structure, failure can occur due to high stress-low cycle fatigue. It is readily apparent from the examination of any typical S-N curve or constant-life fatigue diagram that the number of load applications which can be sustained is relatively low when high loads are involved.

High stress-low cycle fatigue is a phenomenon associated with plastic strain cycling. While failure may not result in one cycle, sufficient damage can accumulate in relatively few cycles to cause rupture. Coffin suggested (Ref. 3-10) an empirical relationship between the range of the plastic strain ($\Delta\epsilon_p$) and the number of cycles to failure (N). The plastic strain range is defined as the difference between the total strain range and the elastic strain range. This is illustrated in Fig. 3-3 for a material being cycled. The plastic strain range is

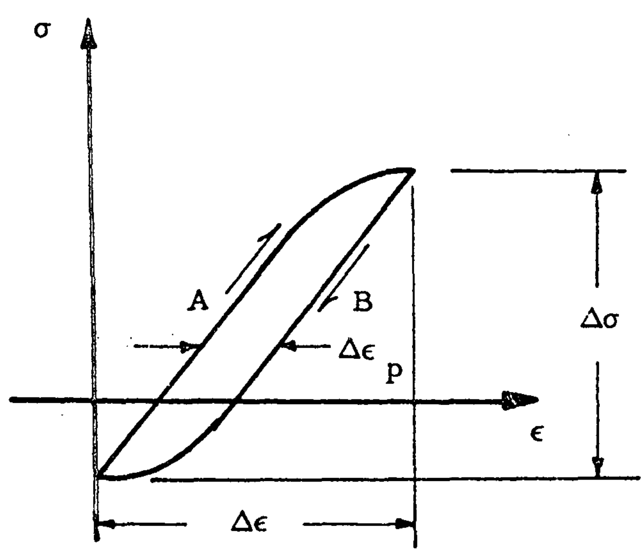

Fig. 3-3 - Cyclic Plastic Strain

$$\Delta\epsilon_p = \Delta\epsilon - \frac{\Delta\sigma}{E} \tag{3.1}$$

where

$\Delta\epsilon$ is the total strain range and $\frac{\Delta\sigma}{E} = \Delta\epsilon_e$, the elastic strain range.

The basic relationship for low cycle fatigue failure is

$$\Delta\epsilon_p = CN^{-\frac{1}{2}} \tag{3.2}$$

where C is a material constant and N is the number of cycles to failure. For many materials the material constant, C, can be found using the elongation, e, corresponding to the ultimate tensile stress, F_{tu}. Letting N = 1/4 cycle at F_{tu} and substituting into the above equation, we have:

$$e = C\,(1/4)^{-\frac{1}{2}} \tag{3.3}$$

or

$$C = e\,(1/4)^{\frac{1}{2}} = \frac{e}{2}$$

Figure 3-4 shows experimental data (Kennedy Ref. 3-11) for some common structural materials which tend to support the empirical relationship.

Equation (3-2) states that failure occurs when

$$\frac{N\,\Delta\epsilon_p^2}{C^2} = 1 \tag{3.4}$$

Equation (3-4) implies that a cumulative damage law exists, but note that it is based on the peak plastic strain in the cycle. This strain can become highly localized. Thus, plastic strain computed from gross properties of a loaded member could give very unconservative results. This supports the often noted situation: Fatigue failures nearly always occur at joints and stress concentrations where the difficulties of analysis are most severe.

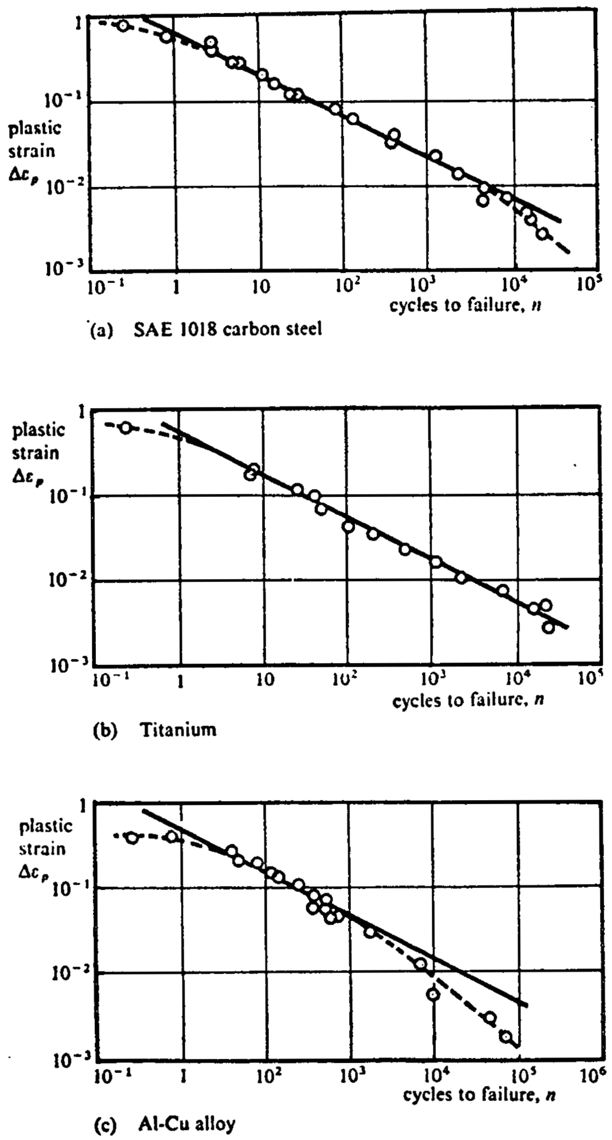

Fig. 3-4 - Experimental Data for Low-Cycle Fatigue (from Ref. 3-11)

The discussion above is brief and is only an introduction to high stress-low cycle fatigue. The next section, 3.3 Fatigue in the Creep Range, discusses low-cycle fatigue in greater detail and relates low-cycle fatigue to thermal fatigue and creep failures at elevated temperatures.

3.3 FATIGUE IN THE CREEP RANGE

When structures are subjected to combined thermal and mechanical stress cycling at elevated temperatures, the mode of fracture can generally be classified as one of two types of failure. If fracture occurs without noticeable deformation it is of the fatigue type, while fracture that is accompanied by noticeable deformation is of the creep type. There are several types of combinations of mechanical and thermal stresses. In the case where both the thermal and mechanical stresses are cyclic and completely reversed the material usually fails without deforming significantly. Whereas in a case where the mechanical stress is constant with a cyclic thermal input and the material is free to elongate, such as a pressurized thick wall cylinder subjected to cyclic temperatures, failure would be by excessive deformation.

In the case of thermal fatigue combined with mechanical mean stress, the stress ratio A is used as a parameter. This is the ratio of the amplitude of the cyclic thermal stress component to the mechanical mean stress, σ_T/σ_m. A simple creep test under steady load and varying temperature corresponds to a zero stress ratio, and an infinite stress ratio corresponds to thermal fatigue under completely reversed strain cycling.

The different combinations of thermal and mechanical fatigue will be discussed in the following paragraphs.

3.3.1 Mechanical Fatigue at Elevated Temperatures

At elevated temperature the fatigue life is greatly affected by the frequency of stress cycling. This is especially true for high stress amplitudes. From the results of Forrest and Tapsell (Ref. 3-15) in Fig. 3-5, the lower frequency stress cycling results in shorter cyclic lives to fracture at the same stress level. For example, at a stress of 19 tons/in^2, the cyclic life time at 10 cpm is 12,000 cycles while the corresponding life at 2000 cpm is 120,000 cycles.

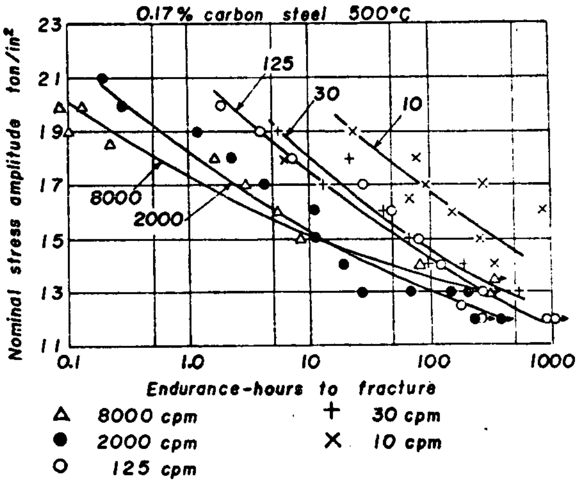

Fig. 3-5 - Fatigue Strength at Various Cycling Speeds (From Ref. 3-13)

Taira (Ref. 3-13) converted the data of Fig. 3-5 into a plot of the plastic strain amplitude versus the log of the number of cycles to fracture, N, Fig. 3-6.

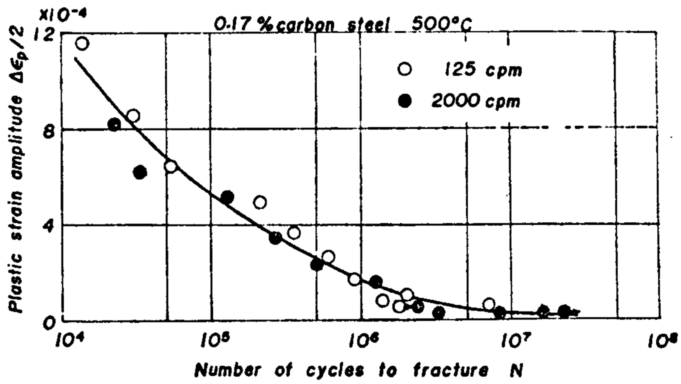

Fig. 3-6 - Plastic Strain Amplitude vs Number of Cycles to Failure

In converting the stress data to plastic strain amplitudes, the dynamic stress-strain curves of Fig. 3-7 were used and fracture time was converted to number of cycles by taking the frequency into account.

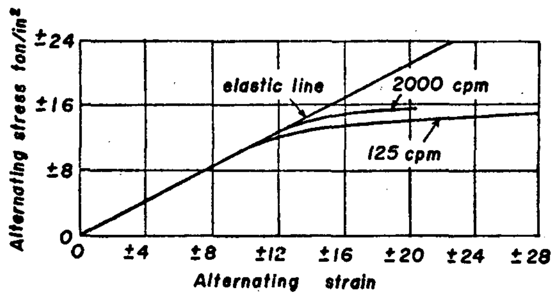

Fig. 3-7 - Dynamic Stress-Strain Curve of 0.17% Carbon Steel at 500°C (From Ref. 3-13)

Based on the data of Fig. 3-6, Taira concluded that the fatigue life at high temperature is strongly dependent on the magnitude of the amplitude of the plastic strain component. Further tests were performed to substantiate this conclusion using other materials. In the range of high strain amplitudes the plastic strain component of the alternating strain was large and the tests results fell on a single curve. In the range of low stress amplitude, where the plastic strain component was small, the cyclic life time was found to be more dependent on the exposure time, and creep was a factor in the failure.

To verify the above conclusions, Taira conducted tests at elevated temperature for the two materials shown in Figs. 3-8 and 3-9. The figures clearly show the divergence in the fatigue life at low strains for the different cyclic rates.

Based on the fact that the log $\Delta\epsilon_p$ - log N is a relatively straight line (Fig. 3-4 of Section 3.2), a relationship between the increment of damage $\Delta\ \phi_f$ caused during one-half cycle of plastic strain $\Delta\epsilon_p$ was derived

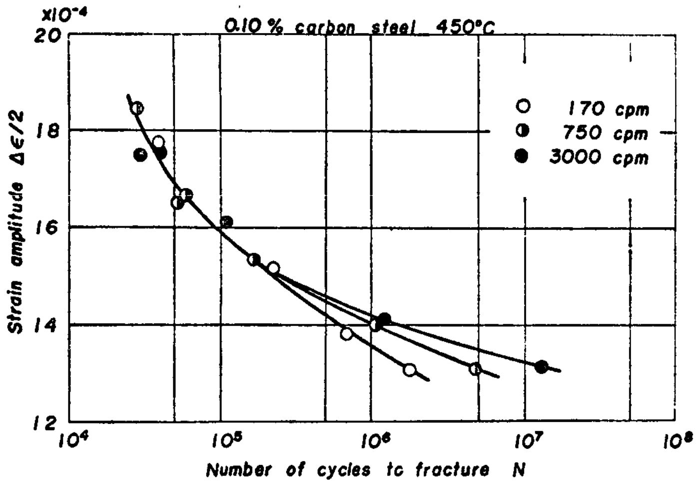

Fig. 3-8 - Strain Amplitude vs Cycles to Fracture for 0.10% Carbon Steel at 450°C (From Ref. 3-13)

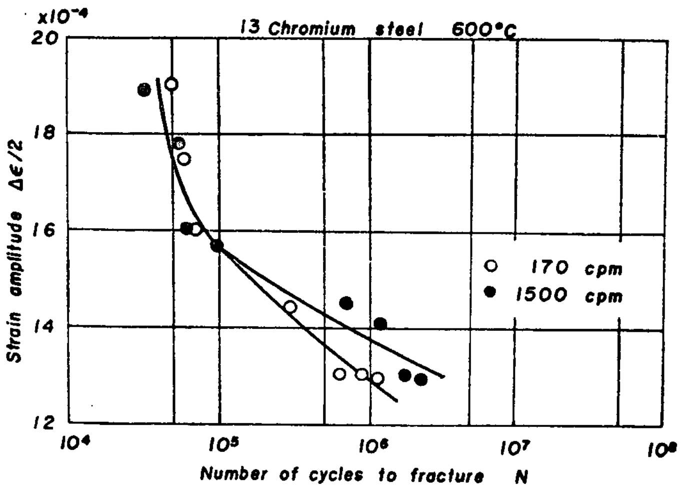

Fig. 3-9 - Fatigue Strength of 13 Chromium Steel at 600°C. Presented in Strain Amplitude vs Number of Cycles to Fracture (From Ref. 3-13)

$$\Delta\phi_f = \lambda (\Delta\epsilon_p)^u \quad (3.5)$$

where λ and u are material constants. It is assumed that failure occurs when the sum of the damage increments reaches a critical value ϕ_o.

$$\phi_o = 2 N \Delta\phi_f \quad (3.6)$$

where N is the number of cycles to failure. From the above two relations the fundamental equation for fatigue at elevated temperature is

$$\Delta\epsilon_p N^{1/u} = (\phi_o/2\lambda)^{1/u} = \text{constant} \quad (3.7)$$

Other results have shown that u is very close to a value of 2. When u = 2 Eq. (3.7) is the same as the equation by Coffin (Ref. 3-10 and Eq. (3-2) of Section 3.2).

3.3.2 Thermal Fatigue

In thermal fatigue the strain amplitude $\Delta\epsilon$ and the cyclic temperature change between the lower temperature level and the upper temperature level are the variables that determine the fracture life.

The stress-strain hysteresis curve for a temperature cycle is shown in Fig. 3-10a and an idealized stress-strain relation for analysis purposes in Fig. 3-10b.

For a simple bar with both ends constrained, the alternating strain induced by the temperature cycle is

$$\Delta\epsilon = \Delta\epsilon_e + \Delta\epsilon_p = \alpha (T_2 - T_1) \quad (3.8)$$

where

$\Delta\epsilon_e$ is the elastic strain component
$\Delta\epsilon_p$ is the plastic strain component
α is the coefficient of thermal expansion.

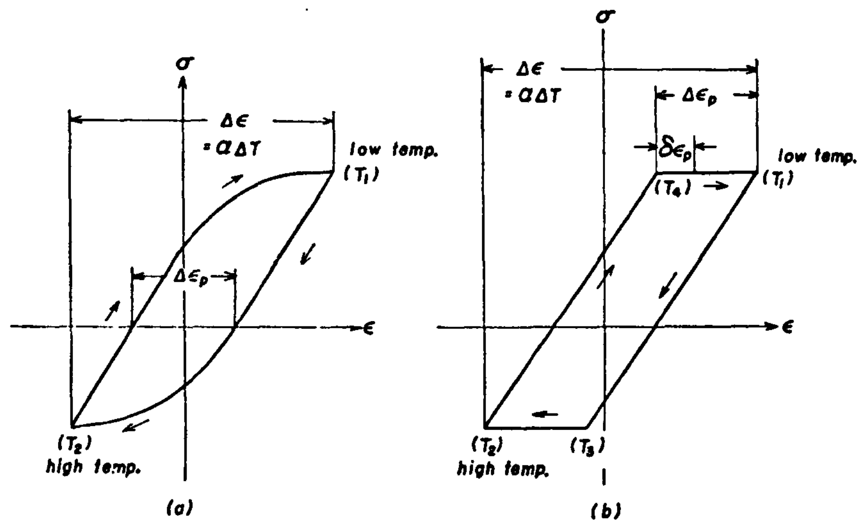

Fig. 3-10 - Stress-Strain Hysteresis Curve for Thermal Stress

It is assumed that the material is elastic during the increase in temperature from T_1 to T_3 and also in the cooling from T_2 to T_4. T_3 is a lower temperature than T_2 and likewise T_4 is higher than T_1. Plastic deformation takes place during the temperature increase from T_3 to T_2 and during the temperature decrease from T_4 to T_1.

$$
\begin{aligned}
T_3 &= T_2 - \xi\ \Delta T \\
T_4 &= T_1 - \xi\ \Delta T
\end{aligned}
\qquad (3.9)
$$

where

ξ is the ratio of plastic strain component to the total strain.

Using the concept of cumulative damage similar to that used in the previous section and taking λ as a function of temperature

$$\Delta\phi = \lambda(T)(\Delta\epsilon_p)^2 \tag{3.10}$$

Putting this equation in differential form and differentiating gives

$$d(\delta\phi) = 2\lambda(T)\,\delta\epsilon_p \cdot d(\delta\epsilon_p) \tag{3.11}$$

Applying the equation to the heating and cooling cycles where plastic deformation occurs, $T_3 - T_2$ and $T_4 - T_1$ respectively, the total increment of damage for one cycle is determined

$$\Delta\phi = \Delta\phi + \Delta\phi_2 = 2\alpha^2 \int_{T_3}^{T_2} \lambda(T)(T - T_3)\,dT$$

$$+ 2\alpha^2 \int_{T_4}^{T_1} \lambda(T)(T - T_4)\,dT \tag{3.12}$$

The coefficient of linear expansion α was assumed constant since the temperature range is usually small.

Tests have been performed for repeated thermal cycles varying the temperature amplitude ΔT and also varying the time that the maximum temperature was held per cycle, Ref. 3-11. The tests show that the value of the maximum temperature reached has more effect on the failure curves than the amplitude of the temperature change. The effect of the time that the maximum temperature was applied had considerable effect on the cycle life time as shown in Fig. 3-11. Life time is significantly shorter for longer time at maximum temperature, leading to the conclusion that failure from thermal fatigue is more of a creep rupture than a true fatigue failure.

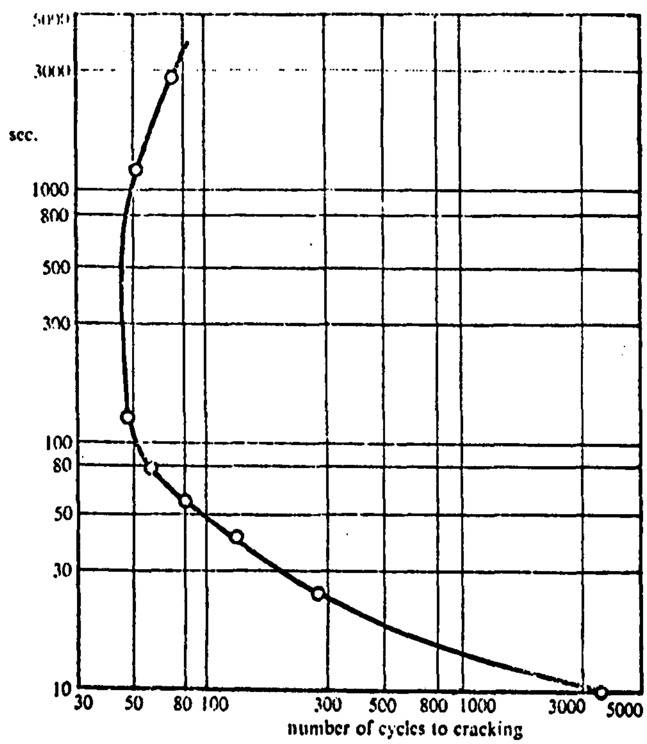

Fig. 3-11 - Variation of Life with Time at Maximum Temperature (T_{max} = 920°C) for Nimonic 90 Under Repeated Thermal Cycles (From Ref. 3-11)

3.3.3 Thermal Fatigue Combined with Mechanical Stress

In analyzing the case of thermal fatigue combined with a steady or mean mechanical stress the cumulative damage theory used in the previous sections is utilized. It is assumed that failure occurs when the damage accumulated by the alternating thermal stress attains a critical value, ϕ_o. In this case failure is produced by the combined effect of fatigue and creep damage, ϕ_f and ϕ_c, respectively.

$$\phi = \phi_f + \phi_c \tag{3.13}$$

Hence failure occurs when $\phi = \phi_o$

$$\frac{\phi_f}{\phi_o} + \frac{\phi_c}{\phi_o} = 1 \tag{3.14}$$

From Eqs. (3.6) and (3.10) of the previous sections

$$\frac{\phi_f}{\phi_o} = \frac{2\,N\,\lambda_f\,(T_e)\,(\Delta\epsilon_p)^2}{\phi_o} \tag{3.15}$$

where $\lambda_f(T_e)$ is the temperature coefficient of fatigue damage.

Using the life-fraction theory of cumulative damage for damage in creep, a material subjected to a stress σ at a temperature T fails by creep rupture at a time t_r when the damage reaches a critical value, ϕ_o. Thus the amount of damage that is absorbed in time, t, is

$$\phi_c = \phi_o \int_o^t \frac{dt}{t_r} \tag{3.16}$$

The life of a material under creep can be expressed as

$$t_r = \lambda_c\,(T)\,\sigma^{-\gamma} \tag{3.17}$$

where $\lambda_c(T)$ and γ are constants. Hence Eq. (3-16) becomes

$$\frac{\phi_c}{\phi_o} = \int_o^t \frac{\sigma^\gamma}{\lambda_c(T)} \, dt \tag{3.18}$$

Substituting Eqs. (3.15) and (3.18) into (3.14)

$$\frac{2 N \lambda_f(T_e) \cdot (\Delta\epsilon_p)^2}{\phi_o} + \int_o^t \frac{\sigma^\gamma}{\lambda_c(T)} \, dt = 1 \tag{3.19}$$

where σ is the sum of the mechanical mean stress and thermal stress.

Using Eq. (3.19) curves similar to those shown in Fig. 3-12 can be constructed. Thermal fatigue tests without mechanical stress and creep rupture tests under a constant load and temperature are used to obtain the ordinate and absissa, respectively.

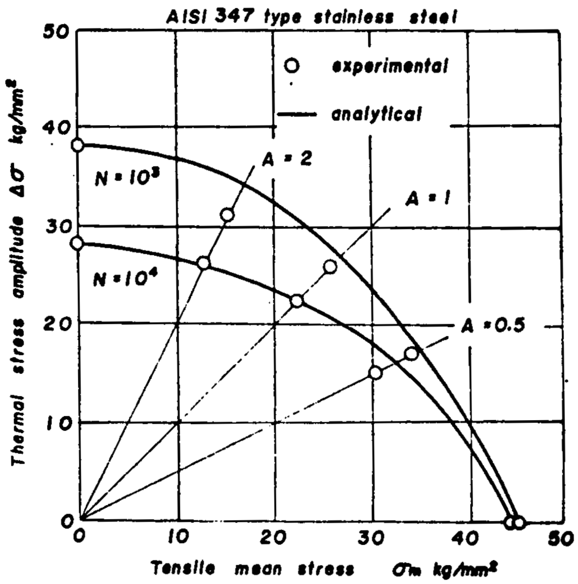

Fig. 3-12 - Stress Fracture Chart for Combined Thermal Fatigue and Steady Mechanical Stress (From Ref. 3-12)

Similarly, design charts can be constructed by using the critical values of the alternating stress, σ_f, that causes fatigue failure, and the mean stress, σ_m, that causes creep rupture, each acting separately for the ordinate and abcissa respectively. Various combinations of static stress, σ_s, and alternating stress, σ_a, that will satisfy the interaction relation are assumed (Ref. 3-11).

$$\sigma_a/\sigma_f + \sigma_s/\sigma_m = 1 \tag{3.20}$$

Figure 3-13 shows this design chart. Other relations can be constructed where the constant p and q depend on the material and tests conditions

$$(\sigma_a/\sigma_f)^p + (\sigma_s/\sigma_m)^q = 1 \tag{3.21}$$

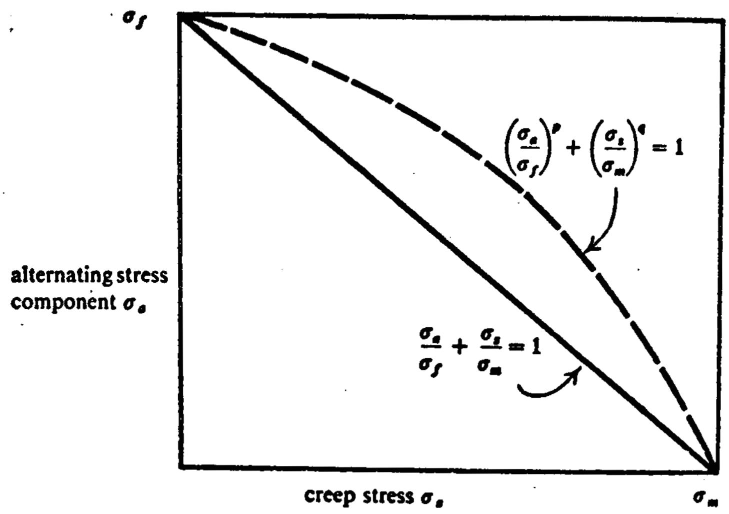

Fig. 3-13 - Interaction Curve for Combined Thermal Fatigue and Steady Mechanical Creep Stress

Experimental data are needed to help in the construction of such plots as those shown in Fig. 3-13.

3.4 FATIGUE BELOW THE CREEP RANGE

Fatigue at elevated temperature is dependent on the load intensity, temperature, number of load cycles, and the duration of the exposure to load and temperature. Below the range where creep becomes a significant factor and at moderate loads, standard room temperature design methods can be used if the fatigue data are based on appropriate elevated temperature fatigue tests. These elevated temperature tests must be performed under conditions of temperature, exposure time, and notch sensitivity similar to the operating conditions of the full-scale structure.

While the life characteristics of fatigue – sensitive structures should be verified by tests, it is necessary to predict the service life with reasonable accuracy during the design phase. The following paragraphs outline methods for fatigue design which can be used when creep is not a significant problem.

The methods for fatigue design which follow are based on procedures outlined in Lockheed's Structural Life – Assurance Manual (Ref. 3-7). Methods used by the Boeing Company (Ref. 3-8) for fatigue design of the supersonic transport (SST) are essentially the same as the Lockheed procedures, with the exception of nomenclature. In each case the type of structure or joint is given a fatigue rating based on tests and past experience.

Lockheed uses a fatigue quality index, K, which is somewhat analogous to the stress concentration factor, K_t. The fatigue quality index is defined as a measure of the ability of a structure to sustain the history of the anticipated service usage. For design the K value of the structure is estimated as discussed in Section 3.4.3C. The K value actually achieved in design is based on the results of representative fatigue tests. The numerical value of the design quality index is defined as the K_t value which yields a D value equal to one, ($\Sigma n/N = 1.0$) for life utilization ratio (D) calculations using the cyclic loads sustained in a full scale flight-by-flight fatigue test. The best quality corresponds to the lowest value of K (see Fig. 3-14).

Boeing uses a detailed fatigue rating (DFR) for components or joints which is based on tests and past experience. The DFR is defined as the maximum cyclic stress in a constant-amplitude loading cycle at which the design detail will withstand 10^5 cycles at a stress ratio, R, of 0.06.

In either case the fatigue quality of the design detail (K or DFR) is based on tests and past experience for similar conditions of stress ratio, temperature, exposure time, etc.

3.4.1 General Considerations

Fatigue analyses are made to provide assurance that the service life of a structure will equal or exceed some specified number of service hours or flights. To show this, fatigue analyses are made at points in the structure using a stress history of anticipated service useage. In addition, fatigue tests are usually specified to substantiate the design life requirements. In some cases the fatigue test requirements are more stringent than the service life requirements. It is the responsibility of the stress engineer to show that the structure will meet both the service life and test life requirements.

When designing a structure to meet the design life requirement, there are three main factors to consider.

1. Choice of material and material processing
2. Detail design quality built into the structure

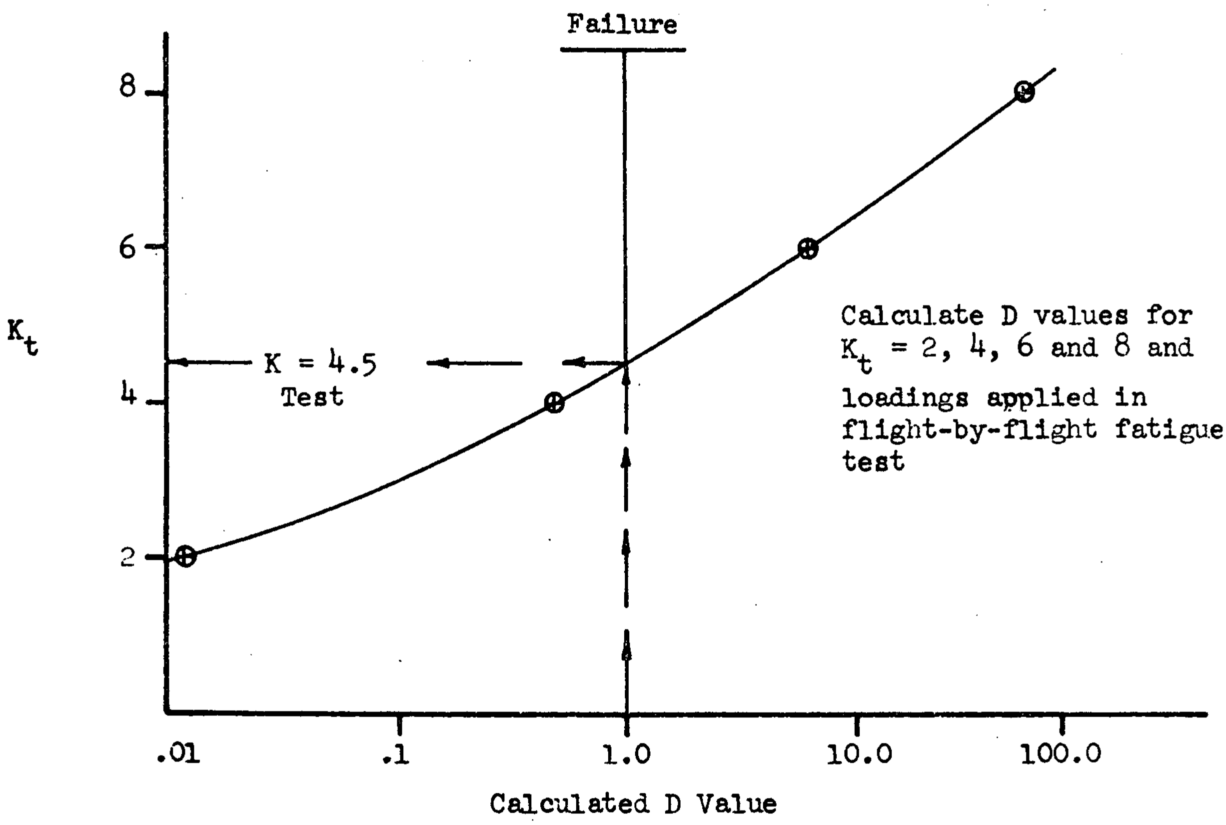

Fig. 3-14 - Illustration of Design Quality Index (K = 4.5 Shown). Obtained from Flight-by-Flight Fatigue Test Data

3. Magnitudes and number of occurrences of constant and alternating stresses at critical locations due to the anticipated service loading conditions.

The order of these three factors vary, depending on whether the structure is basically designed for ultimate strength or fatigue.

The material and material processing must be chosen with the weight, the function of the component and the environmental conditions in mind. The choice of material is usually limited because of other considerations, such as fracture toughness, corrosion resistance, static strength and stiffness. The detail design quality must be kept high by providing gradual changes in load paths and by minimizing induced stress gradients. The constant and alternating stress levels for normal operating conditions must be kept low and consistent with the fatigue quality of the structure and the service life requirements. Finally high frequencies of fatigue damaging alternating stresses must be avoided. The material in the structure must be proportioned to reduce or eliminate resonant conditions.

In selecting a section, on a component or an assembly, for fatigue analysis, one must consider a critical section, i.e., a section with high stresses, stress concentration, susceptability to fretting, such as threads, lugs, joints, etc. However, before conducting a fatigue analysis for a component, the following questions should be considered:

1. Is the component a main load carrying member? If the component is a main load carrying member, and is critical in fatigue, then it must be representatively fatigue tested.
2. Is the structural weight of the component a design consideration? The material must be selected and the structure designed to meet the weight requirements. If the weight of the component is small, the component may be purposely designed overstrength and overweight to eliminate potential problems in service.
3. What is the nature of the normal loading? (Air loads, landing loads, centrifugal loads, inertia loads, towing loads, sonic loads, temperature loads, etc.?). The loads used in the analysis must be as representative as possible of the flight and ground conditions anticipated in service.

4. Is the component subjected to stress concentrations? Stress concentrations occur at notches and section changes along the load paths. These stress concentrations must be evaluated and taken into account.

5. Is a limited or unlimited fatigue life required? The methods of fatigue analysis and fatigue test substantiation may be different for limited life than for unlimited life.

6. Is the component part of a fail-safe structure? In fail-safe structures assurance must be provided by analysis or test that damage of a specified size will be detected using normal inspection techniques before the damage size becomes critical, i.e., catastrophic failure will not occur for fail-safe load conditions. If the structure is designed to be fail-safe, lower scatter factors can be used in the fatigue analysis.

7. What is the quality of inspection during the manufacture of the component?

8. What severity of wear and tear is expected in service? If, due to wear and tear in service, the fatigue quality or loadings at a critical section are affected, this must be considered in the fatigue evaluation of the component.

9. What is the quality of inspection of the component in service? The structure at critical sections, like joints, etc., should be designed so that the critical sections can be inspected. If this is not possible, then a lower design stress must be used.

10. Is the component repairable? If the component cannot be repaired once a fatigue crack has appeared, it must either be designed with sufficient safety margin to prevent cracking or it will have to be replaced at regular intervals.

11. Is the component replaceable? If the component is part of a high cost assembly or if the component itself is prohibitively expensive to replace, then the component must have sufficient safety margin to avoid the necessity for replacement.

12. Do special environmental conditions exist, such as contact with corrosive gases, fluids or solids? The effect of corrosive environments must be considered in the fatigue analysis. To minimize the detrimental effects of corrosive environments, choose materials which are corrosion resistant and/or provide for corrosion protection of the material.

13. Is there a particular type of fatigue problem such as high stress, low cycle fatigue or low stress, high cycle fretting fatigue?

14. Will the component be fatigue tested? Fatigue tests are usually conducted on major components or assemblies to substantiate the fatigue quality of the structure and to establish safe-life replacement times for rotary wing aircraft structure. If fatigue tests are not conducted on the components and the structure cannot be designed to qualify as fail-safe structure, then lower design stresses will have to be used to insure that the structure will have an adequate service life.

3.4.2 Preliminary Selection of Allowable Design Stress

A. Method of Analysis

The curve presented in Fig.3-15 can be used for preliminary estimates of the maximum allowable ultimate design tension stress for typical aircraft structure made from aluminum, steel, and titanium alloys. The curves indicate the scatter in spectrum fatigue tests and constant amplitude fatigue tests of aircraft components. The 50% probability design curve is based on achieving a fatigue quality comparable to previous aircraft such as the P3V, Electra, F-104 and Model 286 Helicopter. The use of design stresses higher than the 50% probability design curve must be accompanied by an improvement in fatigue quality. Fatigue problems are less likely to occur if design stresses below the 50% probability design curve are used.

The maximum allowable ultimate design tension stress (mean plus alternating) is expressed as a percentage of the ultimate strength of the material. The 50% probability design curve is considered to provide a best estimate of the allowable stresses that can be used for the required number of flights or cycles.

To obtain an estimate of the allowable design stresses, the following procedure may be used. <u>This procedure should only be used in the early design stages of the vehicle before spectra loading data become available</u>.

1. Determine the number of flights or cycles for which the structure must be designed. The number of flights is specified by the design specification and/or fatigue and fail-safe policy.

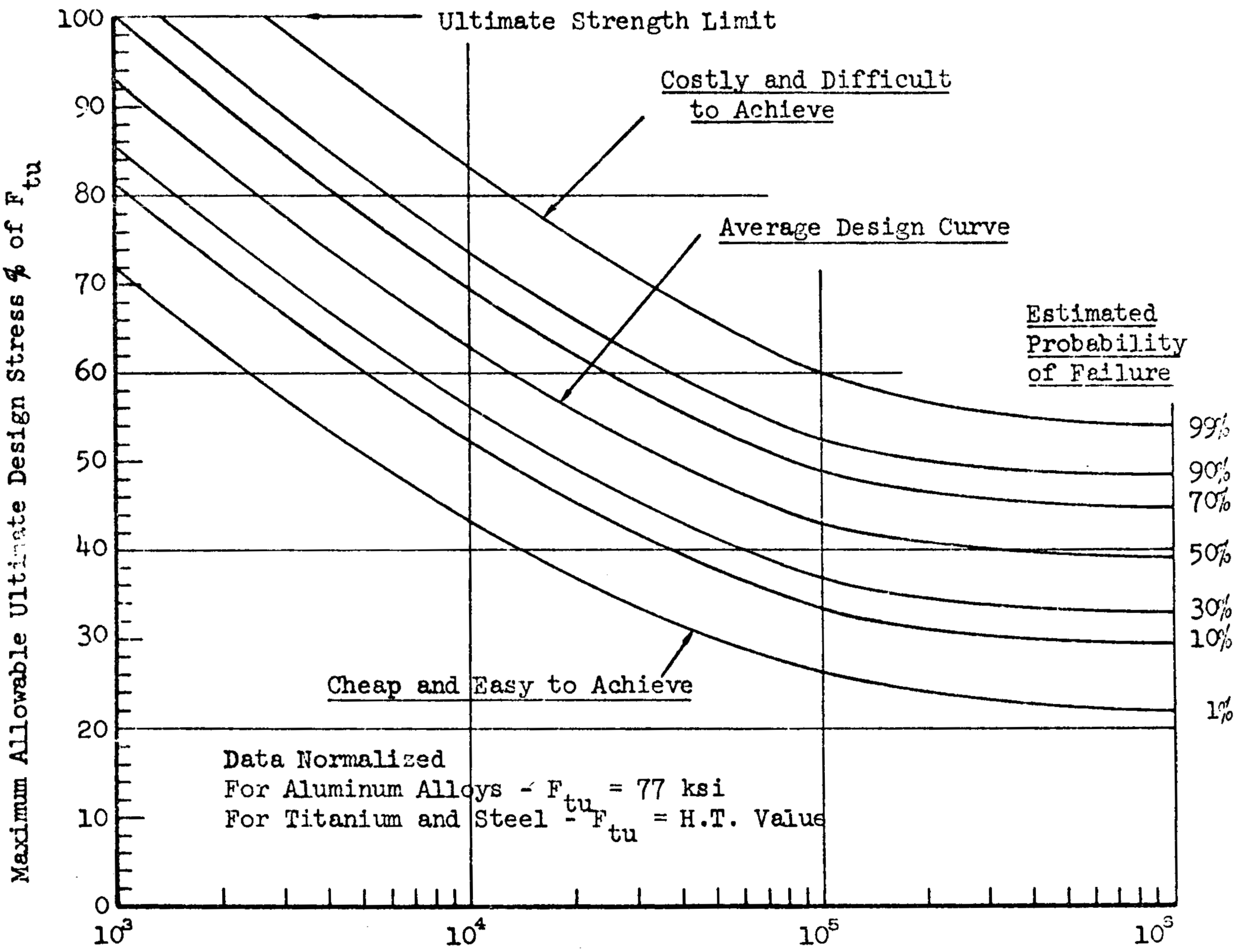

Fig. 3-15 - Flights or Cycles to Failure

2. Enter Fig. 3-15 with the number of flights or cycles obtained in Step 1 and determine the allowable stress as a percentage of the ultimate strength of the material.

3. Multiply the value obtained in Step 2 by the ultimate strength of the material. The value obtained is the maximum allowable gross area tension stress.

3.4.3 Determination of Ultimate Design Stresses using an Equivalent Ground-Air-Ground Cycle

During the early phases of design, design ultimate tension stress levels must be established for the various structural components. The selection of these stress levels must be based on consideration of the anticipated loading history to provide assurance that the design life will be achieved. The equivalent ground-air-ground (GAG) cycle concept provides a relatively rapid means for establishing the permissible design ultimate tension stress for preliminary analyses of structures subjected to complex spectra of loading. This concept may not apply to rotary wing aircraft components where the fatigue loadings are not proportional to the ultimate load conditions.

The equivalent GAG cycle is a measure of the severity of the anticipated loading spectra. In concept, it produces the same fatigue damage to the structure as would be produced if the complete spectra of loadings were considered; and the number of applications of this cycle which can be tolerated by the structure is equal to the estimated fatigue life in terms of number of flights or cycles. At this time, however, no single definition of the equivalent GAG cycle has been shown to be completely adequate. For purposes of preliminary analysis, two GAG cycles are considered:

1. Once per flight peak-to-peak GAG cycle. The loading range for this GAG cycle is determined by the maximum and minimum loadings which are equaled or exceeded once during each flight.

2. Average maximum peak-to-peak GAG cycle. The loading range for this GAG cycle is the average of the range of the maximum and minimum loads which are equaled or exceeded once per flight and the range of maximum and minimum loadings which are equaled or exceeded once during the life of the structure.

The latter value provides a conservative estimate of the equivalent GAG cycle; and the two values together envelope the probable range of the cycle. For preliminary analyses, the average of the two values obtained is used to determine the permissible ultimate design stresses.

A. Analysis Procedure

The analysis procedure starts with the spectra of anticipated loadings for the structure, the design life, and the required quality index (see Section 3.4.3C).

1. Determine the once-per-flight peak-to-peak GAG loading cycle range and the average maximum peak-to-peak GAG loading cycle range from the envelope of the anticipated loading spectra.
2. Calculate the corresponding mean and alternating loadings.
3. Using the static ultimate design loading (or bending) value and a series of selected design ultimate stress values, calculate a series of load-to-stress conversion factors.
4. Calculate the mean and alternating stresses for the two GAG cycles for each selected value of design stress.
5. Enter the appropriate constant-life diagram for the material and determine the fatigue life for the two GAG cycles at each value of design stress.
6. Plot the resultant lives as a function of design stress.
7. Enter the curves at the required design life and obtain the permissible design ultimate stress which is halfway between the two curves.

B. Example Problem

Determine the permissible ultimate design tension stress for a structure subjected to the following conditions:

Design life: 50,000 flights

Material: 7075-T6 aluminum alloy

Quality index level: K = 4.0

Bending moment spectra envelope: Fig. 3-16

Ultimate design bending moment: 30×10^6 in.-lb

1. From Fig. A-3

   Once-per-flight peak-to-peak GAG bending moment range:

   $$M_{max} = 10 \times 10^6 \text{ in.-lb}$$

   $$M_{min} = -2 \times 10^6 \text{ in.-lb}$$

   Average maximum peak-to-peak GAG bending moment range:

   $$M_{max} = 12.5 \times 10^6 \text{ in.-lb}$$

   $$M_{min} = -3 \times 10^6 \text{ in.-lb}$$

2. Once-per-flight peak-to-peak GAG bending moment cycle:

   $$M_{mean} = 4.0 \times 10^6 \text{ in.-lb}$$

   $$M_{alt} = \pm 6.0 \times 10^6 \text{ in.-lb}$$

   Average maximum peak-to-peak GAG bending moment cycle:

   $$M_{mean} = 4.3 \times 10^6 \text{ in.-lb}$$

   $$M_{alt} = \pm 7.7 \times 10^6 \text{ in.-lb}$$

3. $\frac{S}{M}$ = .00233 psi/in. -lb @ $S_{des.}$ = 70,000 psi

   = .00200 = 60,000

   = .00167 = 50,000

   = .00133 = 40,000

   = .00100 = 30,000

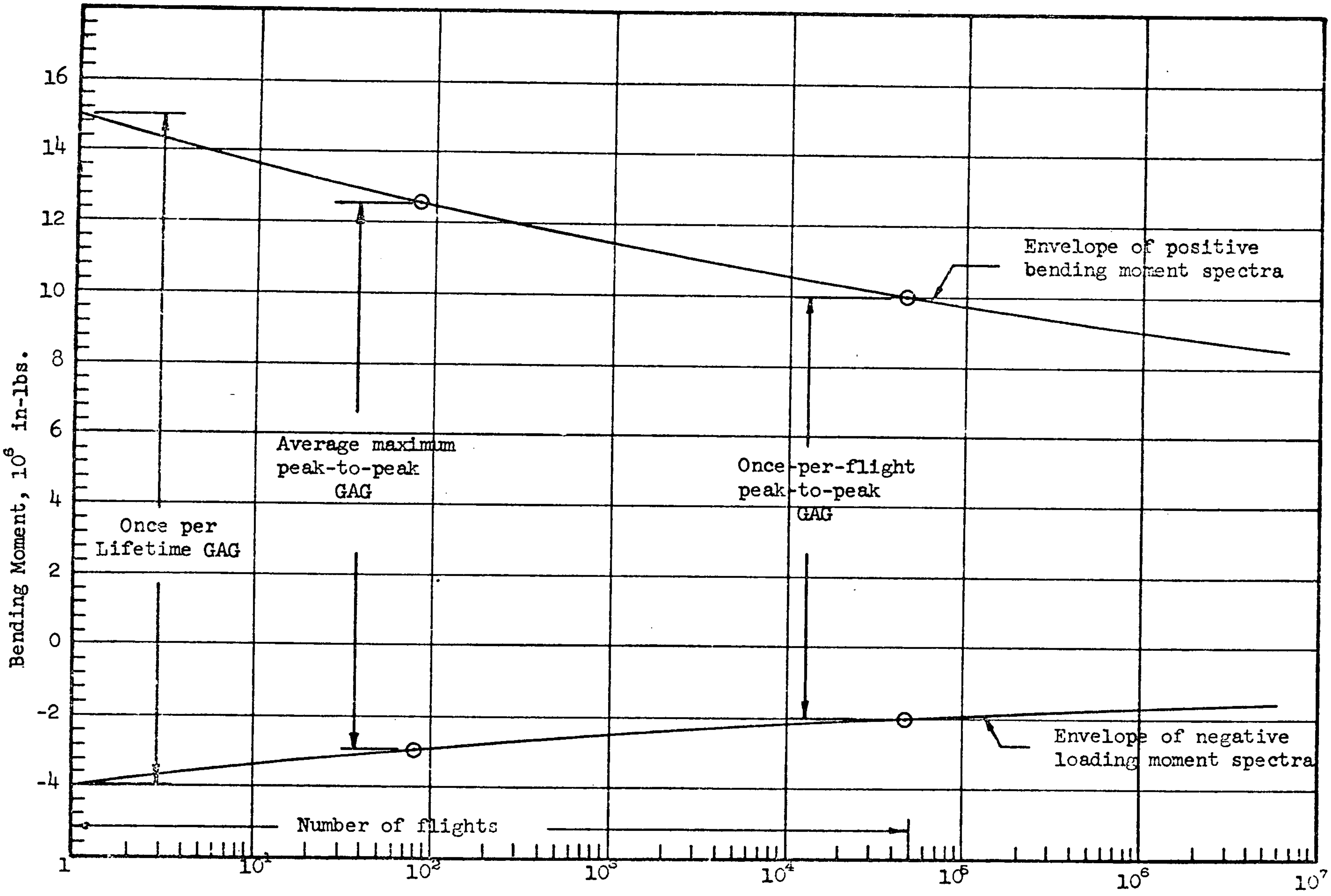

Fig. 3-16- Example of Ground-Air-Ground Loading Cycle Determination

4. Once-per-flight peak-to-peak GAG stress cycle:

S_m	S_a	@ $S_{des.}$
= 9340 psi,	= 14000 psi	= 70,000 psi
= 8000	= 12000	= 60,000
= 6670	= 10000	= 50,000
= 5320	= 8000	= 40,000
= 4000	= 6000	= 30,000

Average maximum peak-to-peak GAG stress cycle:

S_m	S_a	@ S_{des}
= 10000 psi,	= 17900 psi	= 70,000 psi
= 8600	= 15400	= 60,000
= 7180	= 12850	= 50,000
= 5710	= 10250	= 40,000
= 4300	= 7700	= 30,000

5. From Fig. 3-17

Once-per-flight peak-to-peak GAG

N	@ $S_{des.}$
= 9500 cycles	= 70,000 psi
= 22,000	= 60,000
= 70,000	= 50,000
= 370,000	= 40,000
= 3,000,000	= 30,000

Average maximum peak-to-peak GAG

N	@ $S_{des.}$
= 5000 cycles	= 70,000 psi
= 8500	= 60,000
= 22,000	= 50,000
= 85,000	= 40,000
= 600,000	= 30,000

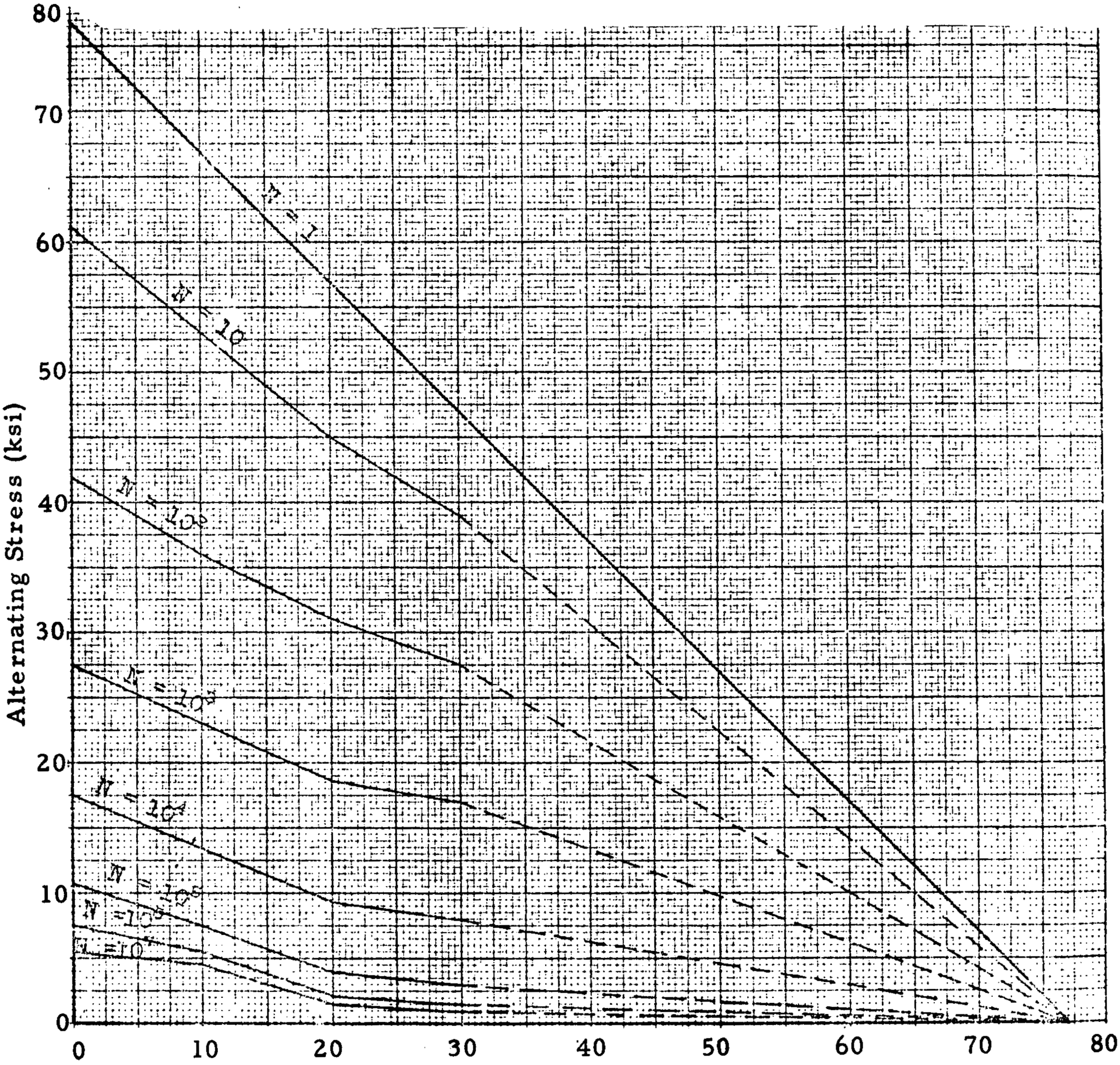

Fig. 3-17- Example of Constant-Life Diagram Material: 7075-T6 Aluminum Alloy Sheet (K_t = 4)

6. These results are plotted in Fig. 3-18.

7. From Fig. 3-18, the permissible design ultimate tension stress is 48,000 psi.

C. Selection of Fatigue Quality Index, K

The fatigue strength of a material is usually evaluated by testing small notched or unnotched standard specimens.

The fatigue strength for a section or a component made from the material will normally be lower than the fatigue strength of standard specimens tested in the laboratory for a number of reasons. In order to account for the effects of conditions not covered by the laboratory tests the fatigue quaity index used in the fatigue analysis must include the effects of the following factors:

K_t stress concentration factor. This is a factor to be used on the nominal local stress at the critical section being considered. Its value depends on the geometry at the section, i.e., notch effect, change in section on the component, etc.

K_x thermal factor allowing for the reduction in allowable due to the exposure at elevated temperature. Fatigue test data conducted at elevated temperatures are usually completed in a relatively short time. If the material will be exposed to elevated temperature for extensive periods of time in service, then the strength degradation effects due to temperature exposure must be accounted for. In lieu of data for the correct exposure conditions the K_x correction factor can be used where K_x is equal to the ultimate strength of the material at temperature for a short period of time (usually $\frac{1}{2}$ hour exposure) divided by the ultimate strength of the material after exposure to temperature for the correct period of time. In order to substantiate the values used, fatigue tests should be conducted under the correct exposure conditions.

K_c corrosion fatigue factor accounting for the effect of corrosion under service conditions. In some cases the environmental conditions may be beneficial, as for example vacuum as compared to air, whereas the more usual environmental conditions will be detrimental as

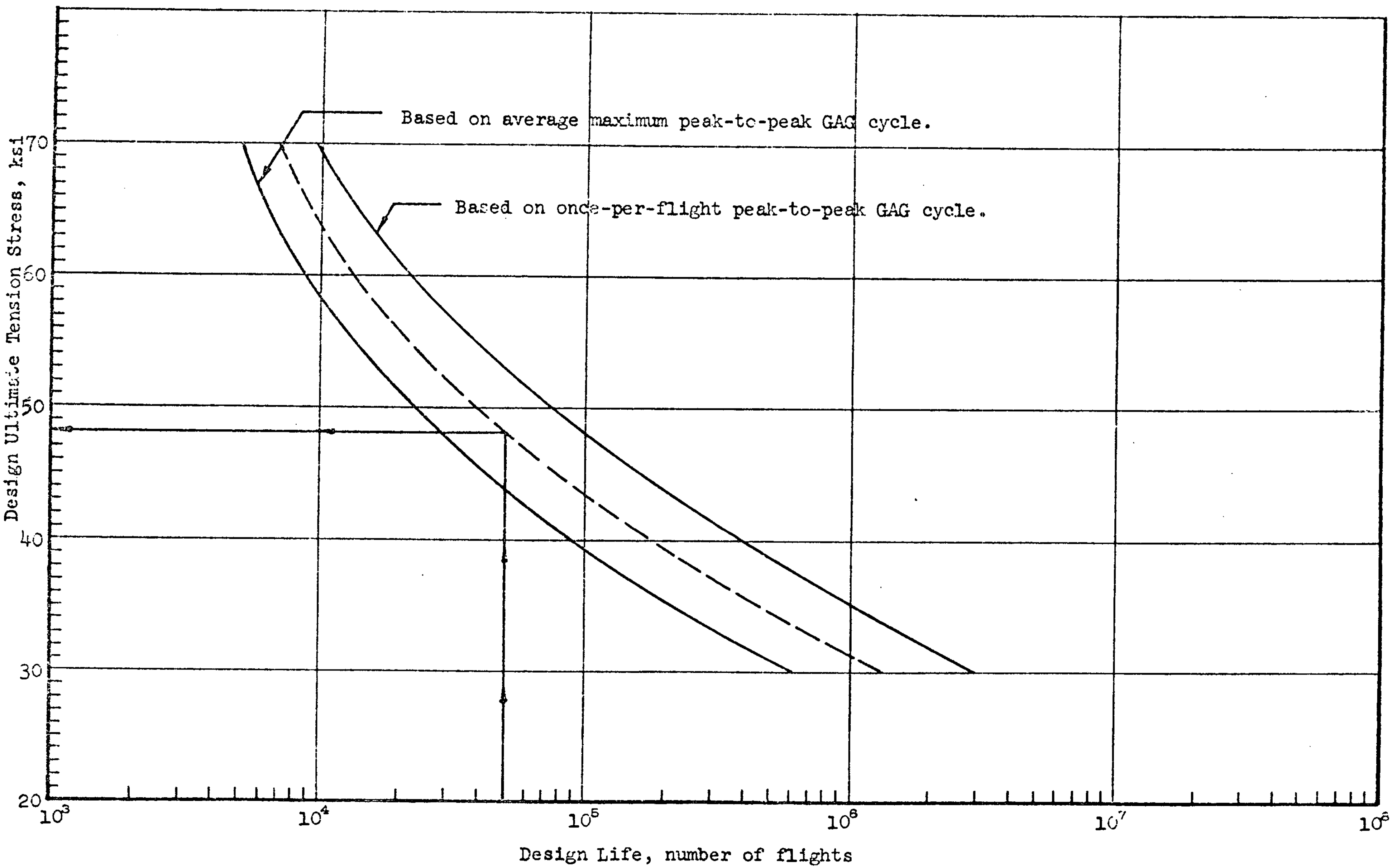

Fig. 3-18 - Example of Design Stress Determination compared to tests conducted in air. Corrosion factors are generally not available. Because the fatigue strength can be greatly reduced by corrosion, corrosion must be avoided whenever possible.

Other effects, such as fretting, joint eccentricity, differences in heat treatment, etc., should also be accounted for.

The above factors should be multiplied together so that the fatigue quality index, K, to be used in conjunction with the nominal local fatigue stress in the fatigue analysis becomes:

$$K = K_t \times K_x \times K_c \tag{3.22}$$

Reduced S-N data can be used in lieu of a K factor if the percent reduction is based on representative fatigue test data.

The design goal is to achieve the lowest practical fatigue quality index. However, the minimum K values that can be used for fatigue analysis at Lockheed Aircraft Corporation are specified in the table below.

Minimum K Values for Fatigue Analysis

Structures that will be repaired if damaged in service such as shell structure	4.0 Aluminum 4.5 Titanium
Structures that will be replaced rather than repaired in service such as landing gear structure, dynamic rotating components, control system components, etc.	2.0

The minimum K value of 4 is based on analysis of previous service experience and test data. Early service failures are characterized by K values greater than 4 whereas parts which have demonstrated adequate service life invariably give K values less than 4. In this manner successful past service history is projected into new design. This comparative base is most important to maintain in new design.

K values less than those given in the preceding table should be used cautiously. For fatigue critical structure, fatigue quality must be substantiated by test of the structure.

3.4.4 Palmgren-Miner Method of Fatigue Analysis

A. Method of Analysis

The method of analysis presented in this section is based on the Palmgren-Miner theory of linear cumulative fatigue damage. While it is recognized that this method of analysis is not precise, it will yield reasonable estimates of the service life of structural components when used as described in this section. The basic equation is expressed as follows:

$$D = \frac{n_1}{N_1} + \frac{n_2}{N_2} + \ldots + \frac{n_i}{N_i} + \ldots + \frac{n_k}{N_k} = \sum_{i=1}^{k} \frac{n_i}{N_i} \quad (3.23)$$

where D = calculated life utilization ratio

n_i = number of loading cycles applied at the i^{th} stress level

N_i = number of loading cycles to failure for the i^{th} stress level from the relevant constant-life diagram. The relevant constant-life diagram is the one which applies to the material and fatigue quality index of the section under consideration.

$\frac{n_i}{N_i}$ = cycle ratio

k = number of stress levels considered. Use ΔS_a = 3 to 4% of F_{tu}.

The method of analysis using Eq.(3.23) above as a basis, follows:

1. Select a fatigue quality index K, for the section under consideration, as described in Section 3.4.3C.

2. Obtain a loading spectra for the section under consideration. These spectra should cover all the ground cases and all the flight cases including the effect of maneuver, gust, etc. A constant and an alternating load should be given for each case, together with the anticipated number of loading cycles for the design life of the vehicle.

   If the loads are given in graphical form as cumulative loading spectra, then discrete loading distributions must be developed.

3. Convert the loads, for each case, to stresses at the section under consideration.

4. Obtain a constant-life diagram for $K_t = K$, for the material under consideration.

5. Calculate the cycle ratio for each loading case, including the effect of the GAG cycle, and add the cycle ratios to obtain the life utilization ratio "D."

6. Calculate the life in hours for the section under consideration from

$$L_C = \frac{R_2 L_1}{D} \tag{3.24}$$

   where L_1 = the life span in hours represented in the spectra used in the analysis.

   R_2 = a reduction coefficient used to assure a specified probability of obtaining a test life equal to or greater than the calculated life. Definitions of the GAG cycles used for fatigue analysis are illustrated in Fig.3-19. Values of R_2 for various probabilities are given in the table below. The values in the table are those used by the Lockheed-California Company for design of aircraft structures. The values of R_2 are based on experience with typical aircraft structures and are presented for information and not as firm recommendations.

Test Life Reduction Coefficient, R_2

Probability of Conservative Prediction of Test Results	For $(GAG)_{PP}$	For Spectrum of GAG
50%	.50	.60
90%	.25	.33
95%	.20	.25

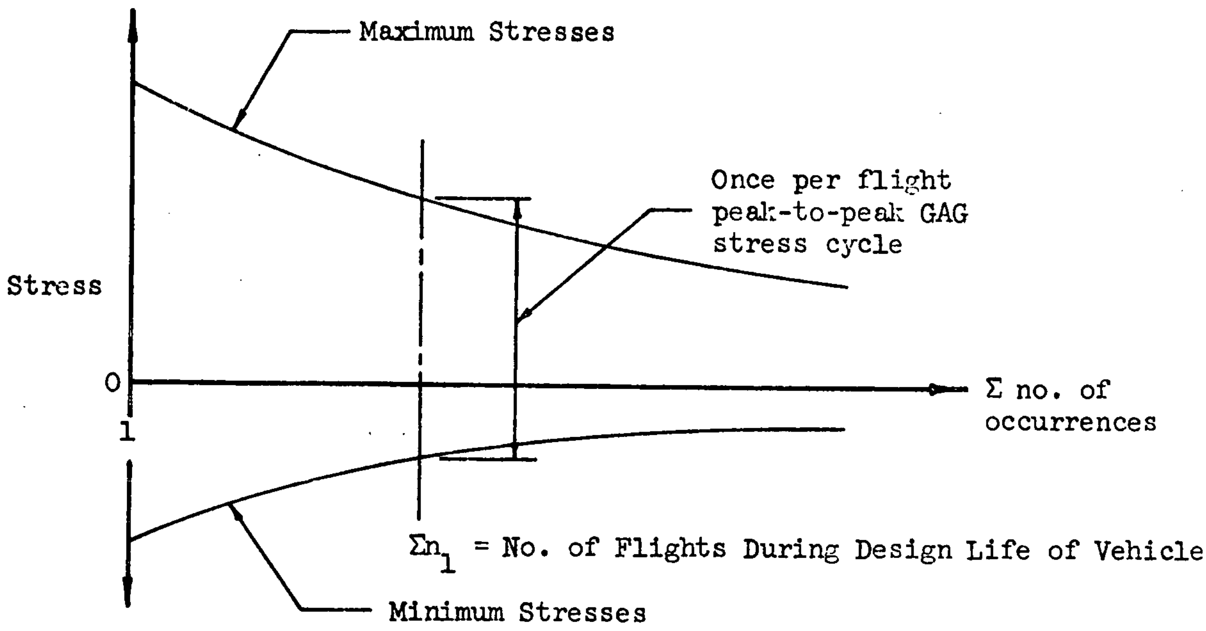

A. For Once per Flight Peak-to-Peak GAG Cycle Used in Analysis,

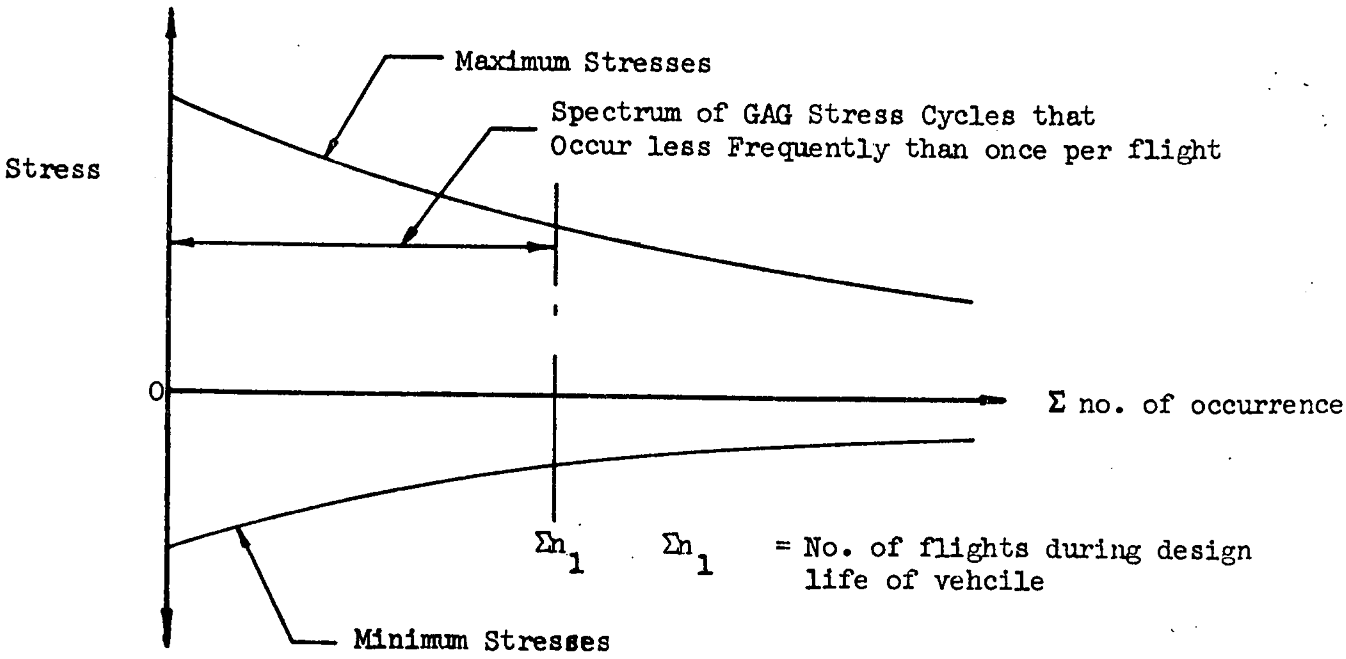

B. For Spectrum of GAG Cycles Used in Analysis,

Fig. 3-19 - Definition of GAG Cycles Used in Fatigue Analysis

7. When the value of the fatigue quality index "K" is not known, evaluate the life utilization ratio and hence the calculated life for several values of "K," as described in Steps 1 to 6.

   Plot K versus the calculated life as shown in the plot below.

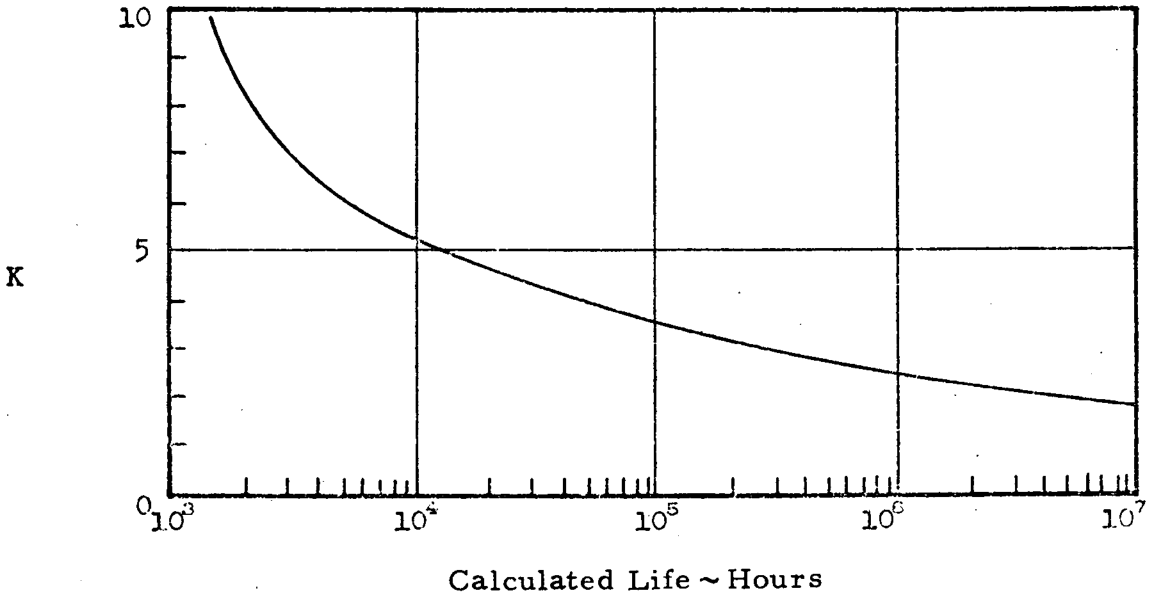

Fig. 3-20 - Relation Between Fatigue Quality Index and Calculated Life

   The calculated life can thus be obtained for any value of "K" within the range considered. Hence, if the range has been chosen correctly, the calculated life for the section under consideration can be obtained at a glance once "K" has been established, as discussed in Section 3.4.3C.

8. If the calculated life is less than the design life, the following steps should be taken in order of priority:

   a. reanalyze the part using more stress levels to represent the loading spectra for cases which have large cycle ratios.

   b. redesign the part to bring the calculated life up to or above the design life.

   c. conduct fatigue tests to demonstrate that the component will meet the design life requirement. The minimum test life required to demonstrate the design life is a function of the type of test, number of tests, type material, and magnitude of the stress levels.

9. Compliance with the design life goal must be demonstrated by either

   a. Representative fatigue tests of the actual part or of parts with similar materials and stress concentrations.

   or b. Previous service experience of parts of similar structural design taking into account the differences in structural design and operating conditions and procedures.

3.5 REFERENCES

3-1. Odqvist, F.K.G., Mathematical Theory of Creep and Creep Rupture, Oxford at the Clarendon Press, London, 1966.

3-2. Parkus, H., Recent Progress in Applied Mechanics, Wiley, New York, 1967, p. 391.

3-3. Odqvist, F.K.G., Creep in Structures, IUTAM Colloquium Stanford, 1960, Academic Press, New York, 1962, p. 137.

3-4. Edstam, U., and J. Hult, Recent Progress in Applied Mechanics, Wiley, New York, 1967, p. 223.

3-5. Lazan, B. J., "Conventional Resonance, and Acoustic Fatigue of Structural Materials at Elevated Temperature," Chapter IV, Proceedings for a Short Course, Material Engineering Design at High Temperatures, Pennsylvania State University, June 1958.

3-6. Lazan, B. J., "Conventional Resonance, and Acoustic Fatigue of Structural Materials at Elevated Temperature," Chapter IV, Proceedings for a Short Course, Material Engineering Design at High Temperatures, Pennsylvania State University, June 1958.

3-7. Structural Life-Assurance Manual, SLM No. 4, "Methods of Fatigue Analysis Lockheed-California Company, Burbank, Calif., November 1971.

3-8. Doty, Ralph J., "Fatigue Design Procedure for the American SST Prototype," presented at the Sixth ICAF Symposium, Advanced Approaches to Fatigue Evaluation, Miami Beach, Fla., May 1971.

3-9. "Methods for Structural Design at Elevated Temperatures, Monthly Progress Report," LMSC-HREC D225925, Lockheed Missiles & Space Company, Huntsville, Ala., 25 May 1972.

3-10. Coffin, L. F., "Thermal Stress and Thermal Stress Fatigue," Chap. V, Proceedings for Short Course Materials Engineering Design for High Temperature, Pennsylvania State University, June 1958.

3-11. Kennedy, A. J., Processes of Creep and Fatigue in Metals, Chap. 5, "Fatigue," Oliver and Boyd, Edenburgh and London, 1962.

3-12. Taira, S., "Lifetime of Structures Subjected to Varying Load and Temperature," Creep in Structures, IUTAM Colloquium, Stanford, 1960, Academic Press, New York, 1962.

3-13. Taira, S., "Thermal Fatigue and its Relation to Creep Rupture and Mechanical Fatigue," High Temperature Structures and Materials, McMillan, New York, 1964.

3-14. Lazan, B. J., "Fatigue of Structural Materials at High Temperature," High Temperature Effects in Aircraft Structures, Pergamon Press, New York, 1958.

3-15. Forrest, P.G., and H.J. Tapsell, Proc. IME 168, 1954, p. 763.

3-16. "Methods for Structural Design at Elevated Temperatures," Monthly Progress Report, LMSC-HREC D306072, Lockheed Missiles & Space Company, Huntsville, Ala., 26 July 1972.

Section 4
PROCEDURES FOR STRUCTURAL ANALYSIS AT ELEVATED TEMPERATURE

Of primary importance and the first step in any structural analysis at elevated temperature is the accurate prediction of the loads and temperature environment. Any conservatism in the predicted loads and temperatures results in an unwarranted weight penalty in the structural design. Accurate temperature predictions are extremely important as the temperature approaches the upper temperature limit of the material. At the upper limit the strength properties decrease sharply, the thermal stresses increase and creep becomes a major consideration in the design.

Most elevated temperature structural design problems are too complex to simplify to handbook or hand calculations without undue conservatism being added to the analysis. Finite element or other mathematical computer models are usually constructed to assist in the analysis. These models offer the capability of varying the material properties, such as E and α, from element to element to correspond to the thermal distributions. This allows a more accurate simulation of the real structure as greater detail can be provided in problem areas. This method is accurate for thin-skin and/or structures approaching the plane-stress state. Based on the results of the initial computer run the math model can be further refined by inputting reduced modulus values in the elements that have been shown to exceed the proportional limit. This procedure has been used to analyze complex structures with large thermal gradients, Refs. 4-1 and 4-2.

In determining the failure stress for the structural components, based on what is considered failure (buckling, plastic yielding, excessive deformation, etc.),the complete temperature and load history must be covered. A flange that might fail by buckling at a room temperature environment could fail by plastic yielding at an elevated temperature environment. A good practice to follow is to construct a plot of critical stress versus temperature, Fig. 4-1, so that the minimum value will always be used at the appropriate temperature.

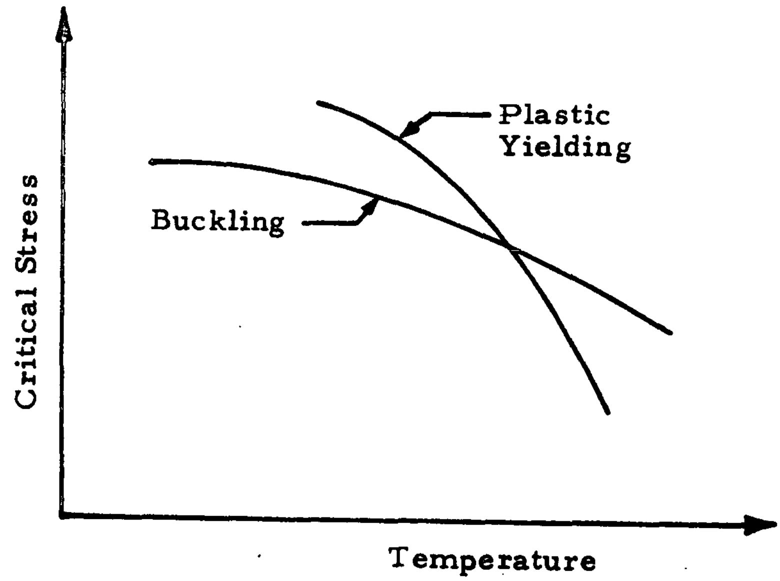

Fig. 4-1 - Critical Stress

4.1 MATERIAL ALLOWABLES AT ELEVATED TEMPERATURE

The material properties used in the analysis for most metallic aerospace structures are taken from MIL-HDBK-5 (Ref. 4-3). The room temperature design allowables are presented on one of four bases:

A basis - The value above which 99% of the population of values is expected to fall with a confidence of 95%.

B basis - The value above which 90% of the population of values is expected to fall with a confidence of 95%.

S basis - The S value is the minimum value specified by the governing group responsible for establishing material specifications. The statistical assurance associated with this value is not known.

Typical basis - The typical value is an average value with no statistical assurance associated with it.

Due to the amount of data required, usually only tensile ultimate and yield strengths are determined on A or B basis. Also, only tensile ultimate and yield strengths and elongation are specified and termed S values. Ratioing procedures have been established with which other property values are computed to have approximately the same assurance levels as the values for tensile ultimate and yield. All elastic modulus values, Poisson's ratio values, and physical properties are presented as average values. A basis values are always used unless the specified value, S value, is lower. Appropriate footnotes are given in MIL-HDBK-5 for these cases.

Elevated temperature properties are usually presented graphically as a percentage of the room temperature value and the effects of time at temperature are included. If the room temperature value has an A basis the elevated temperature values are assumed to have an A basis also.

The stress-strain and stress-tangent modulus curves in MIL-HDBK-5 are "typical" curves. Typical curves means that the stress-strain data have been adjusted to reflect average values of the elastic modulus and typical values of the 0.2% offset yield strength in tension and compression. Where stress-strain curves at elevated temperature levels are given and A basis values are needed, the following method can be used to obtain representative values. It is necessary to reduce the stress values from the typical stress strain curve to make them compatible with the A base table values. The F_{ty} value given in the table is ratioed to the 0.2% offset stress from the curve to obtain an appropriate working value.

$$R = F_{ty}/f_{0.2\%} \tag{4.1}$$

$$f = R \cdot \sigma \tag{4.2}$$

Any stress value (σ) read from the stress-strain curve above the proportional limit is factored by this ratio to make it compatible with the MIL-HDBK-5 tabular data.

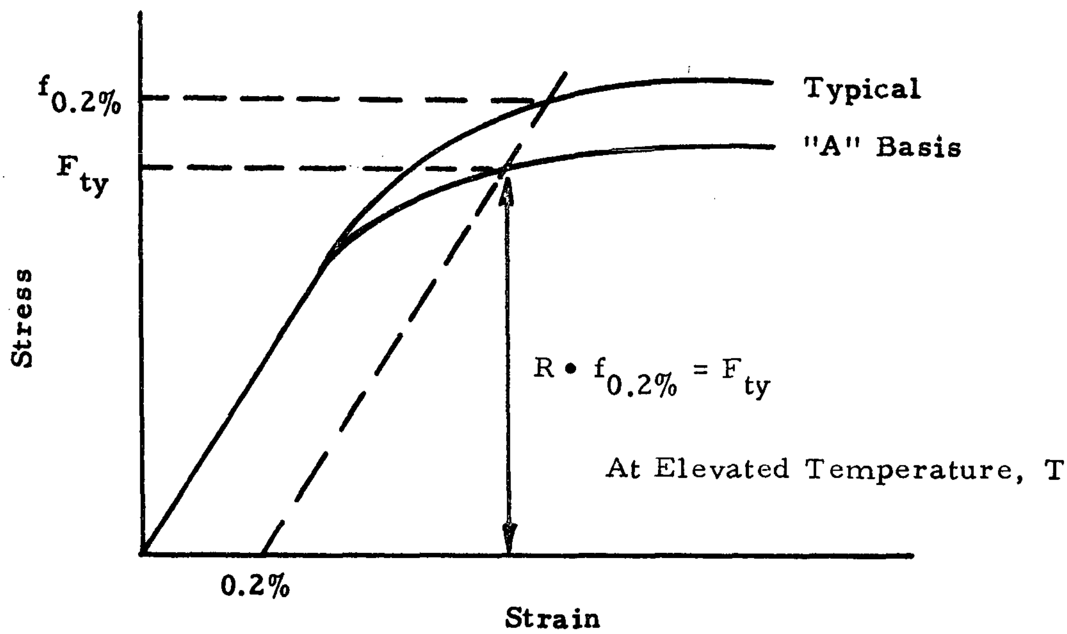

Fig. 4-2 - Elevated Temperature Allowable From Typical Stress-Strain Curves

4.2 STRESSES IN THE INELASTIC RANGE

For the general case of an indeterminate structure subjected to mechanical loads, a nonlinear analysis is required for accurate computation of the load-deflection response. The statically indeterminate structure subjected to mechanical loads differs from both the statically determinate structure and the indeterminate structure with thermal loads:

1. The internal loads in the statically determinate structure are independent of the deformations unless the deformations increase to the point where geometric nonlinearities become significant.

2. The internal loads of an indeterminate structure subjected to thermal loading tend to be self-limiting as the structure goes into the inelastic range, i.e., a small amount of plastic deformation relieves the thermal stresses.

3. Inelastic deformation of an indeterminate structure subjected to mechanical loads only redistributes the internal loads in the structure.

Since most finite element and other general structural analysis programs are linear, the stresses and strains in the elements are always computed using the linear relationship

$$\epsilon = f/E \tag{4.3}$$

For statically determinate structures in the inelastic material range, the stresses computed by a linear analysis are correct and the strain can be determined by referring to the stress-strain curve.

When a structure has only thermal loads and is operating in the nonlinear range of the material, the thermal stresses can be approximated by assuming the strain computed by a linear analysis is correct. The thermal stresses are determined by referring to the stress-strain curve or by using an analytical expression for the stress-strain relationship such as the Ramberg-Osgood model. This approximation probably will be sufficiently accurate if the material is not operating too far into the nonlinear range. The implicit assumption of this approach is that the deformed shape of the structure can be approximated by the deformed shape of a linear structure. For structures operating well into the nonlinear range a nonlinear analysis must be used as for any statically indeterminate structure.

4.3 RECOMMENDATIONS

1. Use a temperature margin ΔT that is added to the limit temperature to account for temperature prediction unknowns and temperature overshoot in variable temperature environments. This temperature margin could be a certain temperature value, $\Delta T = T$, or a percentage of the temperature variation in the structure, $\Delta T = k\,(T_{max} - T_{amb})$.

2. Development of non-linear structural analysis programs that will take variation of material properties as a function of temperature and time.

3. Further material tests at elevated temperature levels to determine material properties on an "A" basis instead of the present typical properties.

4.4 REFERENCES

4-1. Jones, W. E., "Structural Analysis of the Center Tank Section of the TPS Prototype I – Test Article 1," LMSC-HREC D225664-I, Lockheed Missiles & Space Co., Huntsville, Ala., February 1972.

4-2. Ellison, A. M., W. E. Jones and F. D. Tebbenkamp, "Structural Analysis of the TPS Center Section, Test Article I, Vol. I," LMSC-HREC D225790-I, Lockheed Missiles & Space Co., Huntsville, Ala., April 1972.

4-3. "Metallic Materials and Elements for Aerospace Vehicle Structures," MIL-HDBK-5B, Dept. of Defense, Washington 25, D. C., 1 September 1971.

Section 5
DESIGN METHODS FOR COMBINED ENVIRONMENTS

In the previous sections methods for structural design at elevated temperature have been discussed considering creep, creep rupture, fatigue, thermal stresses, and methods of stress analysis. This section discusses methods of combining load-temperature-time environments for structures operating at elevated temperatures.

To define quantitatively the confidence in structural integrity or the reliability of the structural design, one must rely on probability theory. Unfortunately the statistical approach is cumbersome for use during the design phase, and statistical data are seldom available when the structure is being designed (often adequate statistical data never becomes available).

The alternative to the pure statistical approach to structural reliability is to apply design factors, similar to room temperature factors of safety, to the mechanical loads, thermal loads or temperatures, and the service life. The structural reliability cannot be quantitatively determined using this design factor approach; but, if the design factors are applied consistantly with sound reliability principles, confidence in the structural integrity can be established.

Although the general principles of elevated temperature design are applicable to any type structure, the following sections are slanted more to a flight vehicle such as the Space Shuttle.

5.1 DESIGN CONSIDERATIONS

A primary design consideration in flight structures is minimum weight in addition to costs and manufacturing difficulties. When the materials are selected for high temperature application, curves of efficiency parameters for modulus, strength and stiffness (stability) are studied first (Ref. 5-1). For a given configuration, the sensitivity level to high temperatures must then be established. This should give an estimate of: (1) special elevated temperatures design and testing procedures that may be required; (2) if the usual room-temperature design approach is acceptable; or (3) if the configuration is inadmissible.

An acceptable design will avoid both structural and functional failure. Structural failure is characterized by a disintegration of a part of the structure (fracture, rupture). Functional failure is the result of large permanent deformations (plastic or creep strains). In considering creep, a design goal is to make the creep rate extremely low and the time to fracture extremely long. The concept of damage accumulation is essential in design for service life. Structural damage under low intensity loads of long duration reduces the resistance to loads of high intensity and short duration.

Therefore, the designer must consider the following types of structural failure:

1. Failure of the undamaged structure due to short duration loads having an extremely small probability of occurrence (ultimate load failure).
2. Failure of the damaged structure by ultimate loads of a somewhat smaller amplitude but higher probability of occurrence.
3. Functional failure due to excessive deformations from creep or plastic strain.

In designing the structure to resist the above failures it is necessary to consider the interaction of the various loads (sustained and alternating, thermal stresses, etc.) and the temperature environment as functions of time. Numerous methods of estimating the structural response to the combined environments have been proposed (Refs. 5-2 through 5-6), but none of these methods are wholly satisfactory for all cases of loads, temperatures, and materials. In most cases elevated temperature testing which simulates the material load-temperature-time environment is required.

5.2 INTERACTION CURVES

In Section 3 the interaction between thermal fatigue and mechanical stress was discussed. Similar interactions exist between mechanical fatigue and creep stresses at elevated temperature.

Because damage does not accumulate at very low values of sustained stress, the effect of creep damage can be neglected for small values of the ratio of sustained to alternating stress. Similarly, very small alternating stresses have little effect on the creep response of elevated temperature structures. For these reasons elliptic interaction curves are sometimes proposed as a first approximation (Ref. 5-2). Examples of the elliptic interaction curves are shown in Fig. 5-1. These curves show a fracture or damage surface as a function of temperature, T, and a time, t. The creep time, t, and fatigue life, N, are related by a cyclic frequency, ω:

$$t = N/\omega$$

Note that these curves are not the same as the modified Goodman diagrams at normal temperature which relate the mean and alternating components of the fatigue life. The creep-fatigue interaction curves can only be used at elevated temperature when creep damage accumulates under the sustained stress. If a number of these curves are available at different lifetimes, t, a three-dimensional plot can be constructed as shown in Fig. 5-2. In the figure, the intersection of the failure surface with the σ_a-t plane is the S-N curve at temperature T. The intersection with the σ_m-t plane represents the creep rupture curve.

Figures 5-3 through 5-9 are from MIL-HDBK-5B and represent material test data for creep-fatigue interaction. In Figs. 5-3 and 5-4 the constant life diagrams are typical of creep-fatigue data from MIL-HDBK-5B (Ref. 5-8). Figure 5-3 presents fatigue-creep rupture and fatigue-0.2% creep data, while Fig. 5-4 shows fatigue-creep rupture and fatigue-0.5% creep data; both figures

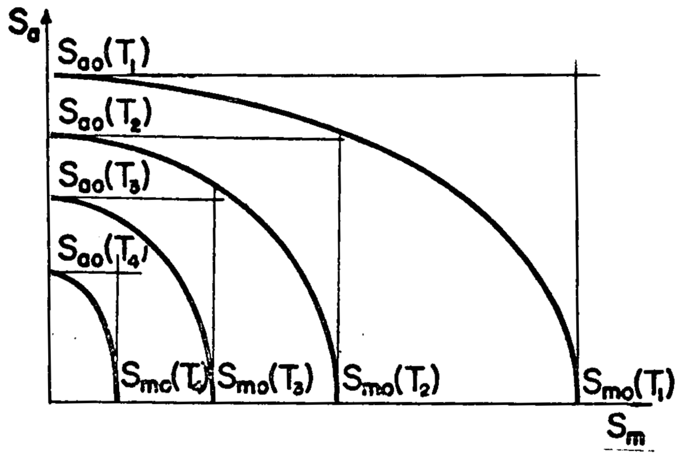

Fig. 5-1 - Elliptic Interaction Curves for Failure at Various Temperatures

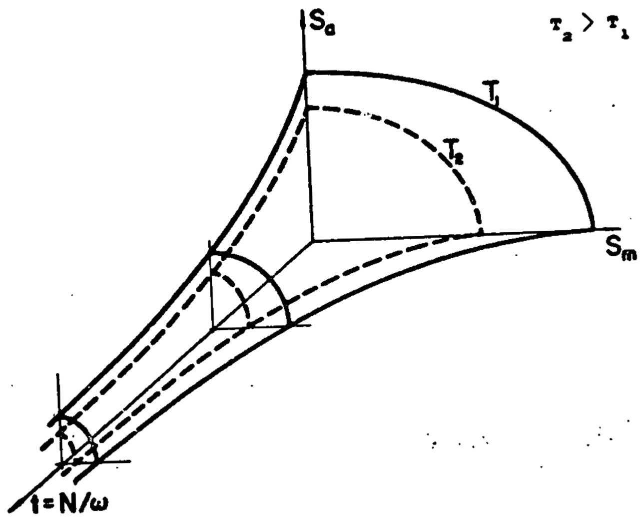

Fig. 5-2 - Interaction Surfaces for Failure

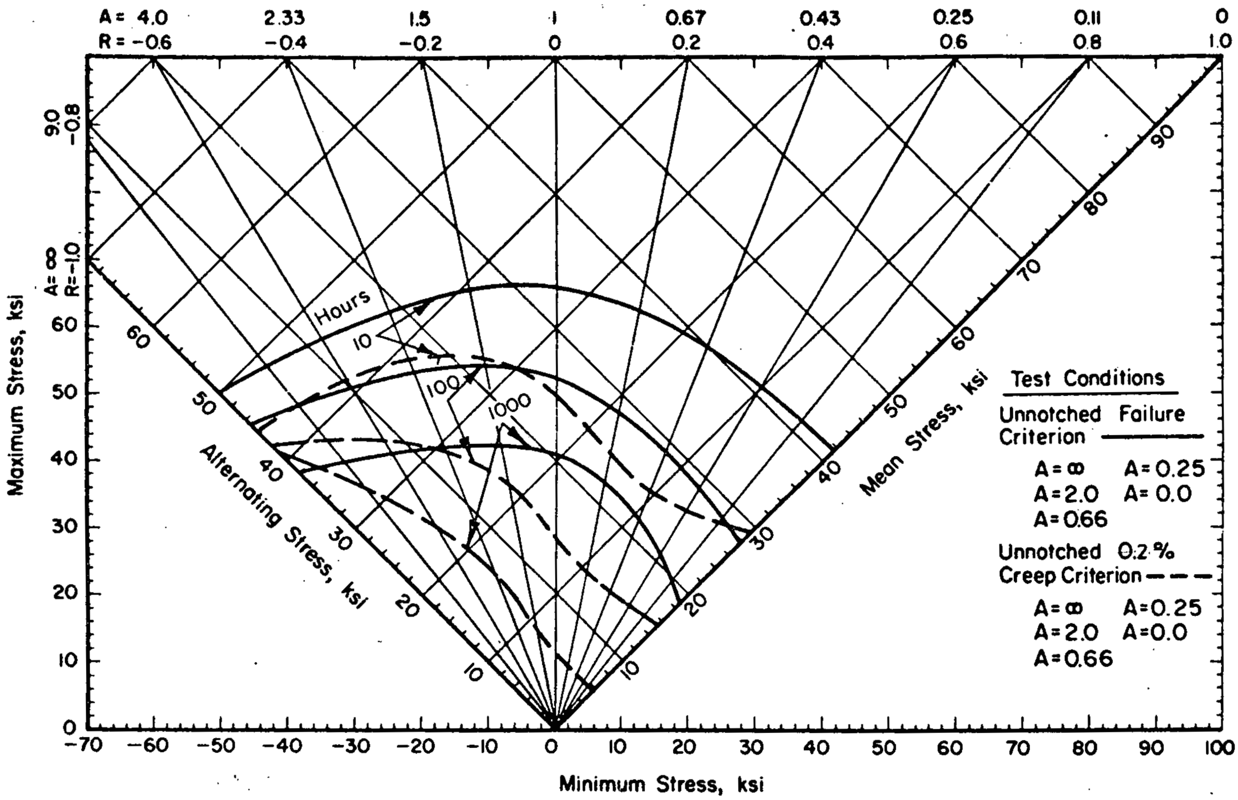

FIGURE 6.3.7.2.8(b). *Typical constant-life diagram for fatigue and dynamic creep behavior of solution treated and aged M-252 forgings at 1500 F.*

Correlative Information for Figure 6.3.7.2.8(b)

Product Form: Forged bar, 1-3/4-inches diameter

Properties:

TUS, ksi	TYS, ksi	Temp, F
176.0	100.0	RT
100.0	73.0	1500 F

Test Parameters:
- Loading - Axial
- Frequency - 1800 cpm
- Temperature - 1500 F
- Atmosphere - Air

Specimen Details: Unnotched
0.250-inch diameter

Surface Condition: Longitudinally polished with 240, 400 and 600 grit belts to provide surface finish of 5-8 RMS.
Heat treatment included solution treatment at 1950 F for 4 hours, air cooled: aging at 1400 F for 15 hours (packed in cast iron chips), air cooled.

Fig. 5-3 - Typical MIL-HDBK-5B Creep-Fatigue Data

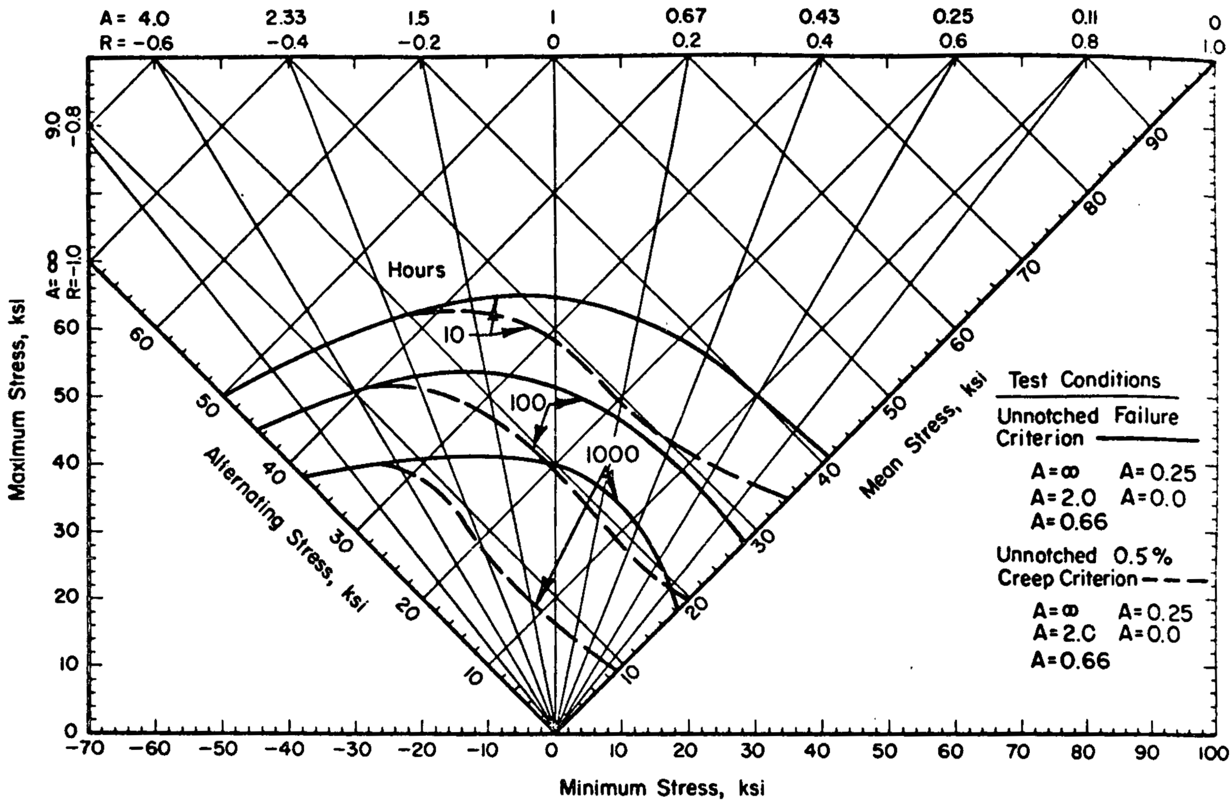

FIGURE 6.3.7.2.8(a). *Typical constant-life diagram for fatigue and dynamic creep behavior of solution treated and aged M-252 forgings at 1500 F.*

Correlative Information for Figure 6.3.7.2.8(a)

Product Form: Forged bar, 1-3/4-inches diameter

Properties:

TUS, ksi	TYS, ksi	Temp, F
176.0	100.0	RT
100.0	73.0	1500 F

Test Parameters:
- Loading - Axial
- Frequency - 1800 cpm
- Temperature - 1500 F
- Atmosphere - Air

Specimen Details: Unnotched
0.250-inch diameter

Surface Condition: Longitudinally polished with 240, 400 and 600 grit belts to provide surface finish of 5-8 RMS.
Heat treatment included solution treatment at 1950 F for 4 hours, air cooled: aging at 1400 F for 15 hours (Packed in cast iron chips), air cooled.

Fig. 5-4 - Typical MIL-HDBK-5B Creep-Fatigue Data

being for M252 forgings at 1500F. The quasi-elliptical shape of the interaction curves are apparent.

Figures 5-5 and 5-6 present fracture interaction data for Udimet 500 alloy at 1200F and 1650F, respectively; the solid lines are for unnotched specimens and the dashed lines for notched speciments. Note that, while the notches greatly reduce the fatigue strength, creep rupture properties are improved for a sustained stress acting alone.

Figures 5-7 through 5-9 are from MIL-HDBK-5B for N-155 bar stock. These figures are similar to Fig. 5-3 through 5-6 except that the data are presented on a cycle-to-failure basis instead of a time basis. As the frequency of loading is given, the conversion to a time scale for creep is apparent.

Material data of the form shown in Figs. 5-3 through 5-9 can be used to generate interaction surfaces of the form shown schematically in Fig. 5-2. These interaction curves will be valid for a particular loading spectra only if the frequency term ω is correct for relating creep time and fatigue cycles.

In the absence of creep-fatigue interaction data, an approach similar to that discussed in Section 3.3.3 and equations (3-13) through (3-21) can be used.

5.3 DESIGN FACTORS AT ELEVATED TEMPERATURE

As stated previously the goal of the designer is to arrive at a structure which has a high probability of survival (reliability) without excessive penalties in terms of weight and cost. A probabilistic approach to structural reliability is desirable if adequate information is available; unfortunately, this is seldom the case during the design phase of new hardware. Since it is not presently practical to use a statistical reliability approach to the design of structure, an alternative procedure is to use reliability principles to arrive at a rational approach for applying design factors.

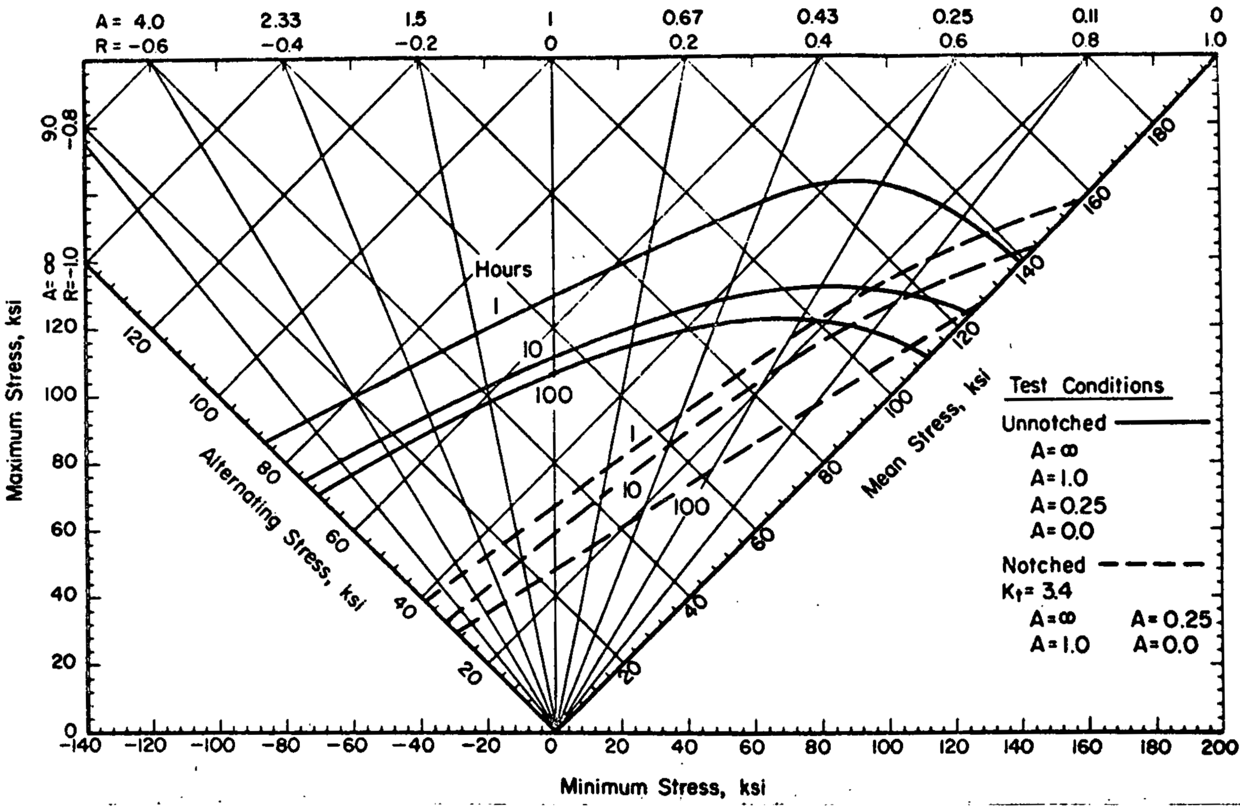

FIGURE 6.3.9.1.8(a). *Typical constant-life diagram for fatigue behavior of solution-treated and aged Udimet 500 alloy bar at 1200 F.*

Correlative Information for Figure 6.3.9.1.8(a)

Product Form: Rolled bar, 3/4-inch diameter

Properties: TUS, ksi TYS, ksi Temp, F
(no properties Given)

Test Parameters:
Loading - Axial
Frequency - 3600 cpm
Temperature - 1200 F
Atmosphere - Air

Speciment Details: Unnotched
0.200-inch diameter

Notched, V-Groove, $K_t = 3.4$
0.375-inch, gross diameter
0.250-inch, net diameter
0.010-inch, root radius, r
60° flank angle, ω

$$K_N = 2.41, \ \rho = 0.0022 \text{ inch, where } K_N = 1 + \frac{K_t - 1}{1 + \frac{\pi}{\pi - \omega}\sqrt{\frac{\rho}{r}}}$$

Surface Condition: Unnotched: Longitudinal polish with 400 grit.
Notched: Notched polish with 600 grit.

Fig. 5-5 - Typical MIL-HDBK-5B Creep-Fatigue Data

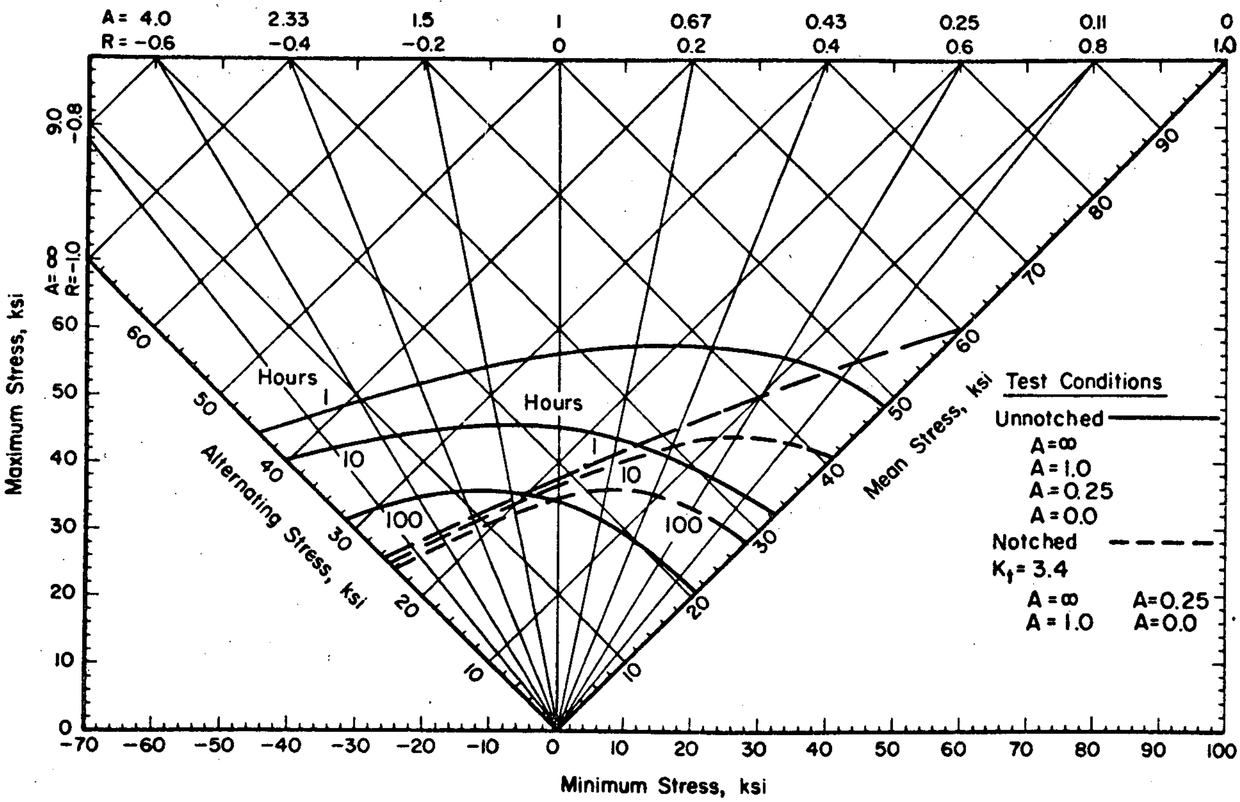

FIGURE 6.3.9.1.8(b). *Typical constant-life diagram for fatigue behavior of solution-treated and aged Udimet 500 alloy bar at 1650 F.*

Correlative Information for Figure 6.3.9.1.8(b)

Product Form: Rolled bar, 3/4-inch diameter

Properties:	TUS, ksi	TYS, ksi	Temp F
	84.0	–	1650 F (Unnotched)
	–	–	1650 F (Notched)

Specimen Details:

Unnotched
0.200-inch diameter

Notched, V-Groove, K_t = 3.4
0.375-inch, gross diameter
0.250-inch, net diameter
0.010-inch, root radius, r
60° flank angle, ω

Surface Condition: Unnotched: Longitudinal polish with 400 grit.
Notched: Notch polish with 600 grit.

Test Parameters:
Loading - Axial
Frequency - 3600 cpm
Temperature - 1650 F
Atmosphere - Air

Fig. 5-6 - Typical MIL-HDBK-5B Creep-Fatigue Data

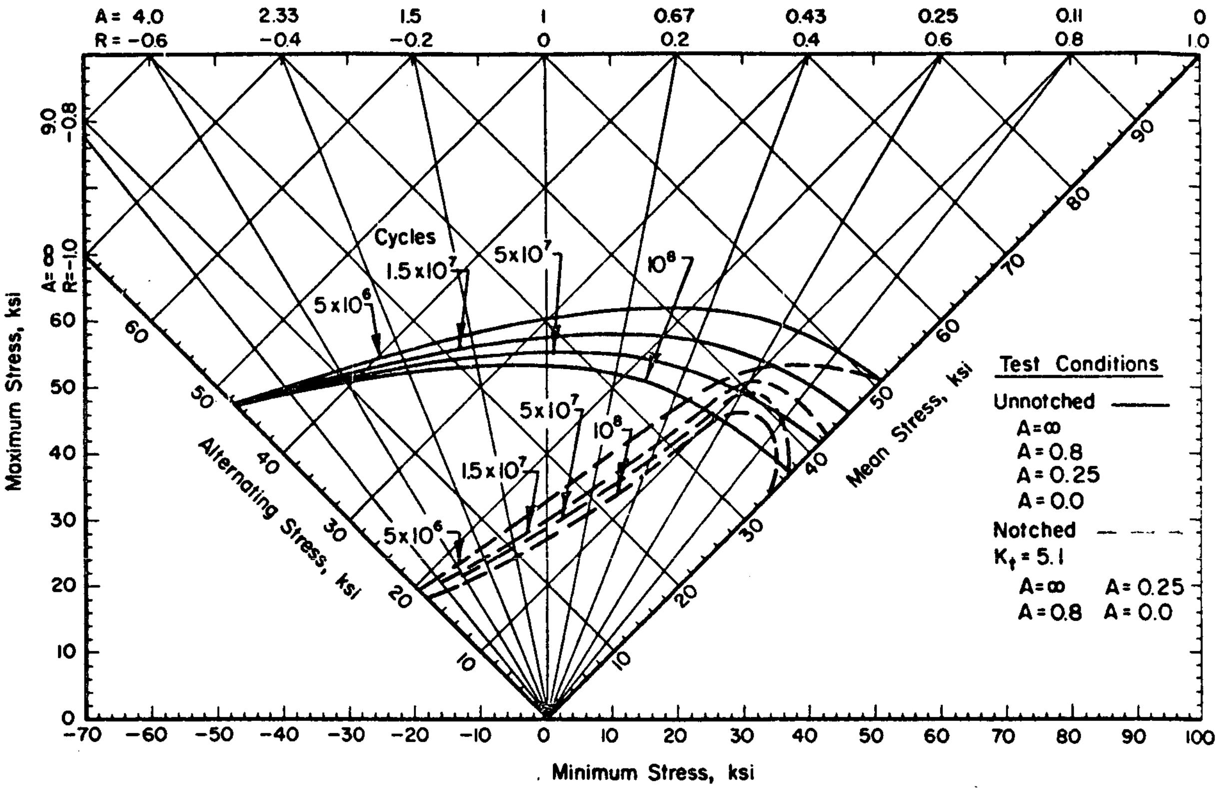

FIGURE 6.2.2.1.8(a). *Typical constant-life fatigue diagram for solution-treated and aged N-155 bar at 1200 F.*

Correlative Information for Figure 6.2.2.1.8(a)

Product Form: Rolled bar, 1-inch diameter

Properties:

TUS, ksi	TYS, ksi	Temp, F
80.0	–	1200 F

Test Parameters:
Loading - Axial
Frequency - 1500 cpm
Temperature - 1200 F
Atmosphere - Air

Specimen Details:

Unnotched	Notched, V-Groove, $K_t = 5.1$
0.225-inch	0.319-inch, gross diameter
	0.225-inch, net diameter
	0.005-inch, root radius, r
	60° flank angle, ω

$K_N = 3.37$, $\rho = 0.0012$ inch, where $K_N = 1 + \dfrac{K_t - 1}{1 + \frac{\pi}{\pi - \omega}\sqrt{\frac{\rho}{r}}}$

Surface Condition: Unnotched specimens were longitudinally polished with 400 grit paper. Notched specimens were lathe turned in the notch with a carbide tool.
Heat treatment involved solution treatment at 2200 F for 1 hour, water quench; aging treatment at 1400 F for 16 hours.

Fig. 5-7 - Typical MIL-HDBK-5B Creep-Fatigue Data

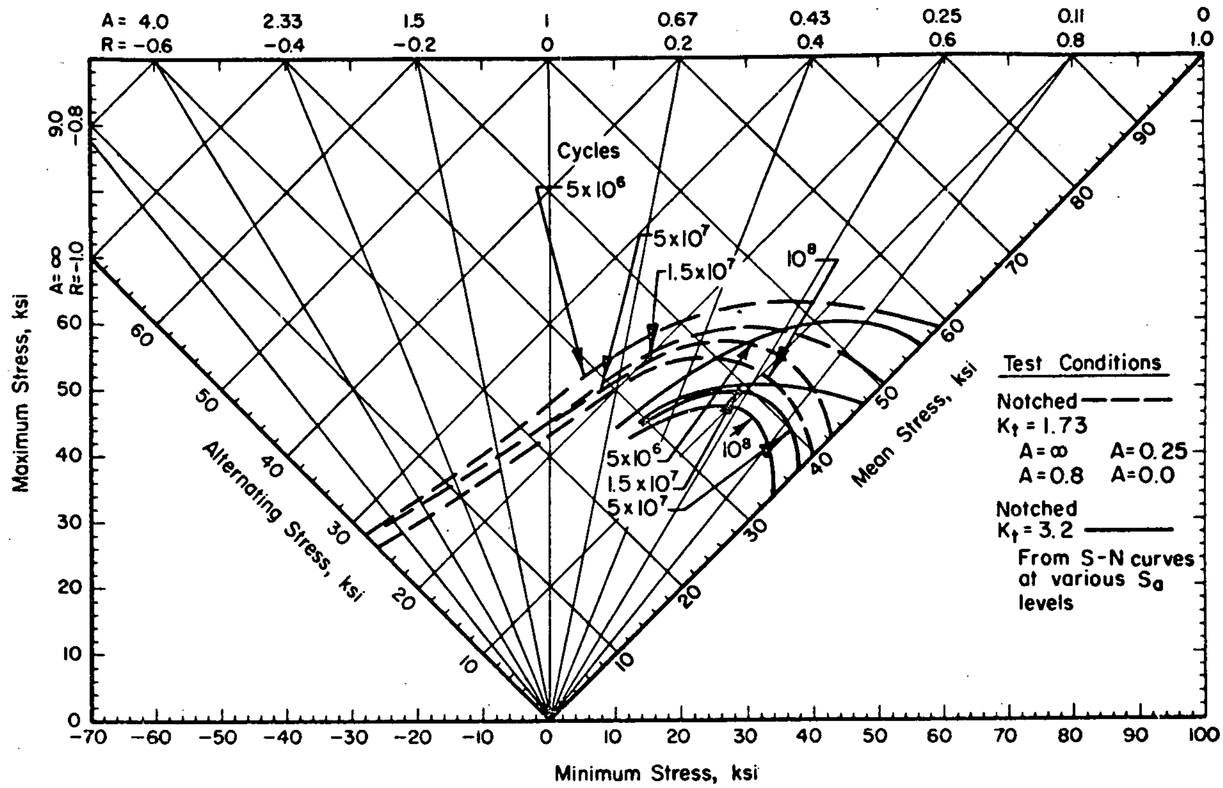

FIGURE 6.2.2.1.8(b). *Typical constant-life fatigue diagram for solution-treated and aged N-155 bar at 1200 F*

Correlative Information for Figure 6.2.2.1.8(b)

Product Form: Rolled bar, 1-inch diameter

Test Parameters:
Loading - Axial
Frequency - 1500 cpm
Temperature - 1200 F
Atmosphere - Air

Properties:	TUS, ksi	TYS, ksi	Temp, F
	80.0	–	1200 F

Specimen Details:

Unnotched
0.255-inch diameter

Notched, V-Groove, $K_t = 1.73$
0.319-inch, gross diameter
0.225-inch, net diameter
0.050-inch, root radius, r
60° flank angle, ω

Notched, V-Groove, $K_t = 3.2$
0.010-inch root radius, r
other dimensions are as given above

Surface Condition: Unnotched specimens were longitudinally polished with 400 grit paper. Notched specimens were lathe turned in the notch with a carbide tool.
Heat treatment involved solution treatment at 2200 F for 1 hour, water quench; aging treatment at 1400 F for 16 hours.

Fig. 5-8 - Typical MIL-HDBK-5B Creep-Fatigue Data

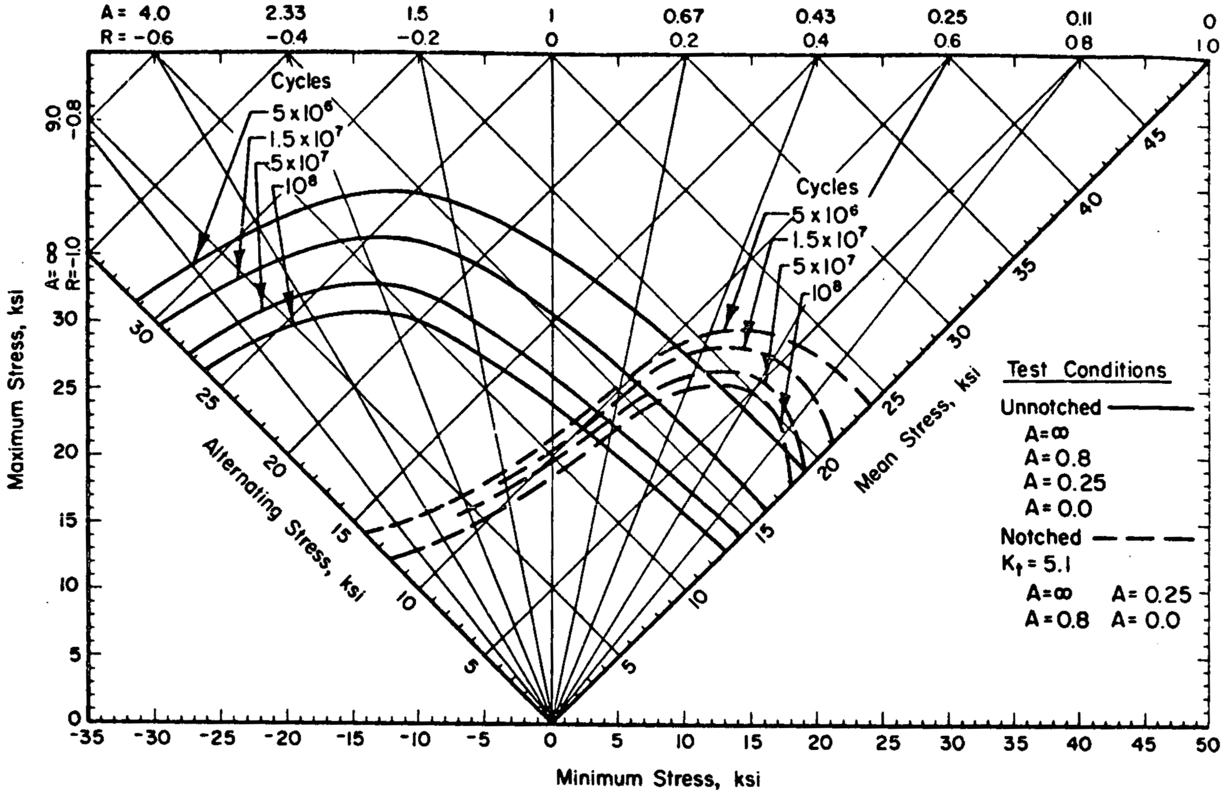

FIGURE 6.2.2.1.8(c). *Typical constant-life fatigue diagram for solution-treated and aged N-155 bar at 1500 F*

Correlative Information for Figure 6.2.2.1.8(c)

Product Form: Rolled bar, 1-inch diameter

Test Parameters:
- Loading - Axial
- Frequency - 1500 cpm
- Temperature - 1500 F
- Atmosphere - Air

Properties:

TUS, ksi	TYS, ksi	Temp, F
50.0	–	1500 F (Unnotched)
–	–	1500 F (Notched)

Specimen Details:

Unnotched
- 0.225-inch diameter

Notched, V-Groove, $K_t = 5.1$
- 0.319-inch, gross diameter
- 0.225-inch, net diameter
- 0.005-inch, root radius, r
- 60° flank angle, ω

$K_N = 2.16$, $\rho = .016$ inch, where $$K_N = 1 + \frac{K_t - 1}{1 + \frac{\pi}{\pi - \omega}\sqrt{\frac{\rho}{r}}}$$

Surface Condition: Unnotched specimens were longitudinally polished with 400 grit paper. Notched specimens were lathe turned in the notch with a carbide tool.
Heat treatment involved solution treatment at 2200 F for 1 hour, water quench; aging treatment at 1400 F for 16 hours.

Fig. 5-9 - Typical MIL-HDBK-5B Creep-Fatigue Data

This section discusses the rationale of applying design factors to a structure operating at elevated temperatures. For purposes of the discussion it is assumed that failure surfaces in terms of load, temperature, and time can be defined; and that reliability values can be associated with the applied loads and temperatures.

Consider Fig. 5-10a which shows a failure surface for a structural component in terms of the normalized failure load, p_A/p_ℓ; the normalized lifetime, t/t_o; and the component temperature, T. Also shown on Fig. 5-10a are the normalized design load, p_D/p_ℓ; the expected or limit temperature, T_ℓ; and the maximum or ultimate temperature, T_u. The loads are considered to be the loads applied to the structure, and the loads and stresses in the component are proportional to the applied loads only for a linear, elastic structure.

p_A is the allowable or failure load as a function of (T, t)
p_ℓ is the limit or maximum expected load in service
p_D is the design load and

$$p_D = K \bullet p_\ell$$

where

K is a design factor of safety on the limit load.

T_ℓ is the limit or maximum expected temperature on the component. T_ℓ is the temperature in the component associated with the limit conditions of heating, $\dot{Q}_\ell(t)$.

T_u $= T_\ell + \Delta T$, the ultimate temperature condition in the component where the ΔT term accounts for unknowns in the heating environment and errors in computing the component temperature.

t_o is the service life of the structure and is associated with the number of flights or cycles by a loading frequency, ω.

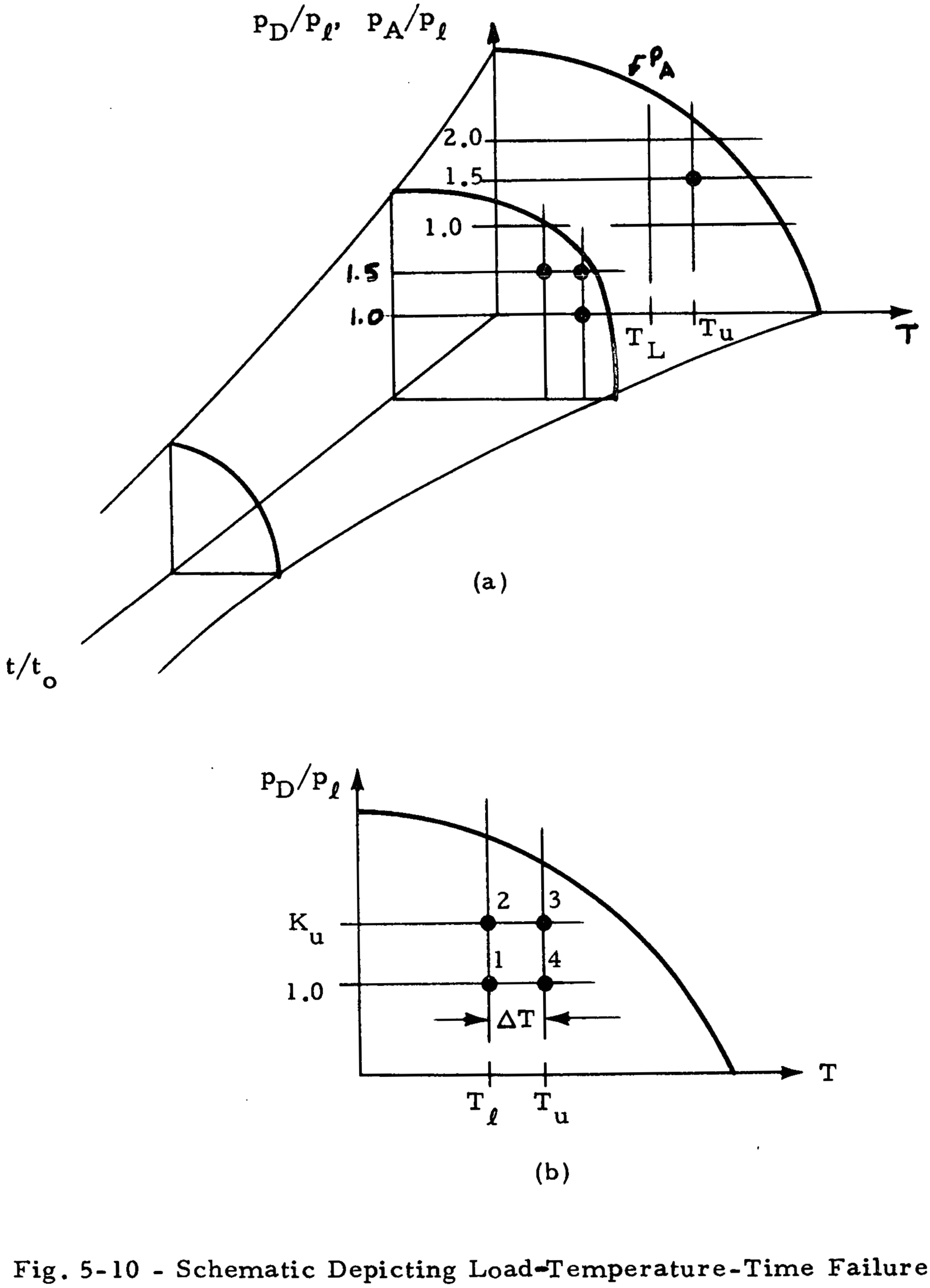

Fig. 5-10 - Schematic Depicting Load-Temperature-Time Failure Surfaces

5.3.1 Reliability Considerations for Design Loads and Temperatures

The undamaged structure should resist ultimate load failure due to a load of a very low probability of occurrence, and the damaged structure should resist failure due to ultimate loads of a somewhat lower probability of occurrence. Structural reliability should be comparable to that given by the factor of safety on mechanical loads at room temperature.

In room temperature design the limit loads are computed with some (generally unknown) probability that the loads will not be exceeded in normal service. The design load is determined using a factor of safety, which, based on experience, gives a reliable structure. The cumulative probabilities for the loads are

$$P(p_\ell) = \text{probability } (p \leq p_\ell)$$

$$P(p_u) = \text{probability } (p \leq K_D \bullet p_\ell = p_u)$$

where K_D is the design factor of safety.

The complement to the cumulative probability is the probability of exceedance:

$$R(p_\ell) = 1 - P(p_\ell) = \text{probability } (p \geq p_\ell)$$

and

$$P(p_u) > P(p_\ell)$$

$$R(p_u) < R(p_\ell)$$

The product rule of probability theory states that the probability that two independent random events will occur concurrently is the product of the individual probabilities of occurrence. If the mechanical load and the temperatures are independent random events the joint probability of exceedance can be expressed as

$$R(p_1, T_1) = R(p_1) \bullet R(T_1)$$

which is the joint probability that:

$$(p \geq p_1) \text{ and } (T \geq T_1)$$

Consider Fig. 5-10b. Loads analyses predict a maximum limit load that the structure will experience and this load has an unknown probability, $P(p_\ell)$. Experience has shown that for room temperature analysis acceptable reliability results when a specified factor of safety is applied to the limit load to obtain a design load. The design load has an unknown but acceptable probability of $P(p_D)$. Similarly, probabilities can be associated with the temperatures, T_ℓ and T_u.

The joint probabilities of exceeding a stress and temperature can be estimated if the probabilities of the stresses and temperatures occurring are written

$$P(p_\ell) = 1 - R(p_\ell)$$
$$P(p_D) = 1 - R(p_D)$$
$$P(T_\ell) = 1 - R(T_\ell)$$
$$P(T_u) = 1 - R(T_u)$$

and

$$R(p_D) < R(p_\ell)$$
$$R(T_u) < R(T_\ell)$$

Consider the joint probability of exceeding the four numbered points on Fig. 5-10b.

$$R_1 = R(p_\ell, T_\ell) = R(p_\ell) \cdot R(T_\ell)$$
$$R_2 = R(p_D, T_\ell) = R(p_D) \cdot R(T_\ell)$$
$$R_3 = R(p_D, T_u) = R(p_D) \cdot R(T_u)$$
$$R_4 = R(p_\ell, T_u) = R(p_\ell) \cdot R(T_u)$$

Table 5-1 is an illustration of the joint probabilities of exceeding the stress and temperature for the following condition:

$$R(p_\ell) = R(T_\ell) = 0.10 \quad \text{or} \quad P(p_\ell) = P(T_1) = 90\%$$

$$R(p_D) = R(T_u) = 0.01 \qquad\quad P(p_D) = P(T_2) = 99\%$$

Table 5-1

Point	Stress	Temperature	Joint Probability of Exceeding Stress and Temperature
1	p_ℓ	T_ℓ	$R_1 = 0.01$
2	p_D	T_ℓ	$R_2 = 0.001$
3	p_D	T_u	$R_3 = 0.0001$
4	p_ℓ	T_u	$R_4 = 0.001$

From the example of Table 5-1 and the joint probability equations it can be seen that the joint probabilities of exceeding points 2 and 3 are less than the probability of exceeding the design stress.

For the limit conditions of stress and temperature, point 1,

$$R_1 \geq R(p_D)$$

If

$$R(p_\ell) \cdot R(T_\ell) \geq R(p_D)$$

In summary, the above discussion shows that if

$$R(T_\ell) \approx R(p_\ell)$$

and

$$R(T_u) \approx R(p_D)$$

the joint probabilities of exceeding either point 2 or point 4 is less than the probability of exceeding the ultimate load. Also, the joint probability of exceeding both the ultimate load and the ultimate temperature (point 3) is much smaller than the probability of exceeding the ultimate load, and design for the conditions of point 4 would be excessively conservative.

5.3.2 Design for Ultimate Load Failure

The reliability discussion of the previous section suggests an approach to design for ultimate load failure at elevated temperature. This approach considers failure of the damaged and the undamaged structure and also considers the sensitivity of the structural integrity to temperature and service life.

In discussing the approach it is assumed that the following criteria are known.

1. The limit loads from which component stresses and loads can be computed.
2. The thermal environment from which component temperatures can be computed.
3. Design factors of safety for the mechanical loads from which:

$$p_D = K_D \cdot p_\ell$$

   K_D can be either yield or ultimate factors, for example:

$$K_u = 1.40$$

$$K_y = 1.10$$

4. The expected service life, t_o, or the number of flights or load cycles, N_o, where

$$t_o = N_o/\omega$$

   and ω is the loading frequency in flights per unit time.

5. A design life factor, k_D, which gives a design life of

$$t_D = k_D \cdot t_o$$

6. A computed temperature, T_ℓ, on the component which has a probability of occurrence approximately the same as that of the limit load, p_ℓ.
7. An ultimate temperature, T_u, which has a very low probability of occurrence.

$$T_u = T_\ell + \Delta T$$

where ΔT is established after considering trajectory considerations, the heating environment, and accuracy of computing the resulting component temperature spectrum.

The proposed approach is as follows:

Step 1 — Ultimate Load Failure of the Undamaged Structure

Figure 5-11a represents a plane in the failure surface of Fig. 5-10a corresponding to the first flight,

$$t/t_o = 0$$

a. For the limit temperature, T_ℓ, compute the allowable load, point 5,

$$p_A/p_\ell\,(T_\ell) = p_5$$

Compare the allowable load and the design load (point 2), and compute the load margin of safety, M.S.

$$\text{M.S.} = p_5/p_2 - 1$$

The M.S. should be positive.

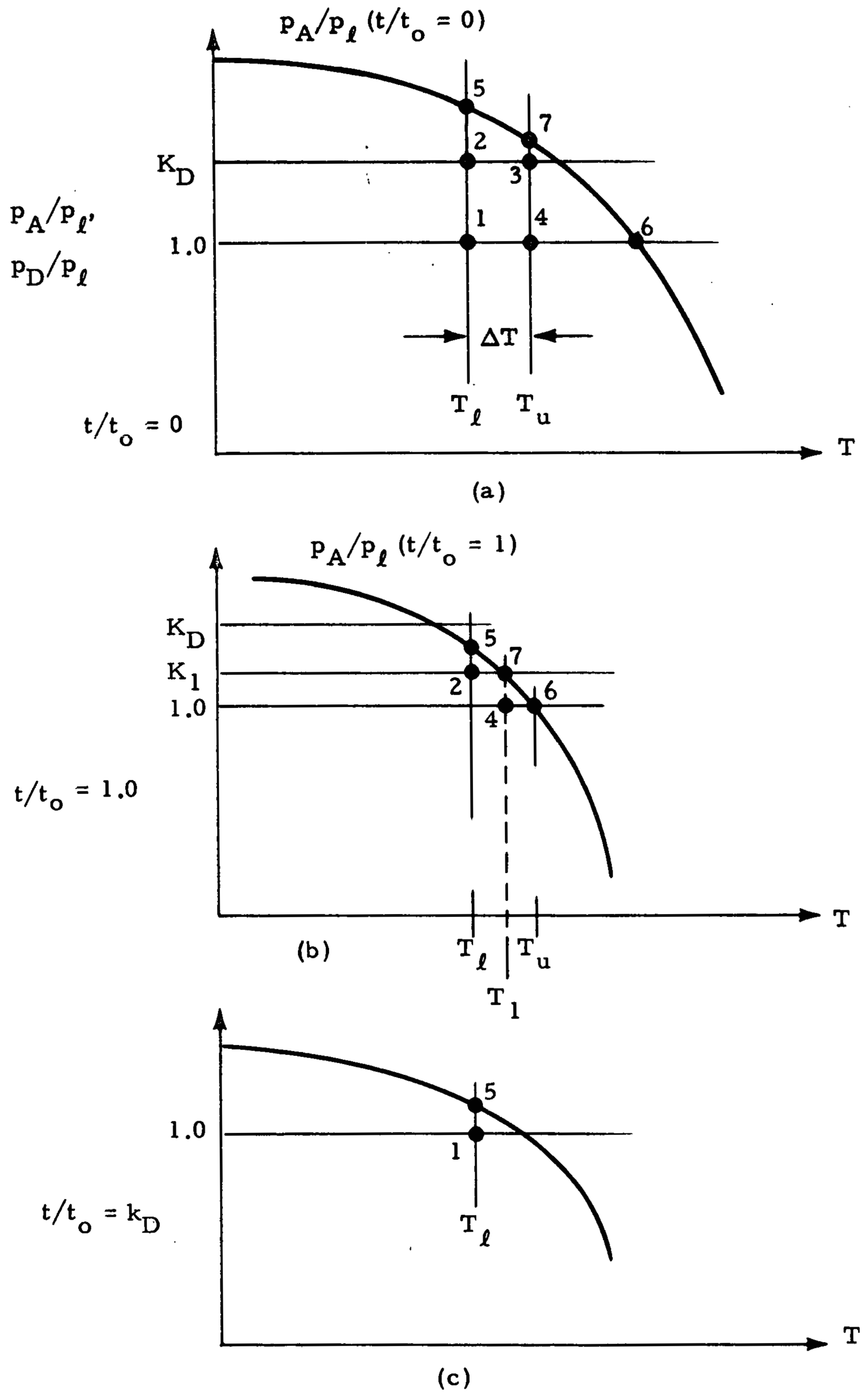

Fig. 5-11 - Allowable and Design Loads and Temperatures vs Service Life

b. For the limit load compute the allowable temperature,

$$T_A(p_A/p_\ell = 1) = T_6$$

Compare the allowable and ultimate temperatures and compute the temperature margin (T.M.)

$$T.M. = T_6 - T_4$$

The T.M. should be positive.

Alternatively, if it is easier to compute the allowable load at T_u, a load M.S. can be computed for conditions of ultimate temperature and limit load:

$$M.S. = p_7/p_4 - 1$$

If all margins are positive the undamaged structure should survive the ultimate conditions. Observe that the approach does not require that the complete failure surface be known. Only two points (5 and 6 or 5 and 7) are required.

Step 2 – Ultimate Failure at $t/t_o = 1$

Figure 5-11b is similar to t-11a except that the failure surface represents the allowable load for a service life factor,

$$t/t_o = 1$$

and K_D and T_u have been replaced by K_1 and T_1, respectively. K_1 is a F.S. which defines the design load and T_1 is the design temperature for the service life factor of one.

$$K_1 \leq K_D$$

and

$$T_\ell \leq T_1 \leq T_u$$

or

$$T_1 = T_\ell + k_1 \Delta T$$

The factors K_1 and k_1 (or T_1) should be specified in the design criteria. A preliminary recommendation is to let

$$K_1 = 1.2$$

when

$$K_u = 1.4$$

and

$$k_1 = 0.5$$

The load M.S. and T.M. are computed in the same manner as for the undamaged structure. That is

$$M.S. = p_5/p_2 - 1$$

and

$$T.M. = T_6 - T_4$$

Some hidden conservatism is included in the above margins. The calculations for the failure surface, after accumulating damage corresponding to a service life factor of one, are based on the factored limit loads and temperature, and the assumption is made that these loads are attained on each flight. In reality limit loads are the maximum expected loads in normal service and most flights will be subjected to loads less than the limit loads. Therefore, the accumulated damage should be less than predicted.

Step 3 — Determine Service Life Margin

Figure 5-11c represents the failure surface at

$$t/t_o = k_D$$

the design life factor.

The scatter in the service life of structures subjected to cyclic and sustained loads at elevated temperature is notoriously large. It is desired to determine the allowable life for limit load and temperature conditions:

$$t_A/t_o\ (p_\ell, T_\ell)$$

If the allowable life is determined, a service life margin (S.L.M.) can be defined

$$S.L.M. = t_A/t_o\ (p_\ell, T_\ell) - k_D$$

The S.L.M. should be positive.

If it is more convenient the existance of a positive S.L.M. can be verified by computing a positive load M.S. for limit load and temperature. On Fig. 5-11c this is shown by the relationship of points 1 and 5:

$$M.S. = p_5/p_1 - 1$$

5.4 DESIGN FOR PERMANENT DEFORMATIONS

Permanent deformations from creep or plastic strain can result in functional failure prior to rupture or ultimate load failure. Methods of predicting creep resulting from sustained loads at elevated temperature are discussed in Section 2 and a creep analysis program is described in Appendix B.

The difficulties of accurately predicting creep deformations increase when a structure must be designed for very long life and very low creep rates. Most creep data are for relatively high creep rates and the test times are too short to be relevant. Utilization of existing data requires extrapolating the data for both creep rate and exposure times. As the required extrapolation can approach two orders of magnitude, confidence in the extrapolated values becomes small. As an example, the design goal for the American SST was 50,000 flight hours (Ref. 5-9), whereas most creep tests are limited to about

500 hours. Additional uncertainties are introduced when the primary creep range is considered as little data are available and the data exhibit considerable scatter.

Freudenthal (Ref. 5-2) considers the primary creep range of principal importance in contributing to the permissible creep but generally unimportant in contributing to damage. The relative importance of primary and secondary creep on allowable deformations also vary with the stress and temperature conditions.

5.4.1 Creep Deformation Surfaces

The dependence of creep deformations on the cyclic stresses is generally small (Ref. 5-3) as illustrated for M252 alloy at 1350F (Figs. 5-3 and 5-4). The design allowable creep condition can be considered independently of the ultimate load failure criteria of Section 5.3.

Figures 5-12 through 5-18 represent typical creep data from MIL-HDBK-5B. Figure 5-12 represents creep data in the form of a nomogram for René 41 alloy sheet. Figures 5-13 and 5-14 show short term, stress-time creep data for 7075 aluminum, and Figs. 5-15 through 5-18 are long term, stress-time creep data for 7075 aluminum.

Figure 5-19 shows constant creep surfaces for 7075 aluminum which were constructed from the data of Figs. 5-13 through 5-18. The constant creep surfaces are shown on a stress-temperature-time plot.

Note that, for high temperatures and long exposure times, the creep strains are very sensitive to small variations in either the temperature or stress environment. This observation is consistant with the analysis of Section 2.4, which considered the case of a small random temperature fluctuation about the mean temperature, and example problem 5 in Section 2.8. The example problem showed that the predicted time for a given creep in a titanium beam was reduced from 1750 to 673 hours when a random temperature fluctuation of $\pm 25^{\circ}F$ was added to a $750^{\circ}F$ mean temperature.

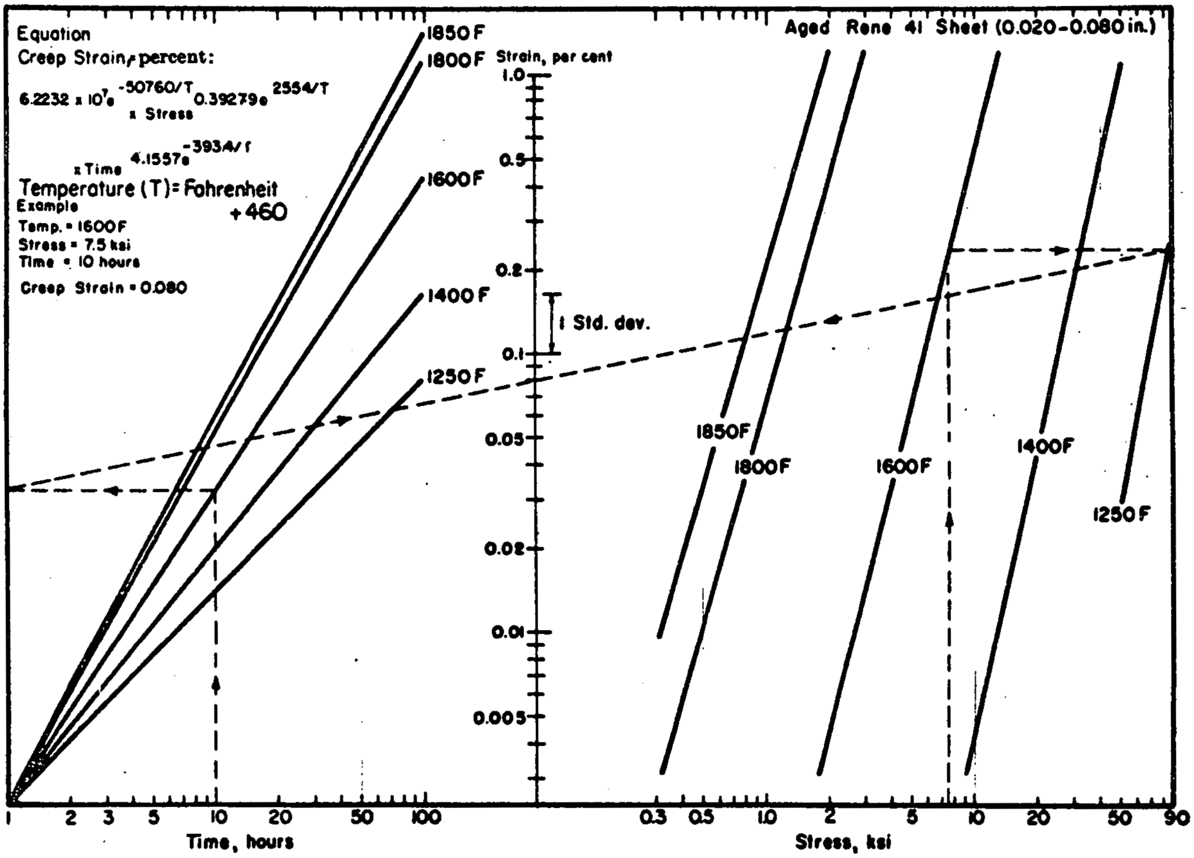

FIGURE 6.3.8.1.7. *Typical creep properties of René 41 alloy sheet.*

Fig. 5-12 - Typical MIL-HDBK-5B Creep Data

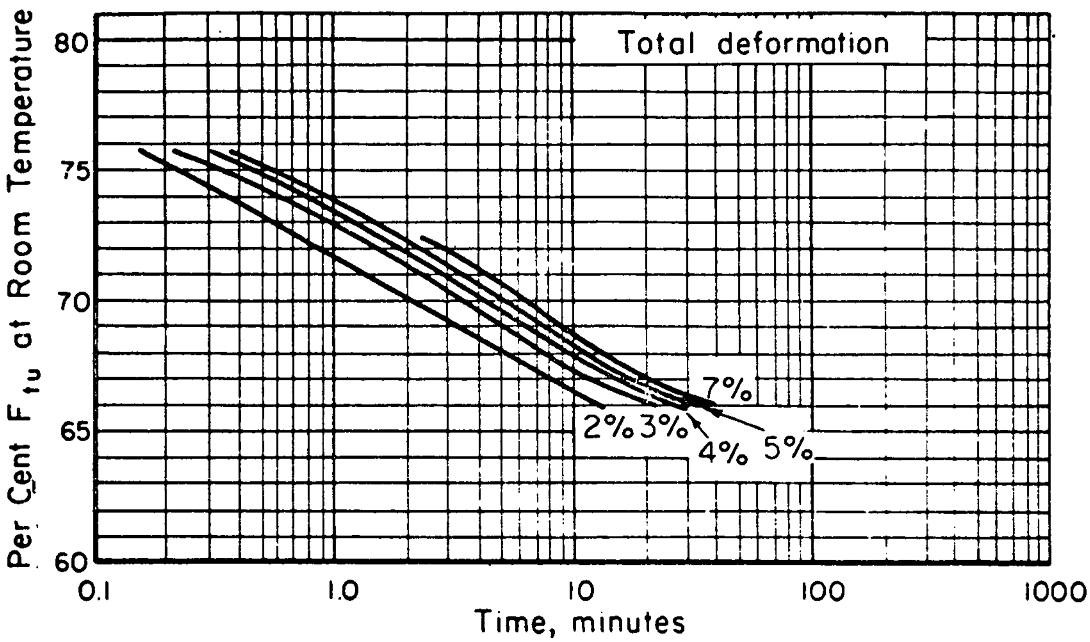

FIGURE 3.7.2.1.7(a). *Creep data for 7075-T6 aluminum alloy (clad sheet) at 300 F. Deformation includes thermal expansion of 0.30 percent. Heating rate 70 F per second.*

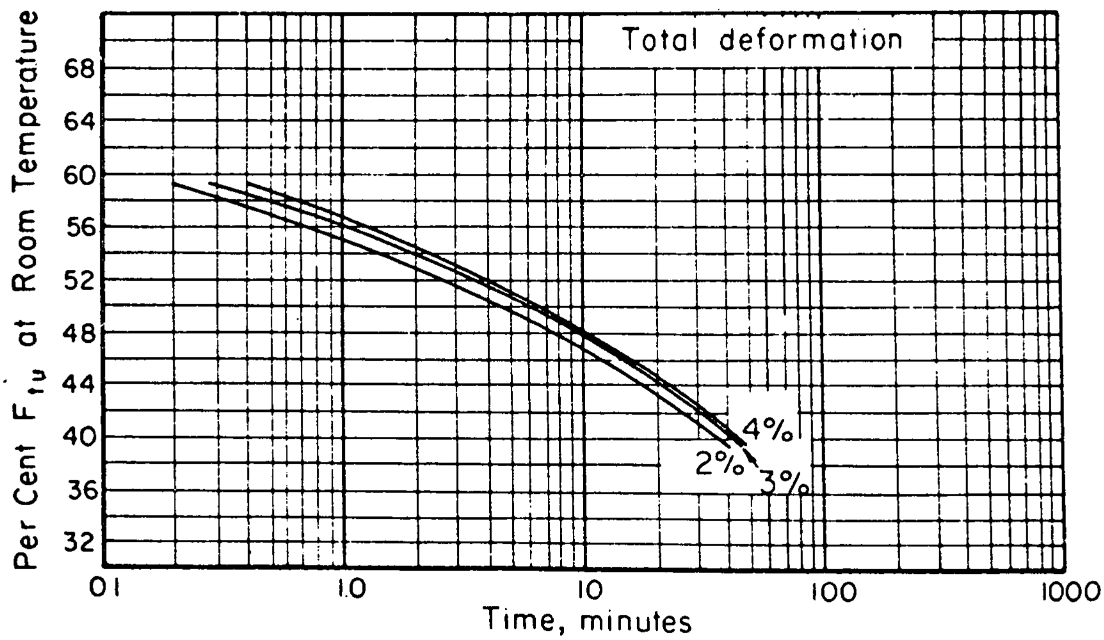

FIGURE 3.7.2.1.7(b). *Creep data for 7075-T6 aluminum alloy (clad sheet) at 400 F. Deformation includes thermal expansion of 0.43 percent. Heating rate 75 F per second.*

Fig. 5-13 - Typical MIL-HDBK-5B Creep Data

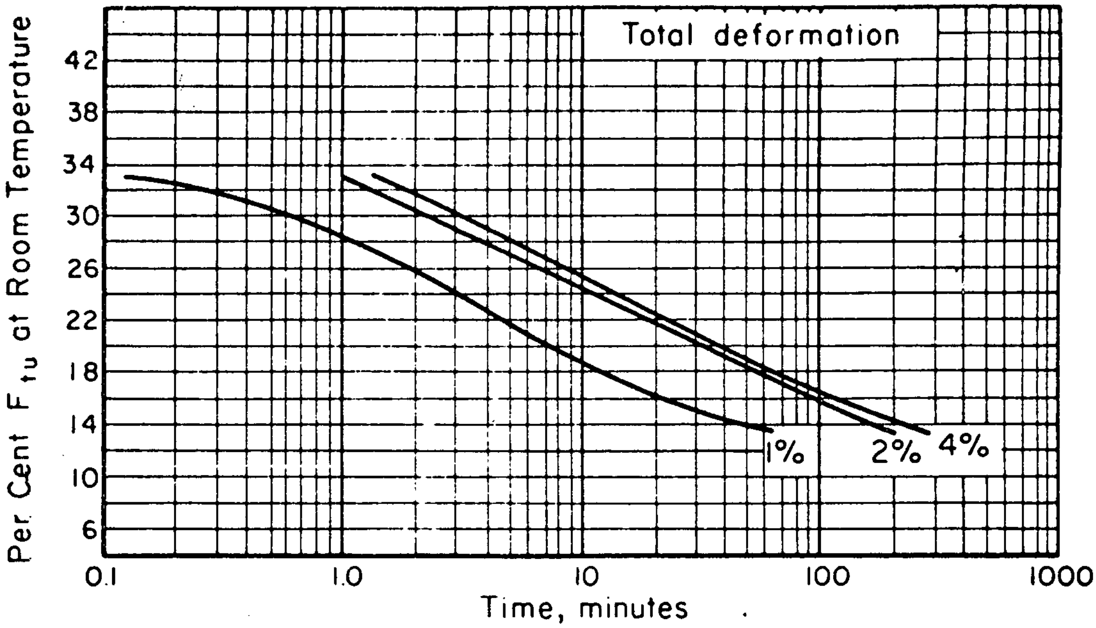

FIGURE 3.7.2.1.7(c). *Creep data for 7075-T6 aluminum alloy (clad sheet) at 500 F.*

Deformation includes thermal expansion of 0.63 percent. Heating rate 75 to 100 F per second.

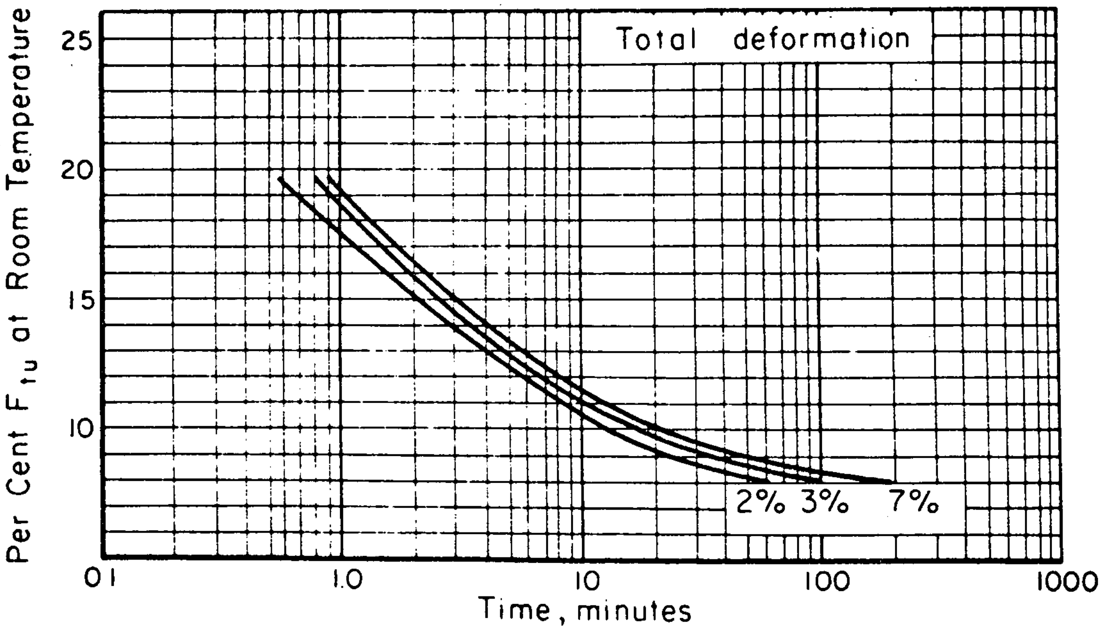

FIGURE 3.7.2.1.7(d). *Creep data for 7075-T6 aluminum alloy (clad sheet) at 600 F.*

Deformation includes thermal expansion of 0.74 percent. Heating rate 80 to 90 F per second.

Fig. 5-14 - Typical MIL-HDBK-5B Creep Data

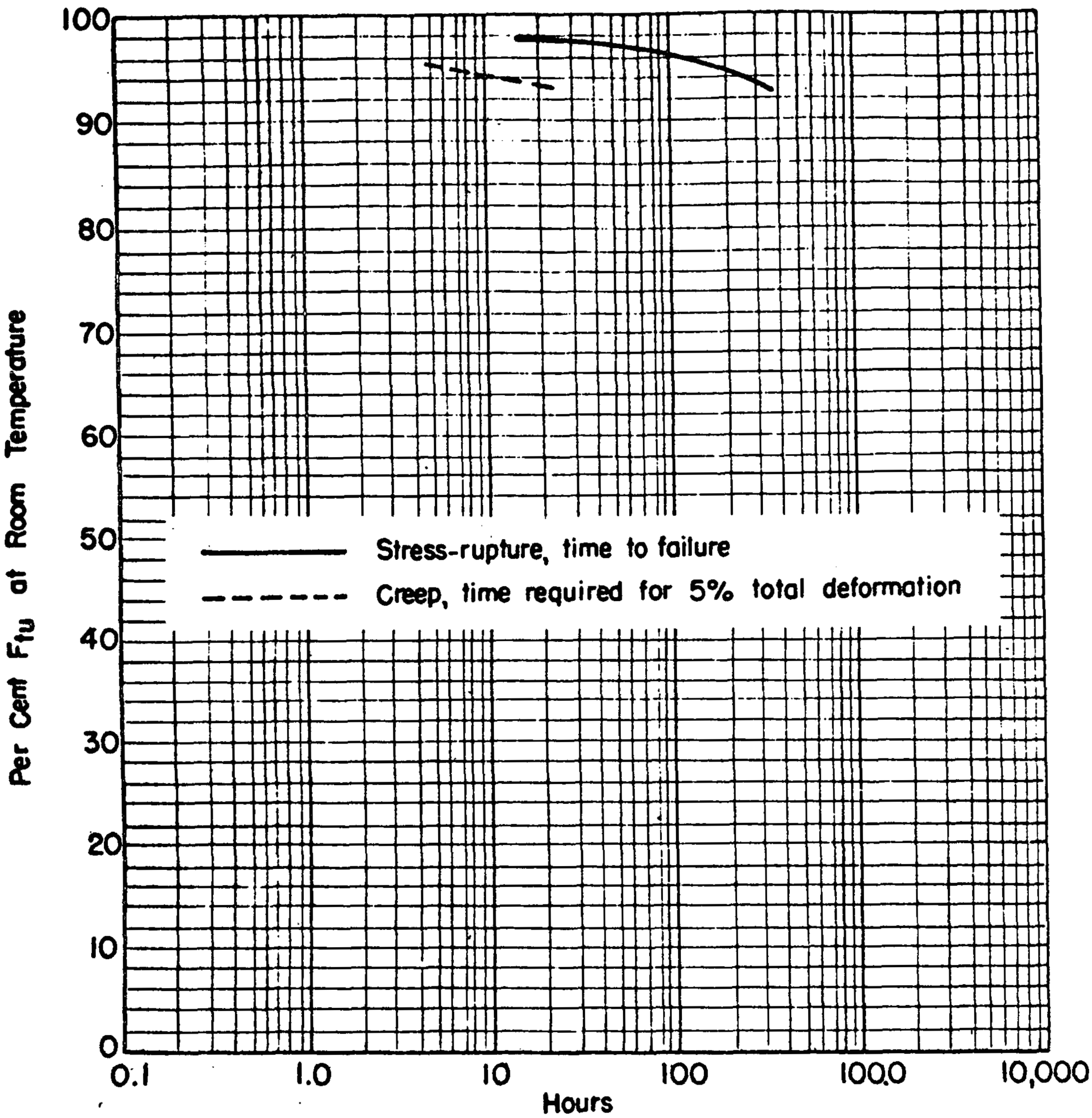

FIGURE 3.7.2.1.7(e). *Creep and stress-rupture properties of wrought 7075-T6 aluminum alloy at 94 F.*

Fig. 5-15 - Typical MIL-HDBK-5B Creep Data

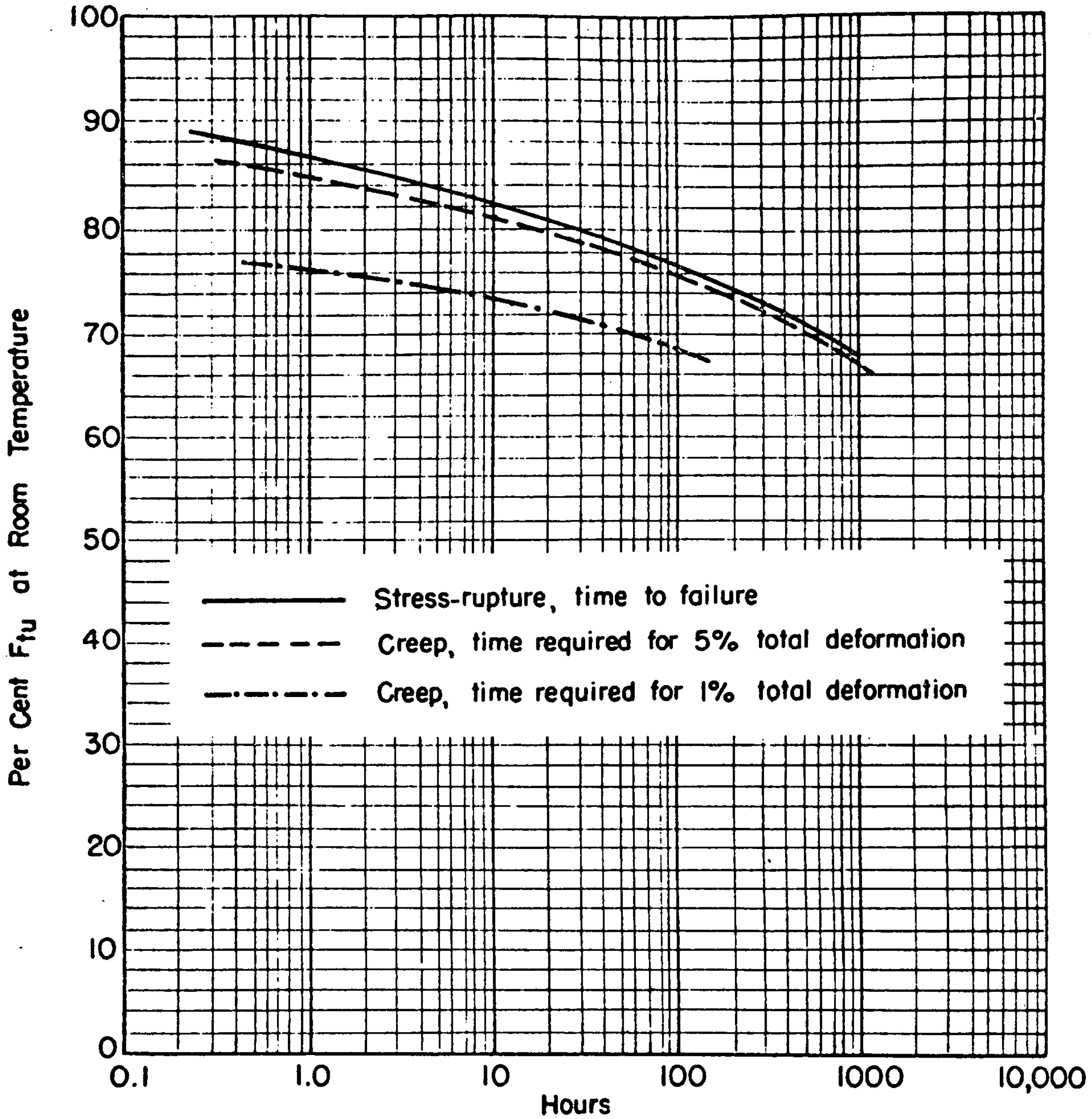

FIGURE 3.7.2.1.7(f). *Creep and stress-rupture properties of wrought 7075-T6 aluminum alloy at 211 F.*

Fig. 5-16 - Typical MIL-HDBK-5B Creep Data

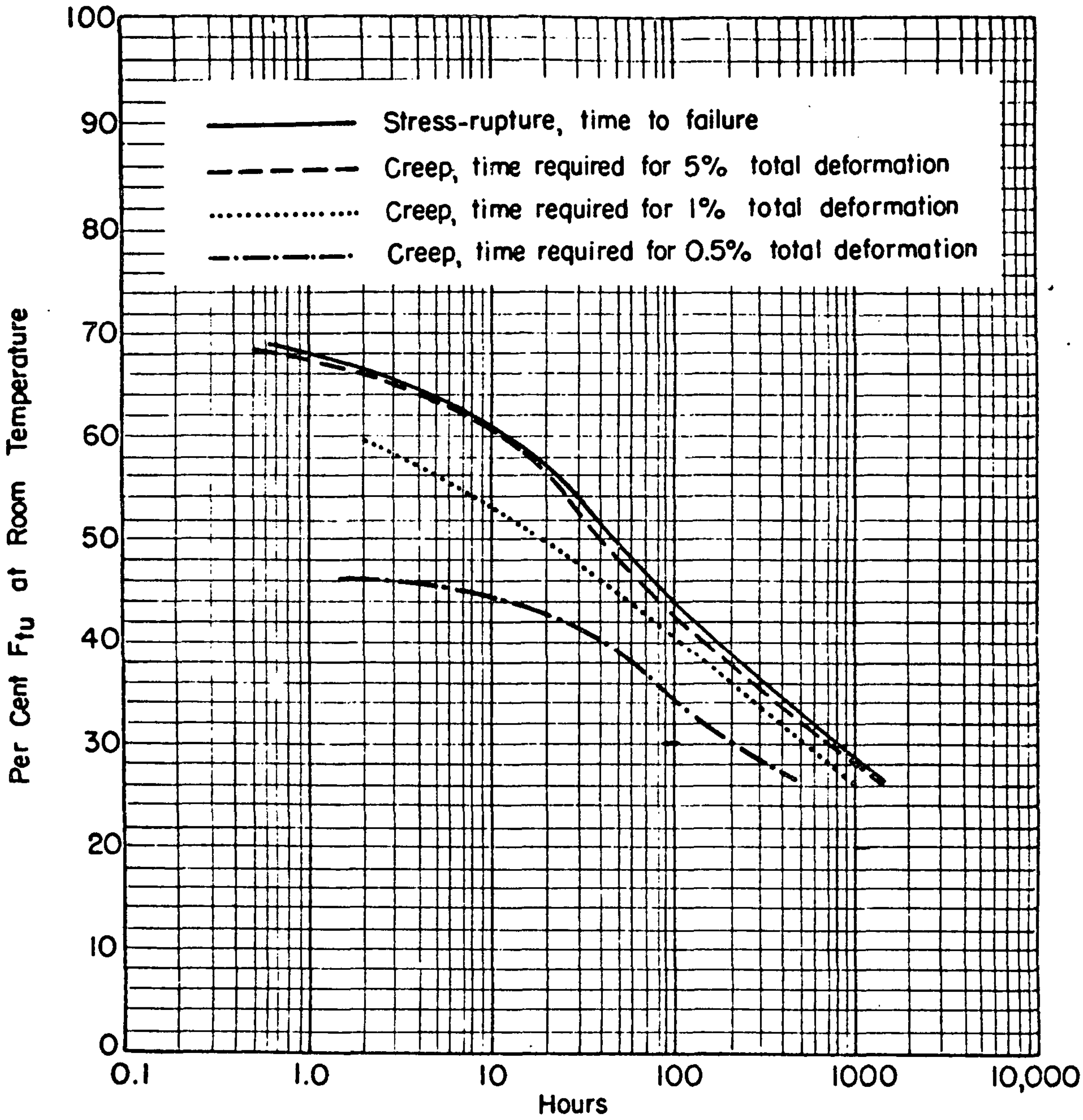

FIGURE 3.7.2.1.7(g). *Creep and stress-rupture properties of wrought 7075-T6 aluminum alloy at 300 F.*

Fig. 5-17 - Typical MIL-HDBK-5B Creep Data

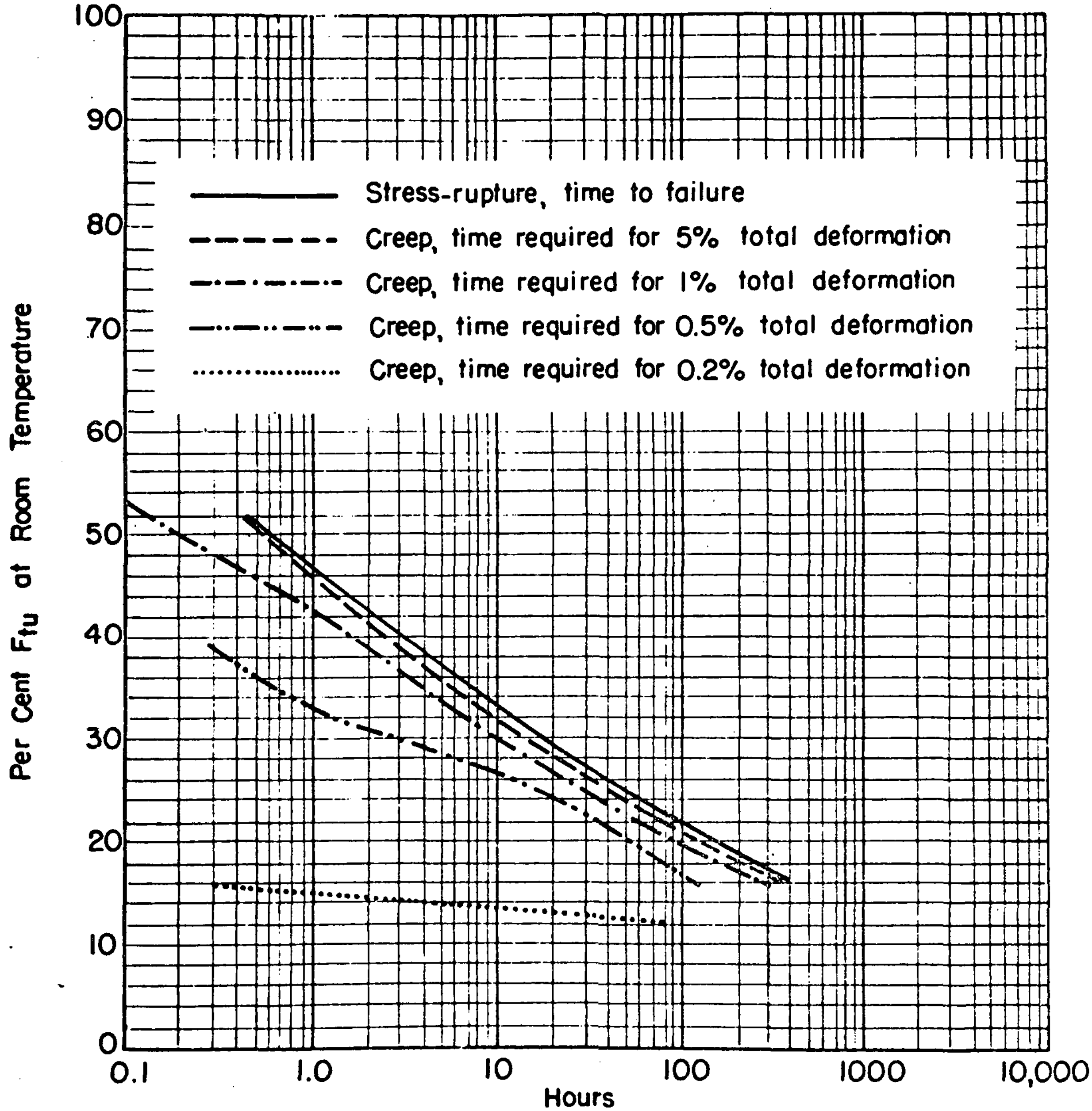

FIGURE 3.7.2.1.7(h). *Creep and stress-rupture properties of wrought 7075-T76 aluminum alloy at 375 F.*

Fig. 5-18 - Typical MIL-HDBK-5B Creep Data

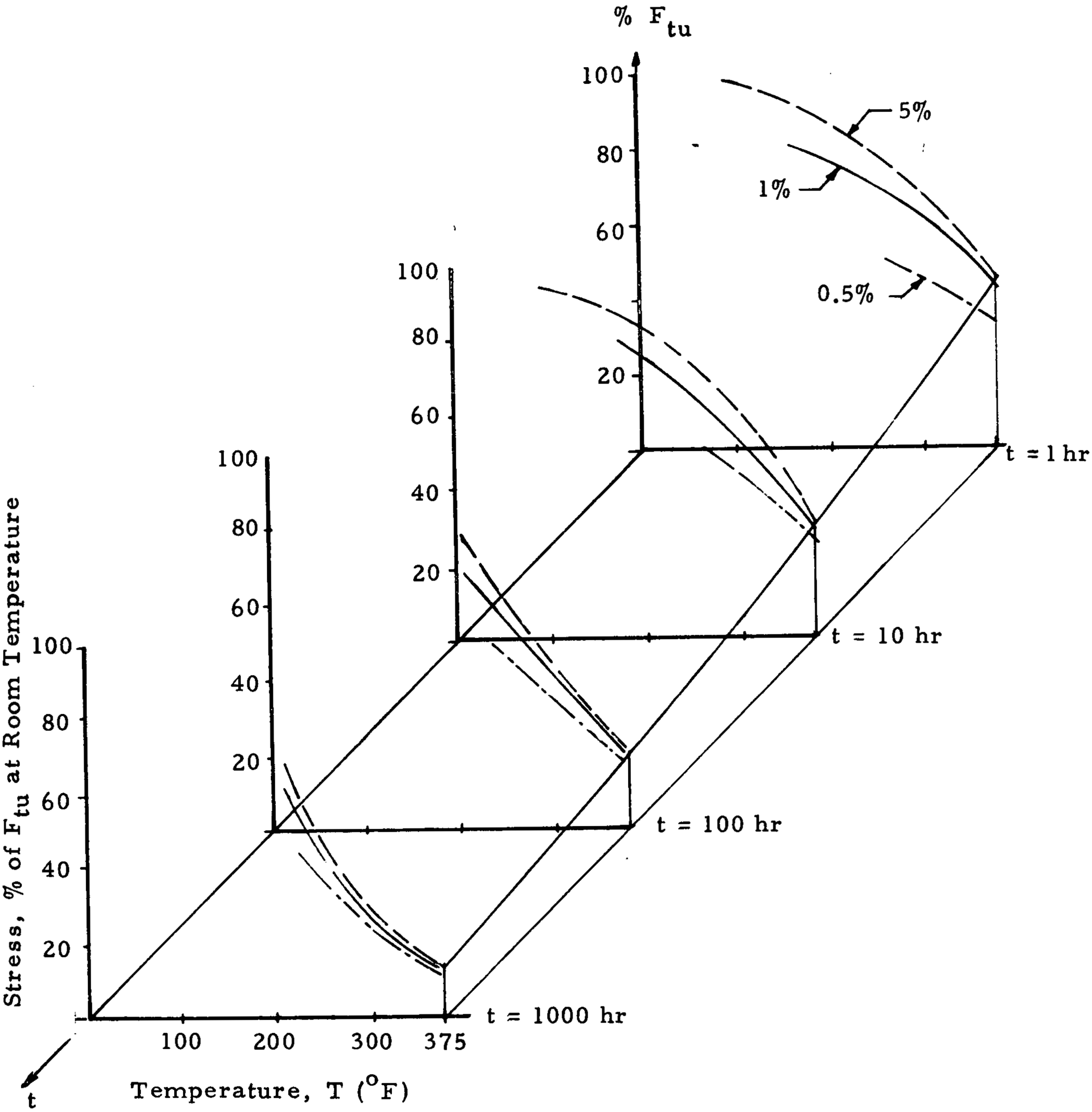

Fig. 5-19 - Creep-Temperature-Time Surface for 7075 Aluminum

5.4.2 Design Factors for Allowable Creep

The proposed approach to design for limiting creep deformations is similar to the approach to design for ultimate load failure. The allowable creep design factors are used to assure that adequate margins on load, temperature and time exist between the design conditions and the allowable creep surface.

Step 1 — Creep at a Service Life Factor of One

At a time equal to a service life factor of one, determine the allowable creep stress (the stress which results in the allowable creep strain) in the component at the limit temperature.

$$F_A(T_\ell, t/t_o = 1)$$

Compute the design stress, f_D,

$$f_D = K_c \cdot f_\ell$$

where

K_c is a creep F.S.
f_ℓ is a stress corresponding to limit load.

Compute the creep stress M.S.

$$M.S. = \frac{F_A\ (T_\ell, t/t_o = 1)}{f_D} - 1$$

Next, determine the allowable temperature which corresponds to f_ℓ

$$T_A(f_\ell, t/t_o = 1)$$

Compute a creep temperature margin

$$T.M. = T_A (f_\ell, t/t_o = 1) - T_\ell$$

The T.M. should be greater than a temperature safety margin, ΔT_c, which is analogous to a F.S. on mechanical loads.

Step 2 — Service Lifetime to Limiting Creep

The final check consists of computing a life margin(S.L.M.)corresponding to conditions of limit temperature and stress. Compute the allowable service life factor,

$$t_A/t_o (f_\ell, T_\ell)$$

Compute the S.L.M. from

$$S.L.M. = t_A/t_o (f_\ell, T_\ell) - t_D/t_o$$

where t_D/t_o is the design service life factor. The S.L.M. should be positive.

5.5 REFERENCES

5-1. Wolfe, M.O.W., "Aspects of Elevated Temperature Design and Design Criteria for Supersonic Aircraft Structures," Proc. of the Third Symposium on Naval Structural Mechanics, New York, 1963, pp.413-438.

5-2. Freudenthal, A.M., "Elevated Temperature Creep and Fatigue," High Temperature Structures and Materials, Pergamon Press, New York, 1958.

5-3. Coffin, L.F., "Thermal Stress and Thermal Stress Fatigue," Chap.V, Proceedings for Short Course Materials Engineering Design for High Temperature, Pennsylvania State University, June 1958.

5-4. Kennedy, A.J., Processes of Creep and Fatigue in Metals, Chap.5, "Fatigue," Oliver and Boyd, Edenburgh and London, 1962.

5-5. Taira, S., "Lifetime in Structures Subjected to Varying Load and Temperature," Creep in Structures, IUTAM Colloquium, Stanford, 1960, Academic Press, New York, 1962.

5-6. Taira, S., "Thermal Fatigue and Its Relation to Creep Rupture and Mechanical Fatigue," High Temperature Structures and Materials, McMillan, New York, 1964.

5-7. Lazan, B.J., "Fatigue of Structural Materials at High Temperature," High Temperature Effects in Aircraft Structures, Pergamon Press, New York, 1958.

5-8. Metallic Materials and Elements for Aerospace Vehicle Structures, MIL-HDBK-5B, Dept. of Defense, Washington, D.C., September 1971.

5-9. Doty, Ralph J., "Fatigue Design Procedure for the American SST Prototype," presented at the Sixth ICAF Symposium, Advanced Approaches to Fatigue Evaluation, Miami Beach, Fla., May 1971.

Appendix A
CREEP DATA FOR METALLIC MATERIALS

Appendix A

Material data for the group of metals listed in Table A-1 have been gathered from references listed in Section A.1 for each of the materials. One of the most striking features of these graphs, shown in Section A.2 is the extreme senstivity of some of the materials to variation of the data with stress and temperature.

A.1 MATERIAL REFERENCES

At elevated temperatures, material properties become greatly temperature and time dependent. These temperature-time-load characteristics must be known with a fair degree of confidence in the accuracy and reliability for the data to be useful in design work. In design handbooks such as MIL-HDBK-5B the following material properties can be found for most aerospace materials:

- Thermal conductivity, thermal expansion coefficient and specific heat versus temperature
- Strength versus temperature for various exposure times
- Charts for strength at test temperatures versus exposure time and exposure temperature
- Strength versus time for given total deformation (creep) at constant temperature
- Constant life diagrams for various exposure times at constant temperature
- Stress-strain diagrams for various temperatures
- Elastic modulus versus temperature
- Tangent moduli versus stress for given temperatures
- Nomogram for computing creep strain for given exposure time to given stress and temperature.

High temperature creep is one area where sufficient data are lacking for quite a few structural materials and in particular those materials applicable to high temperature ranges, Table A-1.

During the course of this study several creep references have been compiled and have been listed here as additional sources of information to supplement MIL-HDBK-5B. The materials are listed alphabetically by their common name with a short description of the information in each reference.

Aluminum

2024-T3

Heimerl, George J., and Arthur J. McEvily, Jr., "Generalized Master Curves for Creep and Rupture," NACA TN 4112, October 1957.

Master curves for creep rupture and minimum creep rate.

2219

Aerospace Structural Metals Handbook, Air Force Materials Laboratory, Wright Patterson AFB, Ohio, 1970.

σ versus t for percent creep and rupture for various temperatures.

Alloy Digest, Engineering Alloys Digest, Inc., Upper Montclair, N. J.

Data table σ versus t, percent creep in specific time.

7075-T6

Heimerl, George J., and Arthur J. McEvily, Jr., "Generalized Master Curves for Creep and Rupture," NACA TN 4112, October 1957.

Master curves for creep rupture and minimum creep rate.

Columbium (Niobium)

CB-753

Conway, J. B., and P. N. Flagella, "Creep-Rupture Data for the Refractory Metals to High Temperatures," Gordon and Breach Science Publishers, 1971.

σ versus t for various percent creep for two temperatures

Table A-1
TEMPERATURE AND MATERIALS

Temperature Range °K (°F)	Material
530 - 590°K (500 - 600°F)	Aluminum 2219-T6
620 - 670°K (650 - 750°F)	Titanium 6Al-4V
810 - 920°K (1000 - 1200°F)	
920 - 1150°K (1200 - 1600°F)	Rene' 41
1030 - 1250°K (1400 - 1800°F)	L 605
920 - 1150°K (1200 - 1600°F)	Inconel 702
1290 - 1480°K (1860 - 2200°F)	Tantalum T-111
1330 - 1370°K (1935 - 2000°F)	Molybdenum TZC
1250 - 1480°K (1800 - 2200°F)	Columbium Cb-753
1250 - 1480°K (1796 - 2200°F)	Columbium D-43

Cb-752

Conway, J. B., and P. N. Flagella, "Creep-Rupture Data for the Refractory Metals to High Temperatures," Gordon and Breach Science Publishers, 1971.

σ versus t for percent creep for three temperatures

D-43

Conway, J. B., and P. N. Flagella, "Creep-Rupture Data for the Refractory Metals to High Temperatures," Gordon and Breach Science Publishers, 1971.

σ versus t for percent creep at three temperatures

Aerospace Structural Metals Handbook, Air Force Materials Laboratory, Wright-Patterson AFB, Ohio, 1970.

Larson-Miller parameter and creep rupture curves for three temperatures.

Inconel (Nickel-base alloy)

Inconel 702

Aerospace Structural Metals Handbook, Air Force Materials Laboratory, Wright-Patterson AFB, Ohio, 1970.

Larson-Miller Parameter of 0.2% creep and creep rupture, 1970.

"Research Investigation to Determine Mechanical Properties of Nickel and Cobalt-Base Alloys for Inclusion in Military Handbook-5," ML-TDR-64-116, Air Force Materials Laboratory, Wright-Patterson Air Force Base, Ohio, October 1964.

σ versus t at various T for various percent deformations

Inconel X

Heimerl, George J., and Arthur J. McEvily, Jr., "Generalized Master Curves for Creep and Rupture," NACA TN 4112, October 1957.

Master curves for creep rupture and minimum creep rate.

L605 (Cobalt base alloy)

"Joint International Conference on Creep, 1963," sponsored by ASME, ASTM and the Institution of Mechanical Engineers, 1963.

σ versus t for 0.5% creep for three T

Aerospace Structural Metals Handbook, Air Force Materials Laboratory, Wright-Patterson AFB, Ohio, 1970.

Manson-Haferd parameter for 0.5% and 1.0% plastic strain

σ versus percent plastic ϵ at 1800°F for various t intervals

Alloy Digest, Engineering Alloys Digest, Inc., Upper Montclair, N. J.

"Research Investigation to Determine Mechanical Properties of Nickel and Cobalt-Base Alloys for Inclusion in Military Handbook-5," ML-TDR-64-116, Air Force Materials Laboratory, Wright-Patterson Air Force Base, Ohio, October 1964.

σ versus t at various T for various percent deformation

Molybdenum

TZC Alloy

Sawyer, J. C., and E. A. Steigerwald, "Generation of Long Time Creep Data of Refractory Alloys at Elevated Temperatures," TRW, Inc., Cleveland, Ohio, (NASA CR-1115).

Larson-Miller parameter, 0.5% creep

TZM Alloy

Aerospace Structural Metals Handbook, Air Force Materials Laboratory, Wright-Patterson AFB, Ohio, 1970.

Creep rupture curves σ versus t for Ts.

σ versus t for percent creep at 2000°F

Rene' 41 (Nickel-base alloy)

"Joint International Conference on Creep, 1963," sponsored by ASME, ASTM and the Institution of Mechanical Engineers, 1963.

σ versus $\dot{\epsilon}$ for various T

Aerospace Structural Materials Handbook, Air Force Materials Laboratory, Wright-Patterson AFB, Ohio, 1970.

Manson-Succop Parameter - Creep Rupture, 1970 edition.

Larson-Miller Parameter - 2% creep + σ versus t for various T, 1966 data.

Gluck, J. V., and James W. Freeman, "Effect of Creep-Exposure on Mechanical Properties of Rene' 41," ASD TR 61-73, Air Force Material Laboratory, Wright-Patterson Air Force Base, Ohio, August 1961.

Plots of ϵ versus t - obtain strain intercept data

"Research Investigation to Determine Mechanical Properties of Nickel and Cobalt-Base Alloys for Inclusion in Military Handbook-5," ML-TDR-64-116, Air Force Materials Laboratory, Wright-Patterson Air Force Base, Ohio, October 1964.

σ versus t at various T for various percent deformation

Steel

Carbon-Molybdenum Steel and 18-8 Cb Stainless Steel

Heimerl, George J., and Arthur J. McEvily, Jr., "Generalized Master Curves for Creep and Rupture," NACA TN 4112, October 1957.

Master curves for creep rupture and minimum creep rate.

Tantalum

T-111 Alloy, and T-222

Sawyer, J. C., and E. A. Steigerwald, "Generation of Long Time Creep Data of Refractory Alloys at Elevated Temperatures," TRW, Inc., Cleveland, Ohio, (NASA CR-1115).

Larson-Miller and Marson-Haferd Parameters of 1% creep at 3000°F

Plots of percent creep versus t for different T and σ (T-111)

Aerospace Structural Metals Handbook, Air Force Materials Laboratory, Wright-Patterson AFB, Ohio, 1970.

Stress rupture curves at 2400°F

TD-Ni Cr

Hirschberg, M. H., David A. Spera and Stanley J. Klima, "Cyclic Creep and Fatigue of TD-Ni Cr, TD-Ni, and Ni Cr Sheet at 1200C," NASA TD D-6649, February 1972.

Creep rupture curves (1200°C)

Titanium

Ti-6Aℓ-4V

"Joint International Conference on Creep, 1963," sponsored by ASME, ASTM and the Institution of Mechanical Engineers, 1963.

ϵ versus t for various T at constant σ

Alloy Digest, Engineering Alloys Digest, Inc., Upper Montclair, N.J.

Plot of total creep versus t for two T and two σ.

Aerospace Structural Metals Handbook, Air Force Materials Laboratory, Wright-Patterson AFB, Ohio, 1970.

σ versus t for various T at specific percent creep.

Tungsten

Conway, J. B., and P. N. Flagella, "Creep-Rupture Data for the Refractory Metals to High Temperatures," Gordon and Breach Science Publishers, 1971.

ϵ versus t curves

Creep rupture curves

σ versus $\dot{\epsilon}$ for various temperatures

Larson-Miller parameter for rupture

Aerospace Structural Metals Handbook, Air Force Materials Laboratory, Wright-Patterson AFB, Ohio, 1970.

Creep rupture curves for four temperatures.

A.2 CREEP CURVES FOR CONSTANT STRESS AND TEMPERATURE

In this section curves of the type of Fig. 2-2 are presented for a variety of metallic materials. This is the form in which the data can be used for creep calculations (Figs. A-1 through A-9).

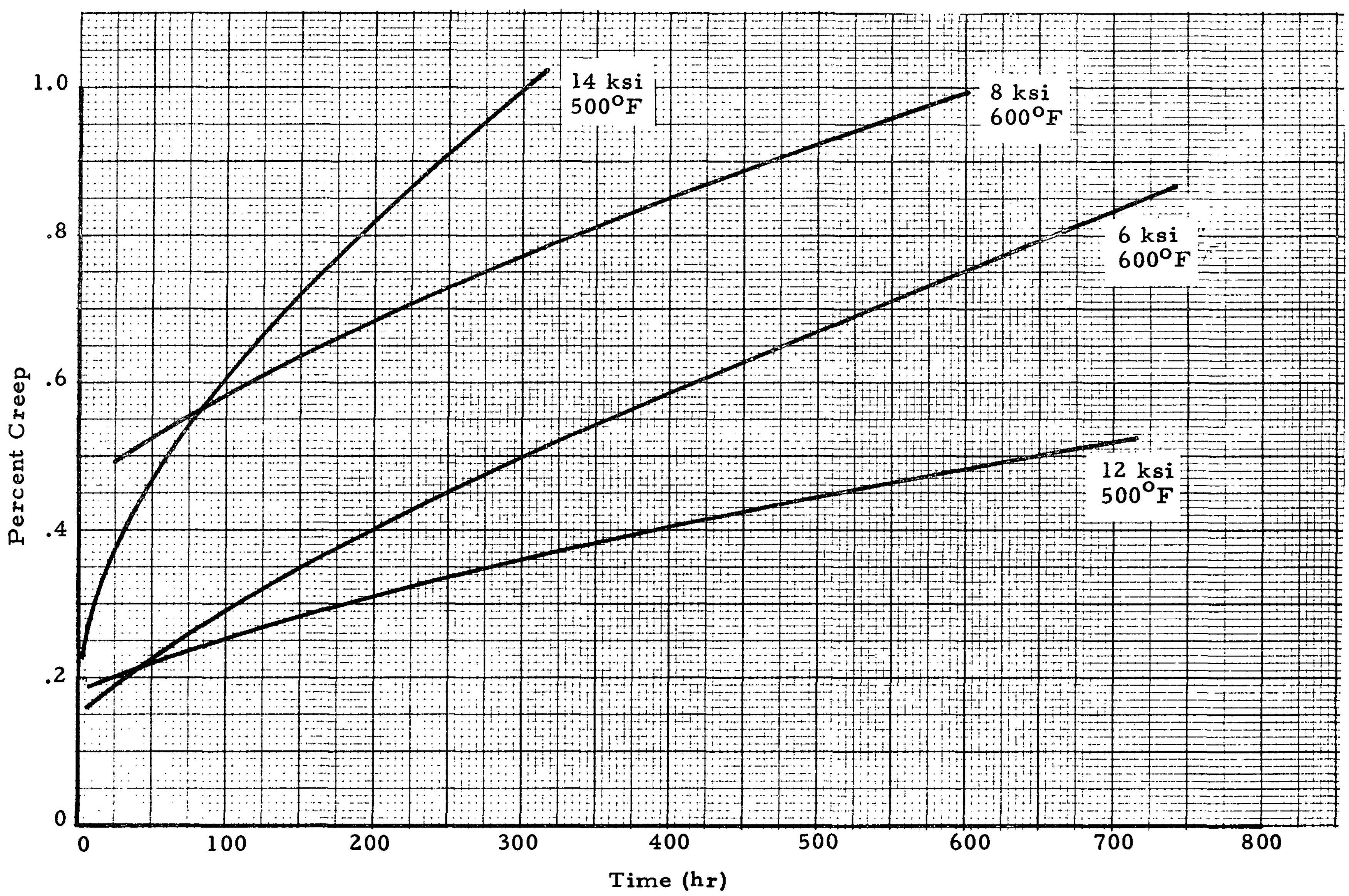

Fig. A-1 - Aluminum 2219-T6

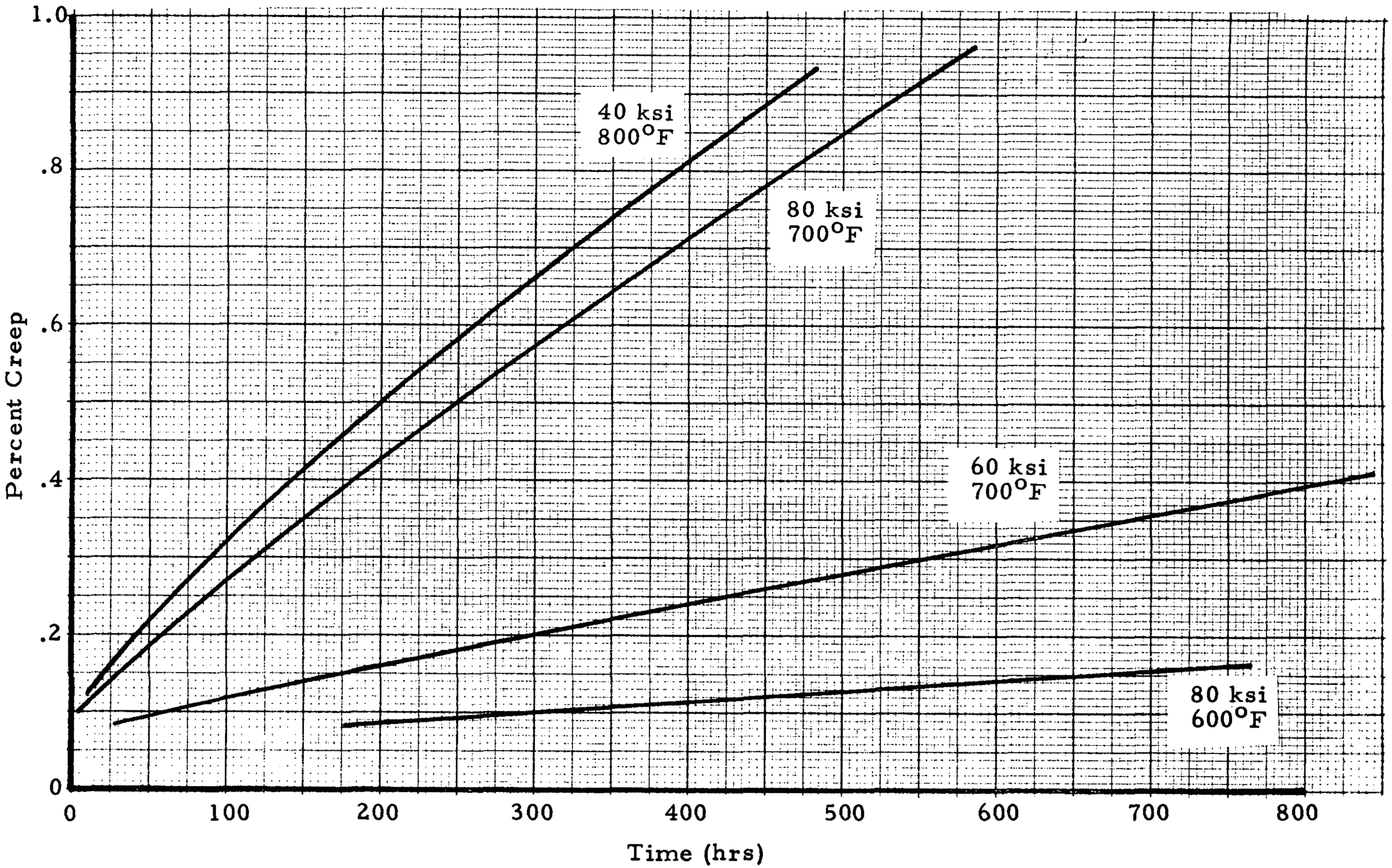

Fig. A-2 - Titanium - 6Aℓ-4V Sheet

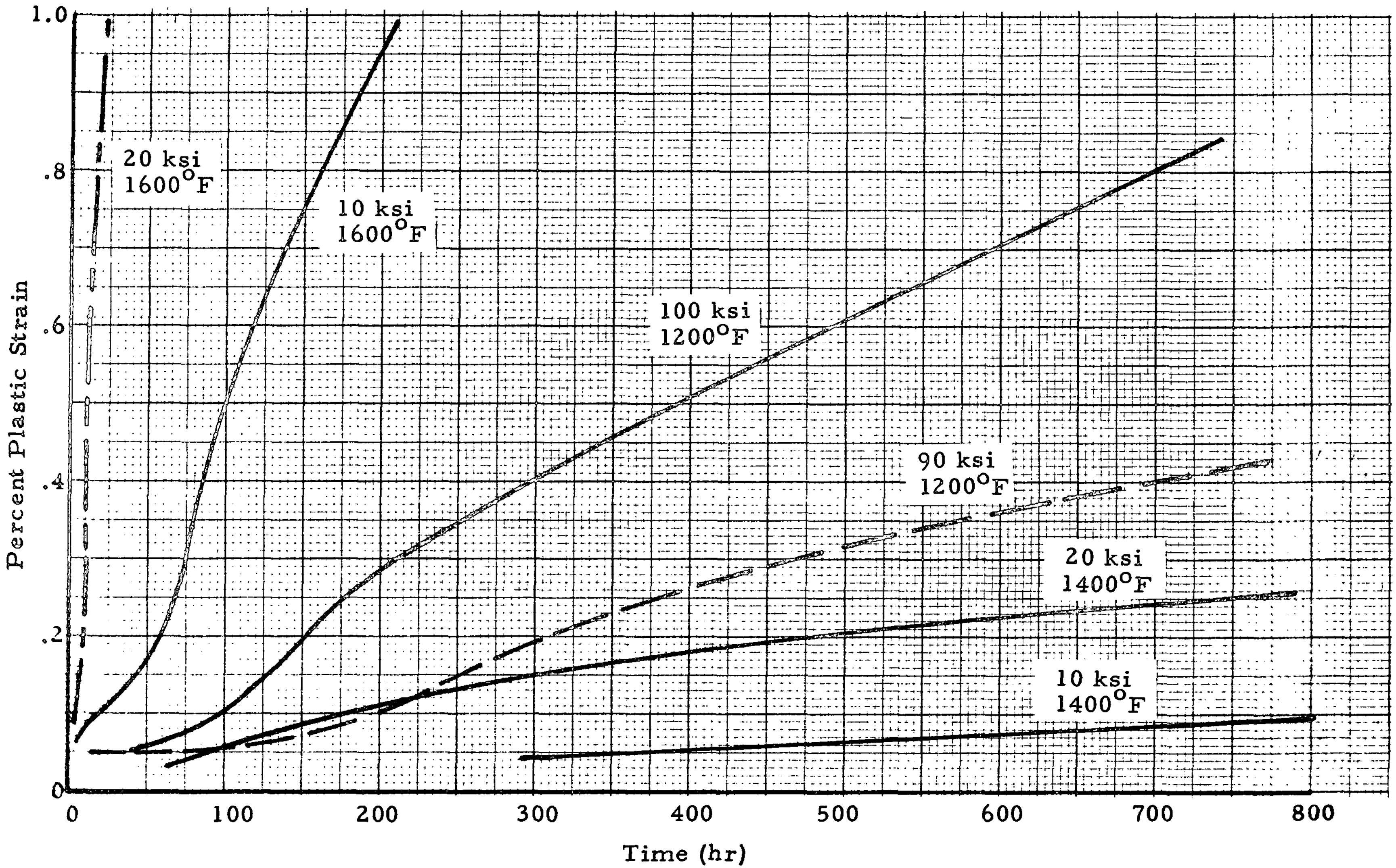

Fig. A-3 - Rene' 41 Sheet

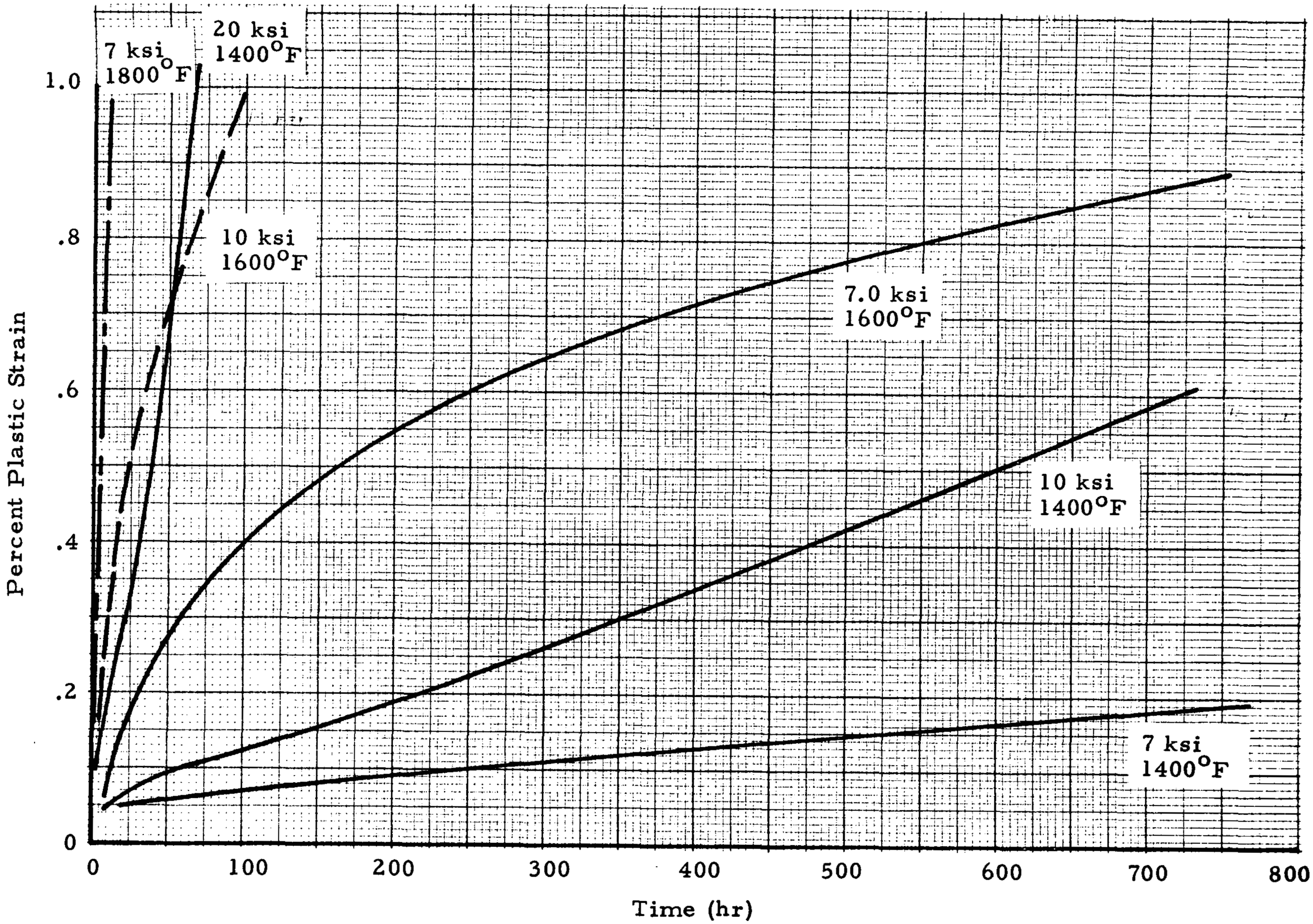

Fig. A-4 - L605 Sheet

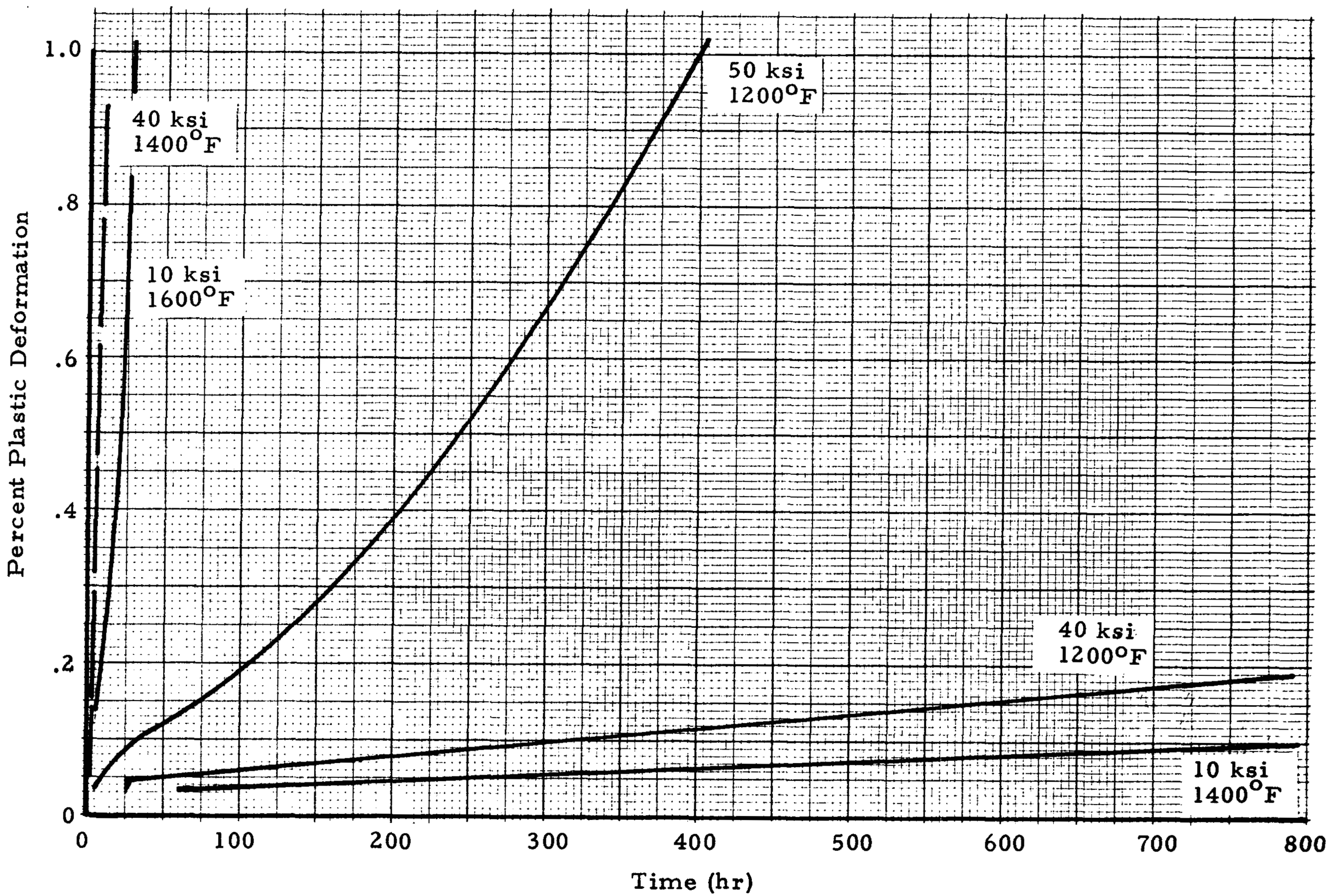

Fig. A-5 - Inconel 702

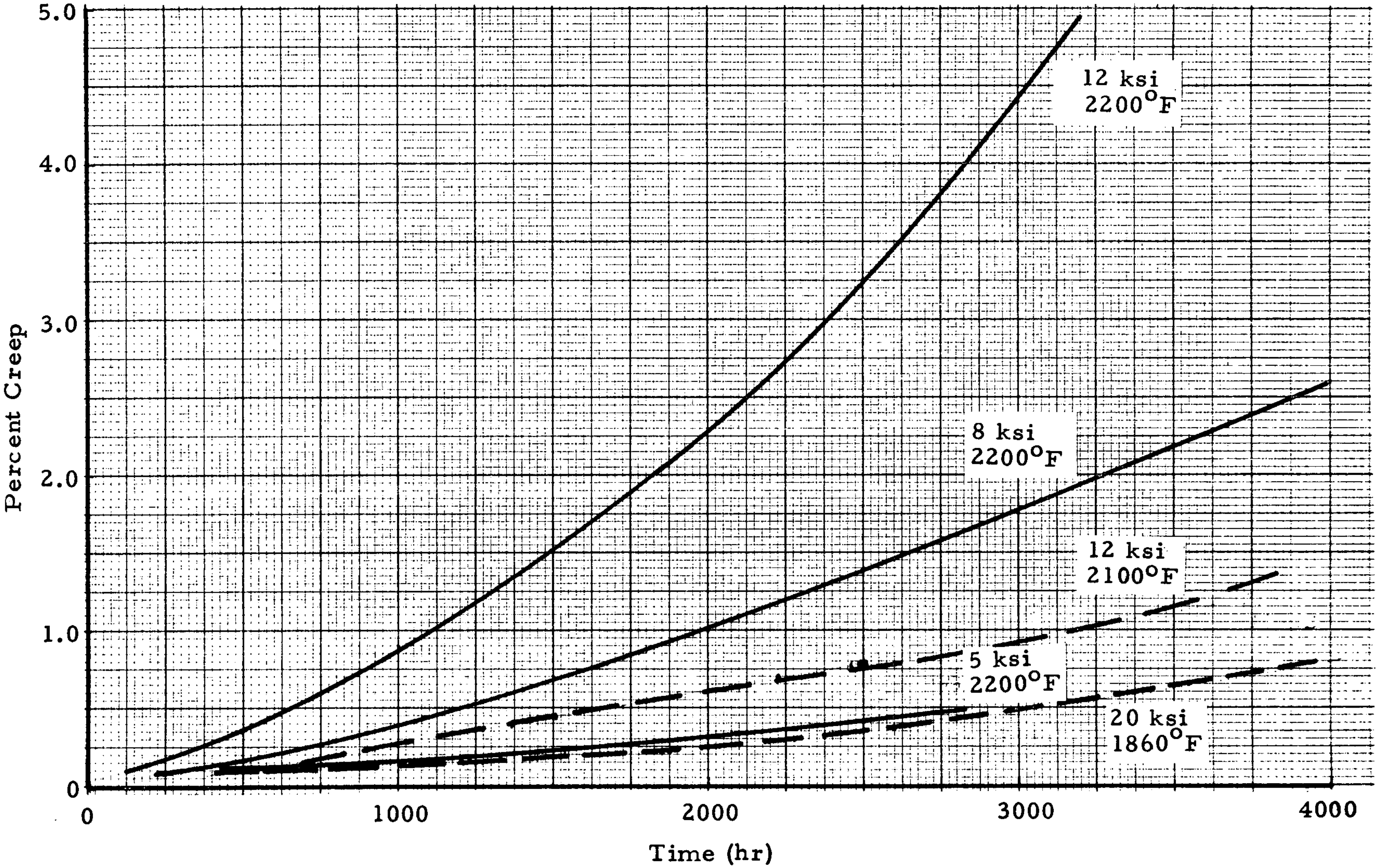

Fig. A-6 - Tantalum T-111 Alloy

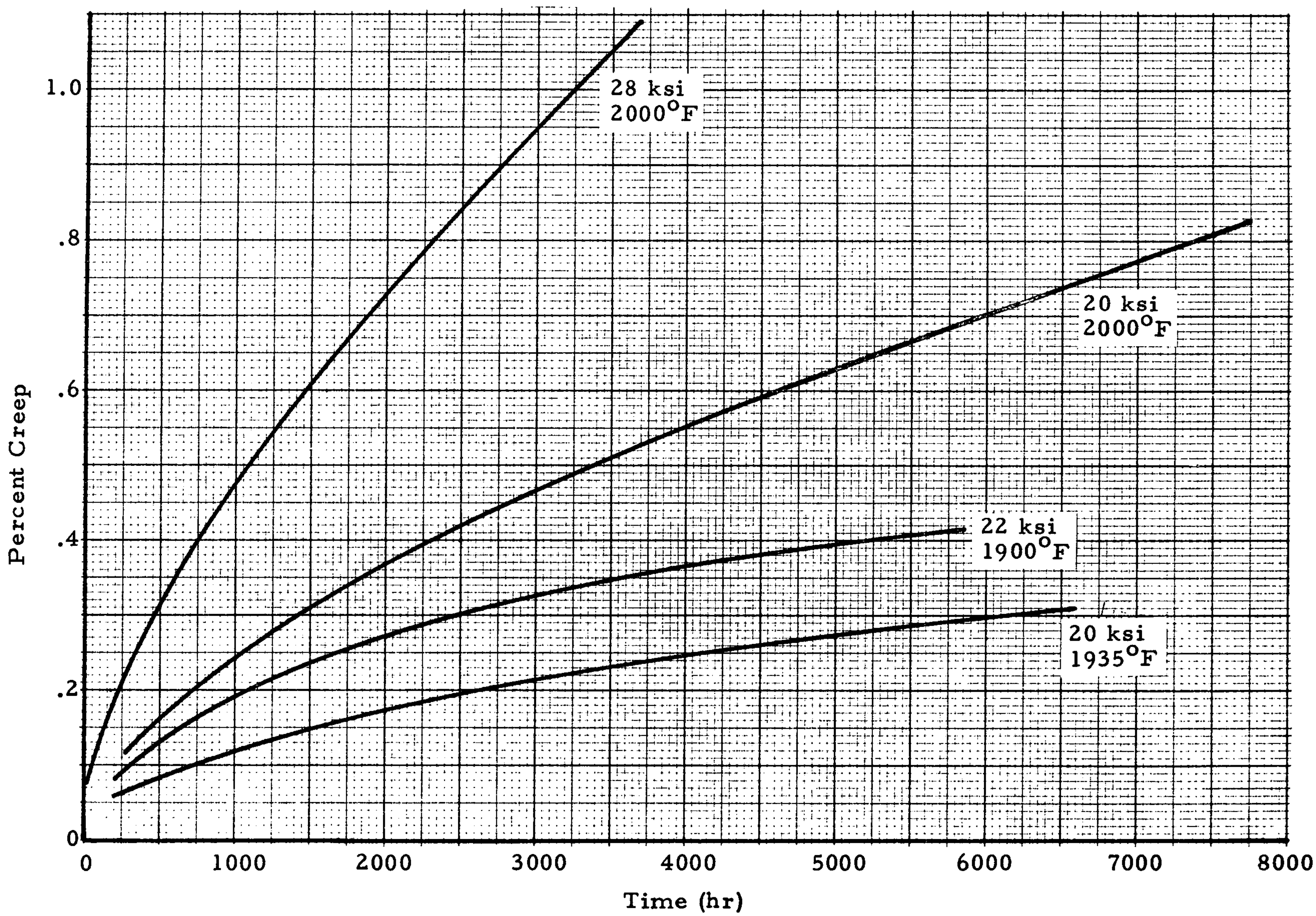

Fig. A-7 - Molybdenum TZC Alloy

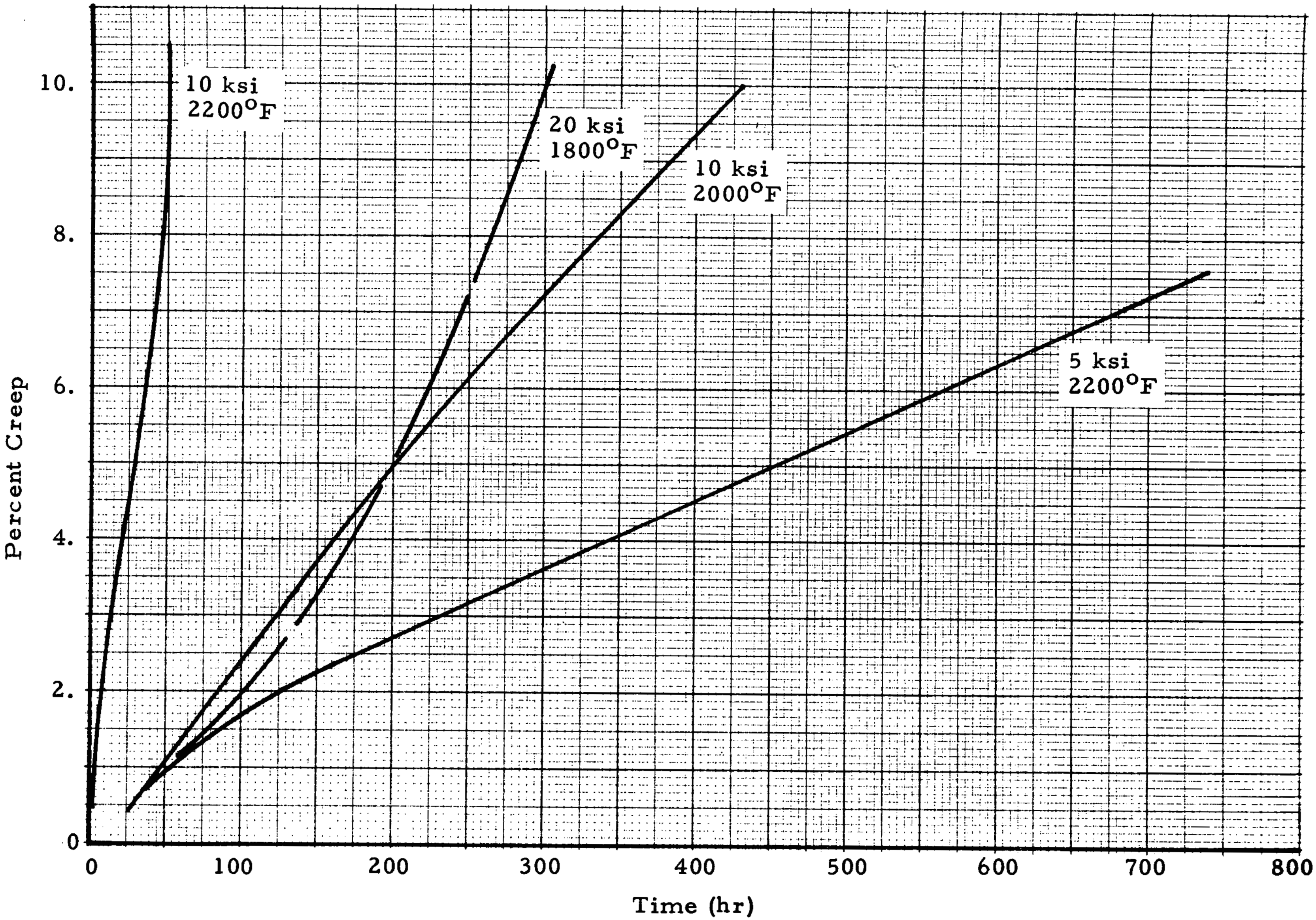

Fig. A-8 - Columbium CB-753 Alloy

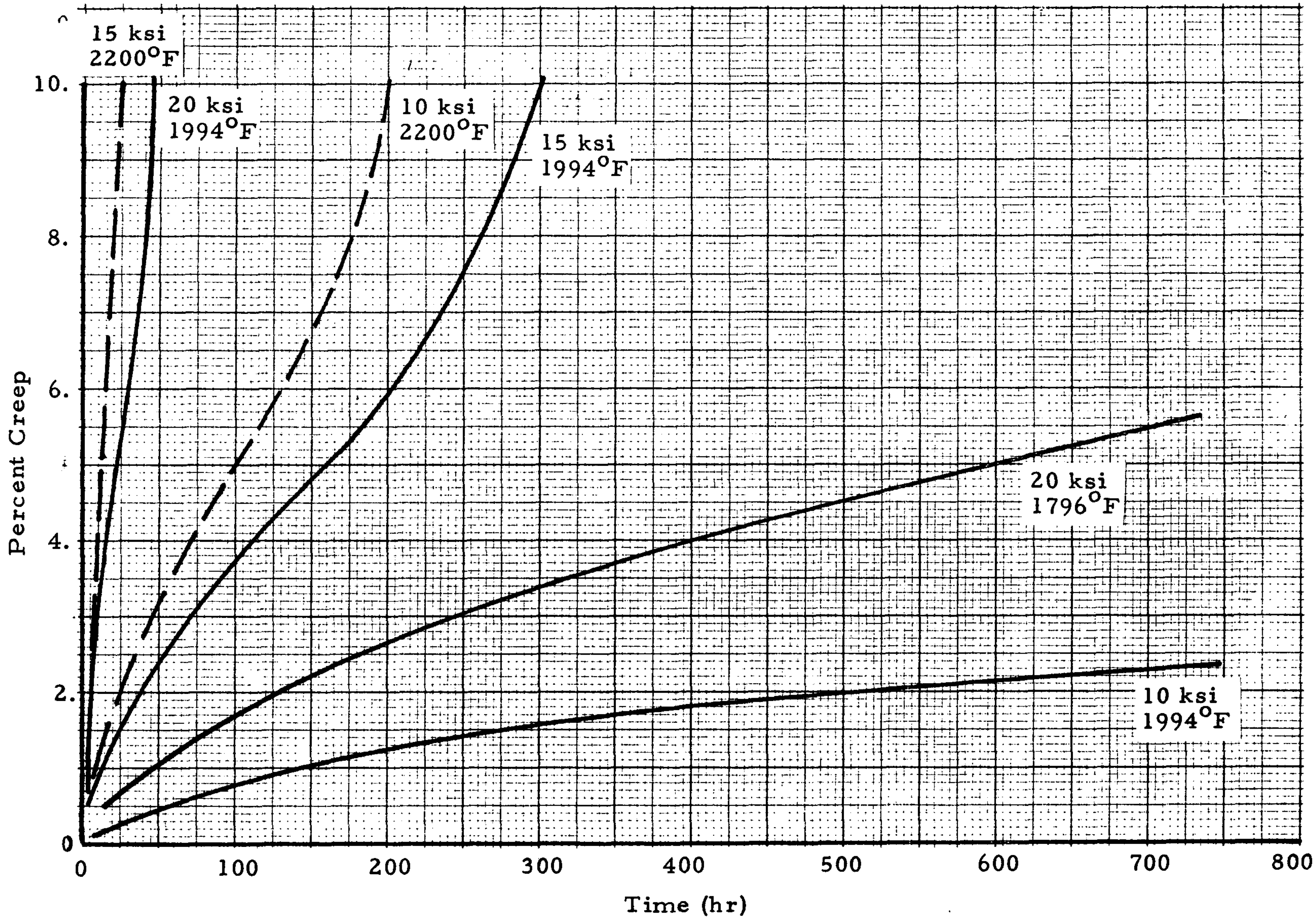

Fig. A-9 - Columbium D-43 Alloy

Appendix B

CREEP ANALYSIS PROGRAM

Appendix B

The program input data, sample problem, program listing and the output for the sample problem are included in this appendix.

B.1 PROGRAM INPUT

The required data input and format to be followed are outlined in the following statements. Note, at least two cards are required in several sections of data, Cards 1, 2, 5 and 6. Number of cards depend on number of data sets to be entered.

Cards 1

NSIG, DTITLE, (SIGMA(I), P(I), I=1, NSIG)
FORMAT (I5, 10A6/(8E10.4))

NSIG	Number of sets of data points to be entered
DTITLE	Title or label for data
SIGMA(I)	Stress value from master creep rupture parameter curve (psi), largest stress value first.
P(I)	Corresponding parameter value

*NOTE: Correct parameter equation must be input into the program corresponding to the parameter data input, see Section 2.9.

Cards 2

NC, STRN, CTITLE, (SIGCR(I), PCR(I), I=1, NC)
FORMAT (I5, E10.4, 9A6/(8E10.4)

NC	Number of sets of data points to be entered

STRN	Percent creep strain for which the parameter data applies, i.e., 0.2% creep strain, etc.
CTITLE	Title or label for data
SIGCR(I)	Stress value from master creep parameter curve (psi), largest stress value first
PCR(I)	Corresponding parameter value

*See note in Cards 1

Card 3

STRMAX
FORMAT (E10.4)

STRMAX	Maximum strain value allowed (in. /in.), card can be left blank.

Card 4

LIREQ
FORMAT (E10.4)

LIREQ	Total life required (hrs)

Cards 5

NS, TITLE, (STRESS(J), TEMP(J), TIME(J), J=1, NS)
FORMAT (I5, 10A6/(3E10.4))

NS	Number of load cases
TITLE	Descriptive label for load cases
STRESS(J)	Stress level (psi)
TEMP(J)	Temperature (°F)
TIME(J)	Time period stress and temperature applied (hrs)

*NOTE: A stress, temperature and time constitute a load case.

Cards 6

NSTR, VSTRES(I), VTEMP(I), (VTIM(J, I), VSR(J, I), J=1, NSTR)
FORMAT (I5, 5X, E10.4, E10.4/(8E10.4))

NSTR	Number of data sets
VSTRES(I)	Stress level for which data applies (psi)
VTEMP(I)	Temperature level for which data applies (°F)
VTIM(J, I)	Time values from plot of transient strain vs time (hr)
VSR(J, I)	Corresponding transient strain value (in. /in.)

*NOTE: NS sets of transient creep data must be input, I=1, NS. The order of the NS sets of data does not have to be the same as the order in the load cases. The program will automatically search for the correct data based on VSTRES and VTEMP.

B.2 SAMPLE PROBLEM

An example problem has been constructed using Rene' 41 material and a variable loading condition. The following stress history was input.

Table 1
LOAD CONDITIONS

NS	Stress (psi)	Temperature (°F)	Time (hr)
1	25,000	1600	4.0
2	35,000	1500	3.5
3	85,000	1300	4.5
4	100,000	1300	1.5

The Manson-Succop creep rupture parameter for Rene' 41 was taken from Ref. B-1 and the Larson-Miller creep parameter for 0.2% creep strain from Ref. B-2. A maximum allowable strain of 0.15 in. /in. and a required life of 200 hours were arbitrarily chosen.

Transient creep strain data were determined for Rene' 41 from the data presented in Ref. B-3. These material data, Fig. B-1, were derived only for use in writing and checking out the operation of the digital computer program and should be used with caution.

The output data and plots for this problem are given in Section B.4.

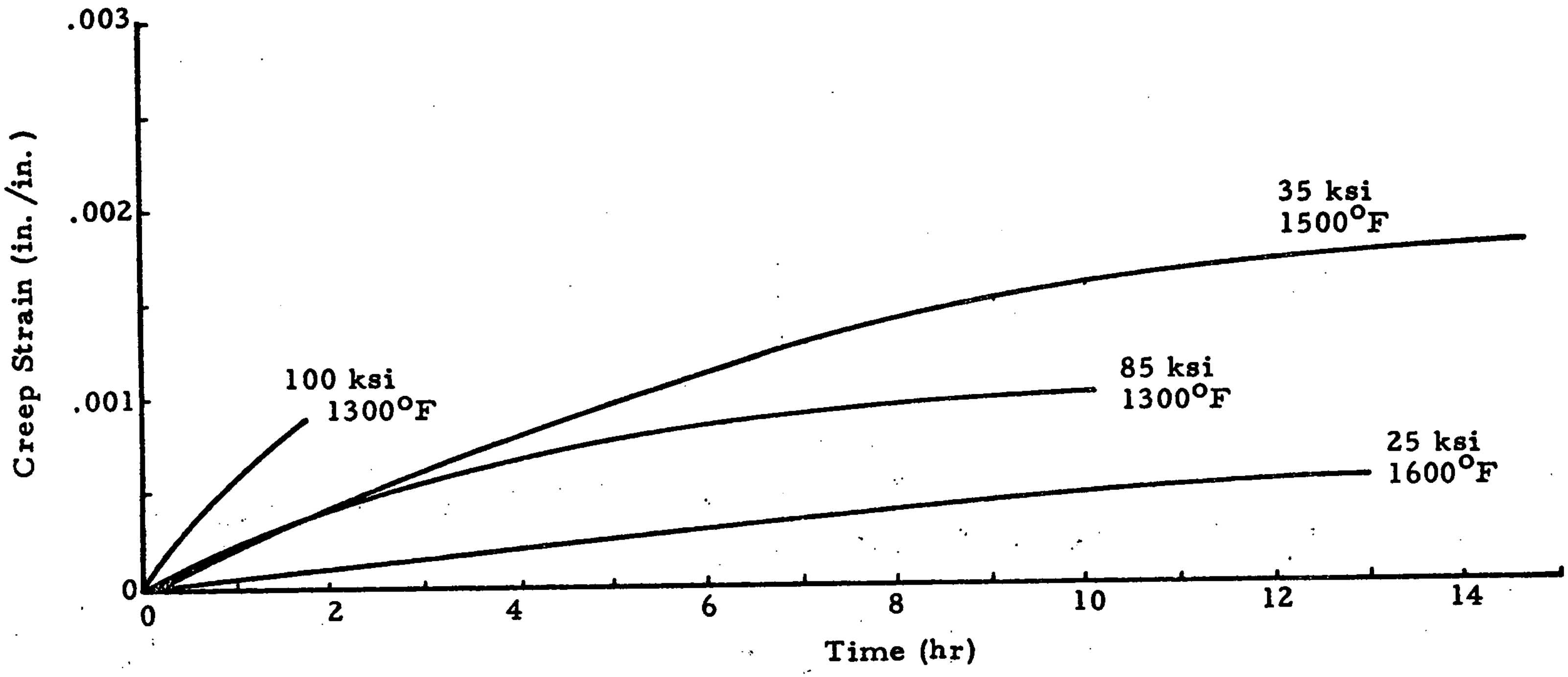

Fig. B-1 - Transient Creep Strain, Rene' 41

0001 002270 920L	0000 I 007055 BCDX	0000 R 007071 BCDY	0000 R 007413 COEFFM	0000 R 001666 CRATE
0000 R 007373 CRATE1	0000 R 007401 CRATE2	0000 R 001750 CREEP	0000 R 007357 CREEPT	0000 R 002222 CTITLE
0000 R 007405 CX	0000 R 007406 DELSTR	0000 R 002210 DTITLE	0000 R 007131 EXPN	0000 R 007414 FS
0000 R 000764 FSUM	0000 R 000702 FT	0000 R 007404 FX	0000 I 007347 I	0000 I 007354 J
0000 I 007361 K	0000 D 007155 K1	0000 D 007225 K2	0000 I 007356 L	0000 R 007345 LIREQ
0000 I 007362 N	0000 I 007350 NC	0000 I 007415 NP	0000 I 007353 NS	0000 I 007346 NSIG
0000 I 007355 NSTR	0000 I 003301 NV	0000 R 000062 P	0000 R 001440 PC	0000 R 001274 PCR
0000 R 007371 PMTL1	0000 R 007377 PMTL2	0000 R 007372 PMT1	0000 R 007400 PMT2	0000 R 000454 PX
0000 R 007370 P1	0000 R 007376 P2	0000 D 007275 Q	0000 R 001356 SIGCLG	0000 R 001212 SIGCR
0000 R 000144 SIGLOG	0000 R 000000 SIGMA	0000 R 001130 STLOG	0000 R 007375 STL1	0000 R 002233 STPRI
0000 R 007363 STPRI1	0000 R 007364 STPRI2	0000 R 007402 STR	0000 R 000226 STRESS	0000 R 007352 STRMAX
0000 R 007351 STRN	0000 R 007365 STRO	0000 R 007374 ST1	0000 R 006627 SY	0000 R 001604 TC
0000 R 001522 TCLOG	0000 R 000310 TEMP	0000 R 000372 TIME	0000 R 005725 TIME1	0000 R 006153 TIME2
0000 R 007410 TISUM	0000 R 002176 TITLE	0000 R 000536 TLOG	0000 R 007412 TMAX	0000 R 007407 TO
0000 R 000620 TR	0000 R 007105 TREM	0000 R 007360 TS	0000 R 002461 TSTR	0000 R 006401 TX
0000 R 007403 TXX	0000 R 002707 T2	0000 R 004544 VSR	0000 R 003135 VSTRES	0000 R 003217 VTEMP
0000 R 003363 VTIM	0000 R 007411 XLIFE	0000 R 001046 XMAR	0000 R 007366 XT1	0000 R 007367 XT2

```
      DIMENSION SIGMA(50),P(50)
      DIMENSION SIGLOG(50),STRESS(50),TEMP(50),TIME(50),PX(50),TLOG(50)
      DIMENSION TR(50),FT(50),FSUM(50),XMAR(50),STLOG(50)
      DIMENSION SIGCR(50),PCR(50),SIGCLG(50), PC(50),  TCLOG(50),TC(50),
     1CRATE(50),CREEP(50,3),TITLE(10),DTITLE(10),CTITLE(9)
      DIMENSION STPRI(50,3),TSTR(50,3),T2(50,3)
      DIMENSION VSTRES(50),VTEMP(50),NV(50),VTIM(25,25),VSR(25,25),
     1TIME1(50,3),TIME2(50,3)
      DIMENSION TX(50,3),SY(50,3),BCDX(12),BCDY(12)
      DIMENSION TREM(20),EXPN(20),K1(20),K2(20),Q(20)
      REAL LIREQ
      INTEGER BCDX
      DOUBLE PRECISION K1,K2,Q
C     THE FOLLOWING DATA ARE THE MANSON-SUCCOP PARAMETER AND STRESS
C     VALUES FOR RENE 41 BAR-CREEP RUPTURE(AERO.STRUCT.METALS HDBK-1970)
C         P=LOG(TIME) + 0.0108TEMP(DEG. F)
C     THE FIRST STRESS VALUE IS THE LARGEST STRESS VALUE IN THE TABLE
C
C     THE CREEP RUPTURE DATA ARE READ IN SIGMA AND P, SIGMA= STRESS AND
C     P= PARAMETER VALUE FROM MASTER CURVE
C
      READ(5,100) NSIG,DTITLE,(SIGMA(I),P(I),I=1,NSIG)
  100 FORMAT(I5,10A6/(8E10.4))
      IF(NSIG.EQ.0) GO TO 205
      WRITE(6,101) DTITLE
  101 FORMAT(1H1,10A6)
      WRITE(6,105) ((SIGMA(I),P(I)),I=1,NSIG)
  105 FORMAT(1H0,8E15.8)
      DO 110 I=1,NSIG
      SIGLOG(I)=ALOG10(SIGMA(I))
  110 CONTINUE
  205 CONTINUE
C
C     THE CREEP MASTER CURVE DATA ARE READ IN SIGCR AND PCR,  STRN= PER-
C     CENT CREEP FOR WHICH THE DATA APPLIES, SIGCR= STRESS AND PCR= PA-
C     RAMETER VALUE FROM THE MASTER CURVE
```

```
00161       C
00162             READ(5,210) NC,STRN,CTITLE,(SIGCR(I),PCR(I),I=1,NC)
00177         210 FORMAT(I5,E10.4,9A6/(8E10.4))
00200             IF(NC.EQ.0) GO TO 240
00202             WRITE(6,220) CTITLE,STRN
00211         220 FORMAT(1H0,9A6/1H0,23HAMOUNT OF CREEP STRAIN=,E15.8)
00212             WRITE(6,230) (SIGCR(I),PCR(I),I=1,NC)
00221         230 FORMAT(1H0,8E15.8)
00222             DO 250 I=1,NC
00225             SIGCLG(I)=ALOG10(SIGCR(I))
00226         250 CONTINUE
00230         240 CONTINUE
00231             READ(5,260) STRMAX
00234         260 FORMAT(E10.4)
00235 *DIAGNOSTIC*  THE TEST FOR EQUALITY BETWEEN NON-INTEGERS MAY NOT BE MEANINGFUL.
00235             IF(STRMAX.EQ.0.0) GO TO 270
00237             WRITE(6,265) STRMAX
00242         265 FORMAT(1H0,22HMAX STRAIN ALLOWABLE=,E15.8)
00243         270 CONTINUE
00244             READ(5,405) LIREQ
00247         405 FORMAT(E10.4)
00250             WRITE(6,406) LIREQ
00253         406 FORMAT(1H0,14HLIFE REQUIRED=,E15.8)
00253       C
00253       C     THE FOLLOWING VALUES ARE THE APPLIED LOADS
00253       C     STRESS IS THE APPLIED STRESS LEVEL AT TEMP. AND THE PERIOD OF TIME
00253       C     THAT THE STRESS IS APPLIED ,  STRESS(PSI),TEMP(F), TIME(HR)
00253       C
00254             READ(5,115) NS,TITLE,(STRESS(J),TEMP(J),TIME(J),J=1,NS)
00271         115 FORMAT(I5,10A6/(3E10.4))
00272             WRITE(6,120)
00274         120 FORMAT(1H1, 54H THE FOLLOWING VALUES ARE THE PRESCRIBED LOADING CY
00274            1CLE/3X,11HSTRESS(PSI),11X,7HTEMP(F),14X,8HTIME(HR))
00275             WRITE(6,125) (STRESS(J),TEMP(J),TIME(J),J=1,NS)
00305         125 FORMAT(1H0,3(E15.8,5X))
00306             WRITE(6,501)
00310         501 FORMAT(1H1, 99HTHE FOLLOWING DATA ARE THE TRANSIENT CREEP STRAIN V
00310            2ALUES FOR THE LOAD STRESS AND TEMPERATURE VALUES)
00311             DO 500 I=1,NS
00314             READ(5,505)NSTR,VSTRES(I),VTEMP(I),(VTIM(J,I),VSR(J,I),J=1,NSTR)
00326         505 FORMAT(I5,5X,E10.4,E10.4/(8E10.4))
00327             WRITE(6,506)NSTR,VSTRES(I),VTEMP(I),(VTIM(J,I),VSR(J,I),J=1,NSTR)
00341         506 FORMAT(1H0,3HNV=,I5,5X,7HSTRESS=,E15.8,5X,5HTEMP=,E15.8/(6(E15.8,
00341            1 5X)))
00342             NV(I)=NSTR
00343         500 CONTINUE
00345             DO 131 L=1,3
00350             CREEPT=0.0
00351             TS=0.0
00352             DO 130 I=1,NS
00355             K=0
00356             IF(NSIG.EQ.0) GO TO 70
00360             IF(STRESS(I)-SIGMA(1))50,50,60
00363          50 CONTINUE
00364             IF(STRESS(I)-SIGMA(NSIG))60,70,70
00367          60 WRITE(6,65) I ,STRESS(I)
00373          65 FORMAT(4X,13HSTRESS VALUE(,I2, 2H)=,E15.8,2X,38HEXCEEDS THE RANGE
```

```
00373          1OF THE RUPTURE TABLE)
00374           TR(I)=0.0
00375           FT(I)=0.0
00376           K=1
00377        70 CONTINUE
00400           IF(NC.EQ.0) GO TO 370
00402           IF(STRESS(I)-SIGCR(1))350,350,360
00405       350 CONTINUE
00406           IF(STRESS(I)-SIGCR(NC))360,370,370
00411       360 WRITE(6,365) I,STRESS(I)
00415       365 FORMAT(4X,13HSTRESS VALUE(,I2,2H)=,E15.8,2X,36HEXCEEDS THE RANGE O
00415          1F THE CREEP TABLE)
00416           CREEP(I,L)=0.0
00417           GO TO 130
00420       370 CONTINUE
00421           STLOG(I)=ALOG10(STRESS(I))
00422           IF(NSIG.EQ.0) GO TO 310
00424           IF(K.GT.0) GO TO 320
00426           CALL  GIR1(STLOG(I),PX(I),SIGLOG,P,NSIG)
00426     C
00426     C     THE FOLLOWING EQUATION IS THE MANSON-SUCCOP PARAMETER EXPRESSION
00426     C
00427           TLOG(I)=PX(I)-(.0108*TEMP(1))
00427     C ****
00427     C ****
00430           TR(I)=10.0**TLOG(I)
00431           FT(I)=TIME(I)/TR(I)
00432           GO TO 320
00433       310 TR(I)=0.0
00434           FT(I)=0.0
00435       320 CONTINUE
00436           DO 510 N=1,NS
00441   *DIAGNOSTIC*  THE TEST FOR EQUALITY BETWEEN NON-INTEGERS MAY NOT BE MEANINGFUL.
00441           IF(STRESS(I).EQ.VSTRES(N)) GO TO 520
00443           GO TO 510
00444   *DIAGNOSTIC*  THE TEST FOR EQUALITY BETWEEN NON-INTEGERS MAY NOT BE MEANINGFUL.
00444       520 IF(TEMP(I).EQ.VTEMP(N)) GO TO 530
00446       510 CONTINUE
00450       530 J=NV(N)
00451           TIME1(I,L)=TS
00452           TIME2(I,L)=TS+TIME(I)
00453           IF (L.EQ.2) GO TO 850
00455           IF(L.EQ.3) GO TO 1000
00457       855 IF(TS.GT.VTIM(J,N)) GO TO 540
00461           CALL INTER1(TS,STPRI1,VTIM(1,N),VSR(1,N),J)
00462           IF(TIME2(I,L).GT.VTIM(J,N)) GO TO 513
00464           CALL INTER1(TIME2(I,L),STPRI2,VTIM(1,N),VSR(1,N),J)
00465           STPRI(I,L)=STPRI2-STPRI1
00466           IF(I.EQ.1) GO TO 508
00470           GO TO 509
00471       508 STRO=STPRI1
00472           TSTR(I,L)=STPRI(I,L)
00473       509 CONTINUE
00474           IF (TIME2(I,L).GT.VTIM(J,N)) GO TO 513
00476           TSTR(I,L)=TSTR(I-1,L)+STPRI(I,L)
00477           GO TO 75
00500       850 [illegible] GO TO 855
```

```
      IF(TSTR(I-1,L).GT.VSR(J,N)) GO TO 540
      CALL INTER1(TSTR(I-1,L),XT1,VSR(1,N),VTIM(1,N),J)
      XT2=XT1+TIME(I)
      IF (XT2.GT.VTIM(J,N)) GO TO 522
      CALL INTER1(XT2,STPRI2,VTIM(1,N),VSR(1,N),J)
      TSTR(I,L)=STPRI2
      GO TO 75
  513 TREM(I)=TIME2(I,L)-VTIM(J,N)
      GO TO 523
  522 TREM(I)=XT2-VTIM(J,N)
  523 STPRI2=VSR(J,N)
      IF(L.EQ.2) GO TO 516
      STPRI(I,L)=STPRI2-STPRI1
      GO TO 550
  540 STPRI(I,L)=0.0
      GO  TO 550
  516 STPRI(I,L)=STPRI2-TSTR(I-1,L)
  550 CONTINUE
      IF(NC.EQ.0) GO TO 300
      CALL GIR1(STLOG(I),PC(I),SIGCLG,PCR,NC)
C
C     THE FOLLOWING EQUATION IS THE LARSON-MILLER PARAMETER
C
      TCLOG(I)= ((PC(I)*1000.)/(TEMP(I)+460.))-20.
C ****
C ****
      TC(I)=10.0**TCLOG(I)
      CRATE(I)=STRN/TC(I)
      IF (TREM(I).GT.0.0) GO TO 531
      IF(TIME1(I,L).GT.VTIM(J,N)) GO TO 511
  531 CREEP(I,L)=CRATE(I)*TREM(I)
      GO TO 512
  511 CREEP(I,L)=CRATE(I)*TIME(I)
  512 CONTINUE
      TSTR(I,L)=TSTR(I-1,L)+STPRI(I,L)+CREEP(I,L)
      GO TO 75
C
C *** PAO-MARIN THEORY
C
 1000 CONTINUE
      CALL GIR1(STLOG(I),P1,SIGCLG,PCR,NC)
      PMTL1=((P1*1000.)/(TEMP(I)+460.))-20.
      PMT1=10.0**PMTL1
      CRATE1=STRN/PMT1
      ST1=STRESS(I)+5000.
      STL1=ALOG10(ST1)
      CALL GIR1(STL1,P2,SIGCLG,PCR,NC)
      PMTL2=((P2*1000.)/(TEMP(I)+460.))-20.
      PMT2=10.0**PMTL2
      CRATE2=STRN/PMT2
      EXPN(I)=ALOG(CRATE2/CRATE1)/ALOG(ST1/STRESS(I))
      K1(I)=VSR(J,N)/(STRESS(I)**EXPN(I))
      K2(I)=CRATE1/(STRESS(I)**EXPN(I))
      CALL INTER1(TIME(I),STR,VTIM(1,N),VSR(1,N),J)
      IF(I.GT.1) GO TO 2990
      XT1=0.0
      XT2=TIME(I)
```

```
               GO TO 2999
         2990 CALL INTER1(TSTR(I-1,L),XT1,VSR(1,N),VTIM(J,N),J)
               XT2=XT1+TIME(I)
         2999 CONTINUE
               Q(I)=(1./TIME(I)  )*ALOG(1./(1.-(STR/(K1(I)*STRESS(I)**EXPN(I)))))
               IF (I.EQ.1) GO TO 3150
               IF (TSTR(I-1,L).GE.VSR(J,N)) GO TO 4000
         3100 IF(XT2.GT.VTIM(J,N)) GO TO 3300
               IF(XT2.LE.VTIM(J,N)) GO TO 3500
               GO TO 3200
         3500 K2(I)=0.0
               GO TO 3200
         3300 TXX=VTIM(J,N)-XT1
               TREM(I)=XT2-VTIM(J,N)
               TSTR(I,L)= (K1(I)*(EXP(-Q(I)*XT1)-EXP(-Q(I)*VTIM(J,N))) +K2(I)*
             1 TREM(I))*((ABS(STRESS(I))**(EXPN(I)-1.))*STRESS(I))+TSTR(I-1,L)
               GO TO 3400
         4000 Q(I)=0.0
               GO TO 3200
         3150 IF(XT2.GT.VTIM(J,N)) GO TO 3200
               K2(I)=0.0
         3200 CONTINUE
               TSTR(I,L)=(K1(I)*(EXP(-Q(I)*XT1)-EXP(-Q(I)*XT2)) +K2(I)*TIME(I))*
             1 ((ABS(STRESS(I))**(EXPN(I)-1.))*STRESS(I))+TSTR(I-1,L)
         3400 CONTINUE
           75 T2(I,L)=TS+TIME(I)
               TS=T2(I,L)
               GO TO 130
          300 CREEP(I,L)=0.0
          130 CONTINUE
          131 CONTINUE
               WRITE(6,116) TITLE
          116 FORMAT(1H1,10A6)
               WRITE(6,141)
          141 FORMAT(1H0,4X,6HSTRESS,12X,4HTEMP,13X,5HHOURS,13X,7HRUPTURE,8X,12H
             1TIME/RUPTURE,7X,8HSUM T/TR,12X,6HMARGIN/5X,5H(PSI),13X,3H(F),13X,7
             2HAPPLIED,13X,4HTIME)
               FX=0.0
               CX=0.0
               DO 135 I=1,NS
               FSUM(I)=FT(I)+FX
*DIAGNOSTIC*  THE TEST FOR EQUALITY BETWEEN NON-INTEGERS MAY NOT BE MEANINGFUL.
               IF (STRMAX.EQ.0.0) GO TO 275
               DO 905 L=1,2
               DELSTR=STRMAX-TSTR(I,L)
          905 CONTINUE
               IF (DELSTR.LE.0.0) GO TO 280
          275 CONTINUE
               IF (NSIG.EQ.0) GO TO 145
               XMAR(I)=(1.0/FSUM(I))-1.0
               IF (XMAR(I).GE.0.0) GO TO 145
               WRITE(6,150) XMAR(I)
          150 FORMAT(48H         A NEGATIVE MARGIN HAS OCCURRED,MARGIN= ,E15.8)
               N=1
               GO TO 155
          145 FX=FSUM(I)
               CX=TSTR(I,L)
```

```
00706          WRITE(6,140)STRESS(I),TEMP(I),TIME(I),TR(I),FT(I),FSUM(I),XMAR(I)
00717      140 FORMAT(1H0,7(E15.8,3X))
00720      135 CONTINUE
00722          WRITE(6,142)
00724      142 FORMAT(1H1,86HTHE FOLLOWING VALUES ARE THE CREEP STRAIN VS TIME VA
00724         1LUES FOR THE TIME HARDENING THEORY/5X,4HTIME,15X,12HCREEP STRAIN/5
00724         2X,4H(HR),16X,7H(IN/IN))
00725          TO=0.0
00726          WRITE(6,143) TO,STRO
00732      143 FORMAT(1H0,E15.8,5X,E15.8)
00733          WRITE(6,144) (T2(I,1),TSTR(I,1),I=1,NS)
00742      144 FORMAT(1H0,E15.8,5X,E15.8)
00743          WRITE(6,146)
00745      146 FORMAT(1H1,88HTHE FOLLOWING VALUES ARE THE CREEP STRAIN VS TIME VA
00745         1LUES FOR THE STRAIN HARDENING THEORY/5X,4HTIME,15X,12HCREEP STRAIN
00745         2/5X,4H(HR),16X,7H(IN/IN))
00746          WRITE(6,143) TO,STRO
00752          WRITE(6,144) (T2(I,2),TSTR(I,2),I=1,NS)
00761          WRITE(6,147)
00763      147 FORMAT(1H1,81HTHE FOLLOWING VALUES ARE THE CREEP STRAIN VS TIME VA
00763         1LUES FOR THE PAO-MARIN THEORY/5X,4HTIME,15X,12HCREEP STRAIN/5X,4H(
00763         2HR),16X,7H(IN/IN))
00764          WRITE(6,143) TO ,STRO
00770          WRITE(6,144) (T2(I,3),TSTR(I,3),I=1,NS)
00777          GO TO 165
01000      280 WRITE(6,290) TSTR(I,L)
01003      290 FORMAT(1H0,55HTOTAL STRAIN HAS EXCEEDED MAX STRAIN ALLOWABLE, STRA
01003         1IN=,E15.8)
01004          GO TO 165
01005      155 WRITE(6,160) STRESS(N),TEMP(N),TIME(N)
01012      160 FORMAT(28H RUPTURE OCCURRED AT STRESS=,E15.8,5X5HTEMP=,E15.8,5X,5H
01012         1TIME=,E15.8)
01013      165 CONTINUE
01014          TISUM=0.0
01015          DO 400 I=1,NS
01020          TISUM=TISUM + TIME(I)
01021      400 CONTINUE
01023          XLIFE= TISUM/FSUM(NS)
01024          TMAX=TEMP(1)
01025          WRITE(6,425) XLIFE
01030      425 FORMAT(1H1,5X,14HLIFE EXPECTED=,E15.8)
01031          IF (XLIFE.GT.LIREQ) GO TO 455
01033          WRITE(6,460) XLIFE,LIREQ
01037      460 FORMAT(1H0,17HTHE LIFE EXPECTED,E15.8,31H IS LESS THAN THE LIFE RE
01037         1QUIRED,E15.8)
01040          GO TO 465
01041      455 CONTINUE
01042          DO 410 I=1,NS
01045          IF(TMAX.GE.TEMP(I)) GO TO 420
01047          TMAX=TEMP(I)
01050      420 CONTINUE
01051      410 CONTINUE
01053          COEFFM=(PCR(3)-PCR(2))*1000./((TMAX+460.)*(ALOG10(SIGCR(2))-ALOG10
01053         1(SIGCR(3))))
01054          WRITE(6,430) TMAX
01057      430 FORMAT(1H0,5X,9HMAX TEMP=E15.8)
01060          WRITE(6,435) COEFFM
```

```
01063         435 FORMAT(1H0,5X,2HM=,E15.8)
01064 *DIAGNOSTIC*  THE TEST FOR EQUALITY BETWEEN NON-INTEGERS MAY NOT BE MEANINGFUL.
01064             IF(LIREQ.EQ.0.0) GO TO 436
01066             FS=(XLIFE/LIREQ)**(1.0/COEFFM)
01067             WRITE(6,440) FS
01072         440 FORMAT(1H0,5X,17HFACTOR OF SAFETY=,E15.8)
01073         436 CONTINUE
01074         465 CONTINUE
01075             NP=NS+1
01076             DO 800 I=1,NP
01101             IF (I.GT.1) GO TO 805
01103             TX(1,1)=TO
01104             SY(1,1)=STRO
01105             GO TO 800
01106         805 CONTINUE
01107             TX(I,1)=T2(I-1,1)
01110             SY(I,1)=TSTR(I-1,1)
01111         800 CONTINUE
01113             CALL IDENT(9)
01114             CALL QUIK3V(1,35,BCDX,BCDY,-NP,TX,SY)
01115             DATA BCDY /12*6H      /
01117             DATA BCDX / 6HTIME (,6HHR)    ,10*6H      /
01121             CALL APRNTV(0,-14,20,20HCREEP STRAIN (IN/IN),0,652)
01122             CALL PRINTV(21,21HTIME HARDENING THEORY,80,1007)
01123             DO 910 I=1,NP
01126             IF(I.GT.1) GO TO 920
01130             TX(1,2)=TO
01131             SY(1,2)=STRO
01132             GO TO 910
01133         920 CONTINUE
01134             TX(I,2)=T2(I-1,2)
01135             SY(I,2)=TSTR(I-1,2)
01136         910 CONTINUE
01140             CALL QUIK3V(-1,35,BCDX,BCDY,-NP,TX(1,2),SY(1,2))
01141             DATA BCDY /12*6H      /
01143             DATA BCDX /6HTIME (,6HHR)    ,10*6H      /
01145             CALL APRNTV(0,-14,20,20HCREEP STRAIN (IN/IN),0,652)
01146             CALL PRINTV(23,23HSTRAIN HARDENING THEORY,80,1007)
01147             DO 1010 I=1,NP
01152             IF(I.GT.1) GO TO 1020
01154             TX(1,3)=TO
01155             SY(1,3)=STRO
01156             GO TO 1010
01157        1020 CONTINUE
01160             TX(I,3)=T2(I-1,3)
01161             SY(I,3)=TSTR(I-1,3)
01162        1010 CONTINUE
01164             CALL QUIK3V(-1,35,BCDX,BCDY,-NP,TX(1,3),SY(1,3))
01165             DATA BCDY /12*6H      /
01167             DATA BCDX /6HTIME (,6HHR)    ,10*6H      /
01171             CALL APRNTV(0,-14,20,20HCREEP STRAIN (IN/IN),0,652)
01172             CALL PRINTV(16,16HPAO-MARIN THEORY,80,1007)
01173             CALL QUIK3V(-1,24,BCDX,BCDY,-NP,TX(1,2),SY(1,2))
01174             DATA BCDY /12*6H      /
01176             DATA BCDX /6HTIME (,6HHR)    ,10*6H      /
01200             CALL APRNTV(0,-14,20,20HCREEP STRAIN (IN/IN),0,652)
01201             CALL QUIK3V(0,25,BCDX,BCDY,-NP,TX(1,1),SY(1,1))
```

```
01202    374*        DATA BCDY /12*6H      /
01204    375*        DATA BCDX /12*6H      /
01206    376*        CALL QUIK3V(0,21,BCDX,BCDY,-NP,TX(1,3),SY(1,3))
01207    377*        DATA BCDY /12*6H      /
01211    378*        DATA BCDX /12*6H      /
01213    379*        CALL ENDJOB
01214    380*        END

     END OF COMPILATION:        5 DIAGNOSTICS.
```

```
GFOR,IS GIR
FOR 0E10A-01/03/73-11:11:34 (,0)

   SUBROUTINE GIR1       ENTRY POINT 000100

   STORAGE USED: CODE(1) 000116; DATA(0) 000026; BLANK COMMON(2) 000000

   EXTERNAL REFERENCES (BLOCK, NAME)

    0003   NERR3$

   STORAGE ASSIGNMENT  (BLOCK, TYPE, RELATIVE LOCATION, NAME)

    0001     000014 105G       0001     000024 20L       0001     000031 30L       0001     000065 40L       0000 R 000004 A1
    0000 R 000001 A2           0000 R 000005 DA         0000 R 000006 D1         0000 R 000007 D2         0000 I 000000 I
    0000     000010 INJP$      0000 I 000003 I1         0000 I 000002 I2


00101                   SUBROUTINE GIR1(A,B,C,D,N)
00103                   DIMENSION C(50),D(50)
00104                   DO 10 I=1,N
00107                   IF(A-C(I))10,20,30
00112                10 CONTINUE
00114                20 B=D(I)
00115                   GO TO 40
00116                30 A2=C(I)
00117                   I2=I
00120                   I1=I-1
00121                   A1=C(I1)
00122                   DA=(A1-A)/(A1-A2)
00123                   D1=D(I1)
00124                   D2=D(I2)
00125                   B=D1+DA*(D2-D1)
00126                40 RETURN
00127                   END

      END OF COMPILATION:        NO  DIAGNOSTICS.
```

```
@FOR,IS INTER
FOR 0B10A-01/03/73-11:11:36 (,0)

   SUBROUTINE INTER1    ENTRY POINT 000102

   STORAGE USED: CODE(1) 000121; DATA(0) 000030; BLANK COMMON(2) 000000

   EXTERNAL REFERENCES (BLOCK, NAME)

    0003   NERR3$

   STORAGE ASSIGNMENT  (BLOCK, TYPE, RELATIVE LOCATION, NAME)

    0001   000014 105G     0001   000024 20L     0001   000031 30L     0001   000066 40L     0000 R 000004 A1
    0000 R 000001 A2       0000 R 000005 DA     0000 R 000006 D1     0000 R 000007 D2     0000 I 000000 I
    0000   000010 INJP$    0000 I 000003 I1     0000 I 000002 I2


00101               SUBROUTINE INTER1(A,B,C,D,N)
00103               DIMENSION C(20),D(20)
00104               DO 10 I=1,N
00107               IF(A-C(I))30,20,10
00112            10 CONTINUE
00114            20 B=D(I)
00115               GO TO 40
00116            30 A2=C(I)
00117               I2=I
00120               I1=I-1
00121               A1=C(I1)
00122               DA=(A2-A)/(A2-A1)
00123               D1=D(I1)
00124               D2=D(I2)
00125               B=D2-DA*(D2-D1)
00126            40 RETURN
00127               END

     END OF COMPILATION:        NO  DIAGNOSTICS.


@PRT,T
FURPUR 023A-01/03-11:11

CREEPANALYSI*TPF$ ELEMENT TABLE
```

D	NAME	VERSION	TYPE	DATE	TIME	SEQ #	SIZE-PRE	TEXT	(CYCLE	WORD)	PSRMODE	LOCATION
	MAIN		FOR SYMB	03 JAN 73	11:11:25	1		90	5	0	1	1792
	MAIN		RELOCATABLE	03 JAN 73	11:11:33	2	2	103				1882
	GIR		FOR SYMB	03 JAN 73	11:11:34	3		3	5	0	1	1987
	GIR		RELOCATABLE	03 JAN 73	11:11:36	4	1	5				1990

MANSON-SUCCOP PARAMETER FOR CREEP RUPTURE FOR RENE 41 BAR

.10000000+06	.16250000+02	.80000000+05	.16900000+02	.60000000+05	.17750000+02	.40000000+05	.18700000+02
.30000000+05	.19300000+02	.20000000+05	.20100000+02	.15000000+05	.20700000+02	.10000000+05	.21300000+02

LARSON-MILLER PARAMETER FOR .2 0/0 CREEP,RENE 41 BAR

AMOUNT OF CREEP STRAIN= .20000000-02

.10500000+06	.36000000+02	.10000000+06	.36200000+02	.80000000+05	.37700000+02	.60000000+05	.39550000+02
.40000000+05	.41850000+02	.20000000+05	.44750000+02	.10000000+05	.46800000+02		

MAX STRAIN ALLOWABLE=, .15000000+00

LIFE REQUIRED= .20000000+03

THE FOLLOWING VALUES ARE THE PRESCRIBED LOADING CYCLE

STRESS(PSI)	TEMP(F)	TIME(HR)
.25000000+05	.16000000+04	.40000000+01
.35000000+05	.15000000+04	.35000000+01
.85000000+05	.13000000+04	.45000000+01
.10000000+06	.13000000+04	.15000000+01

LMSC-HREC TR D306579

THE FOLLOWING DATA ARE THE TRANSIENT CREEP STRAIN VALUES FOR THE LOAD STRESS AND TEMPERATURE VALUES

NV= 9 STRESS= .25000000+05 TEMP= .16000000+04

.00000000	.00000000	.10000000+00	.10000000-04	.10000000+01	.50000000-04
.50000000+01	.25000000-03	.80000000+01	.40000000-03	.10000000+02	.48000000-03
.11000000+02	.52500000-03	.12000000+02	.55000000-03	.13000000+02	.57000000-03

NV= 11 STRESS= .85000000+05 TEMP= .13000000+04

.00000000	.00000000	.10000000+00	.40000000-04	.50000000+00	.15000000-03
.10000000+01	.25000000-03	.30000000+01	.52000000-03	.50000000+01	.75000000-03
.60000000+01	.85000000-03	.70000000+01	.92000000-03	.80000000+01	.96000000-03
.90000000+01	.99000000-03	.10000000+02	.10000000-02		

NV= 13 STRESS= .35000000+05 TEMP= .15000000+04

.00000000	.00000000	.10000000+00	.40000000-04	.50000000+00	.15000000-03
.10000000+01	.25000000-03	.20000000+01	.44000000-03	.40000000+01	.80000000-03
.55000000+01	.10500000-02	.75000000+01	.13500000-02	.90000000+01	.15000000-02
.12000000+02	.17000000-02	.13000000+02	.17500000-02	.14000000+02	.17700000-02
.15000000+02	.18000000-02				

NV= 6 STRESS= .10000000+06 TEMP= .13000000+04

.00000000	.00000000	.10000000+00	.10000000-03	.50000000+00	.32500000-03
.10000000+01	.56000000-03	.15000000+01	.79000000-03	.17500000+01	.89000000-03

SAMPLE PROBLEM- TIME AND STRAIN HARDENING,TRANSIENT + SD.

STRESS (PSI)	TEMP (F)	HOURS APPLIED	RUPTURE TIME	TIME/RUPTURE	SUM T/TR	MARGIN
.25000000+05	.16000000+04	.40000000+01	.23973314+03	.16685219-01	.16685219-01	.58933286+02
.35000000+05	.15000000+04	.35000000+01	.60047882+03	.58286818-02	.22513901-01	.43417003+02
.85000000+05	.13000000+04	.45000000+01	.48239762+03	.93284041-02	.31842304-01	.30404762+02
.10000000+06	.13000000+04	.15000000+01	.16218102+03	.92489241-02	.41091228-01	.23336094+02

THE FOLLOWING VALUES ARE THE CREEP STRAIN VS TIME VALUES FOR THE TIME HARDENING THEORY

TIME (HR)	CREEP STRAIN (IN/IN)
.00000000	.00000000
.40000000+01	.20000000-03
.75000000+01	.75000001-03
.12000000+02	.10689137-02
.13500000+02	.18797622-02

THE FOLLOWING VALUES ARE THE CREEP STRAIN VS TIME VALUES FOR THE STRAIN HARDENING THEORY

TIME (HR)	CREEP STRAIN (IN/IN)
.00000000	.00000000
.40000000+01	.20000000-03
.75000000+01	.84166667-03
.12000000+02	.10539404-02
.13500000+02	.18647889-02

LMSC-HREC TR D306579

THE FOLLOWING VALUES ARE THE CREEP STRAIN VS TIME VALUES FOR THE PAO-MARIN THEORY

TIME (HR)	CREEP STRAIN (IN/IN)
.00000000	.00000000
.40000000+01	.20000000-03
.75000000+01	.83764221-03
.12000000+02	.10279986-02
.13500000+02	.18388472-02

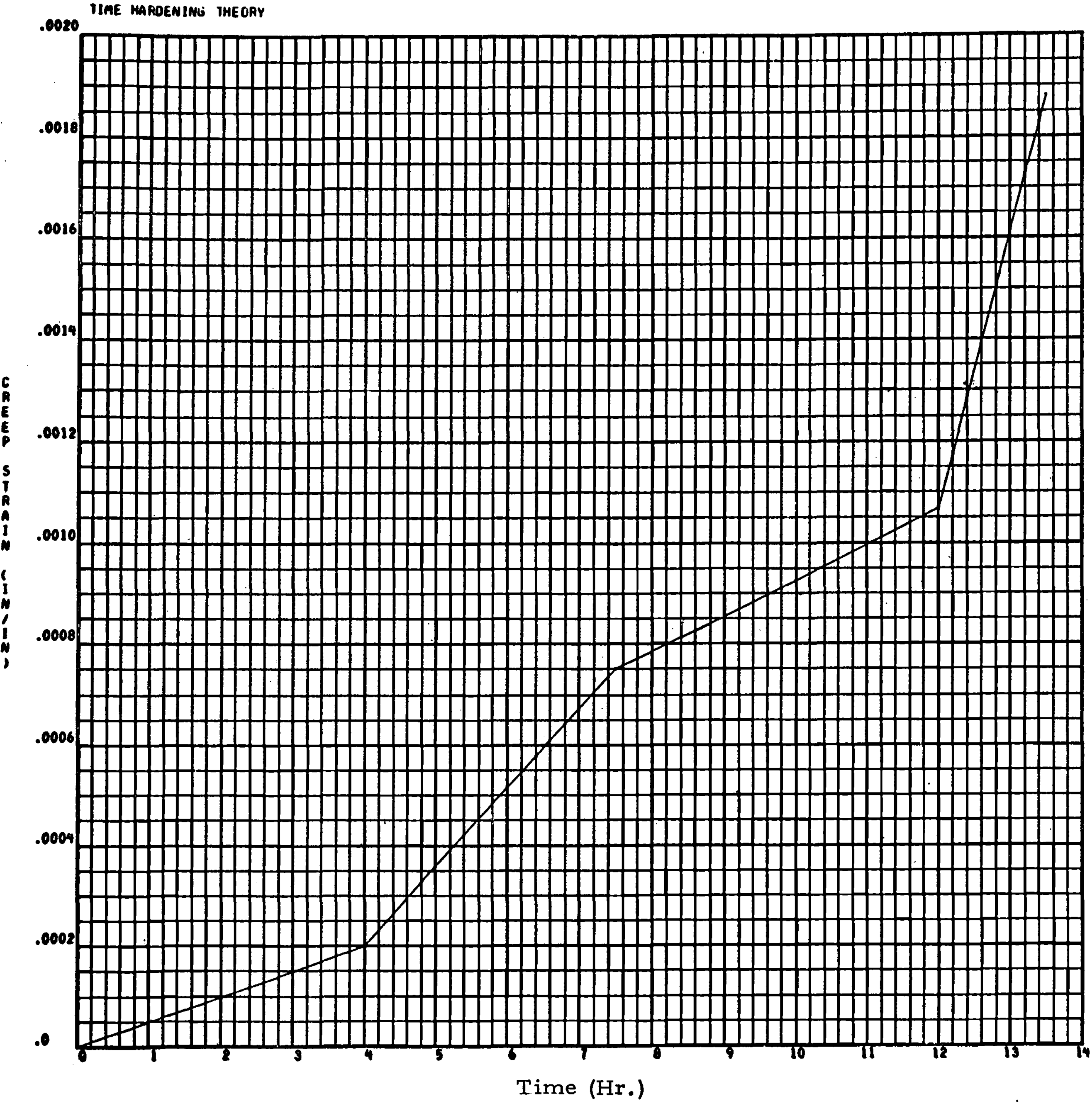

Fig. B-2 - Creep Strain, Time Hardening Theory

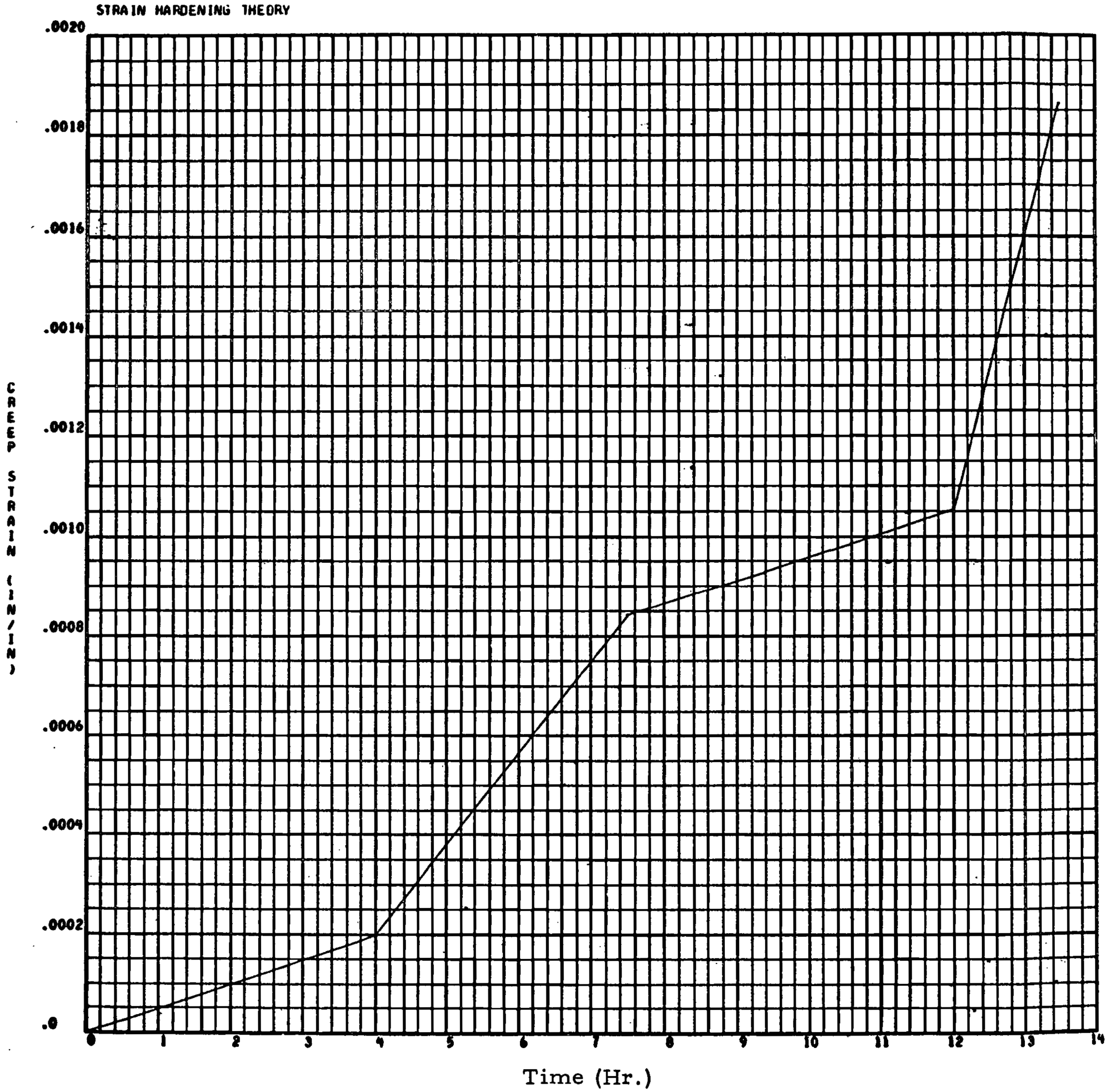

Fig. B-3 - Creep Strain, Strain Hardening Theory

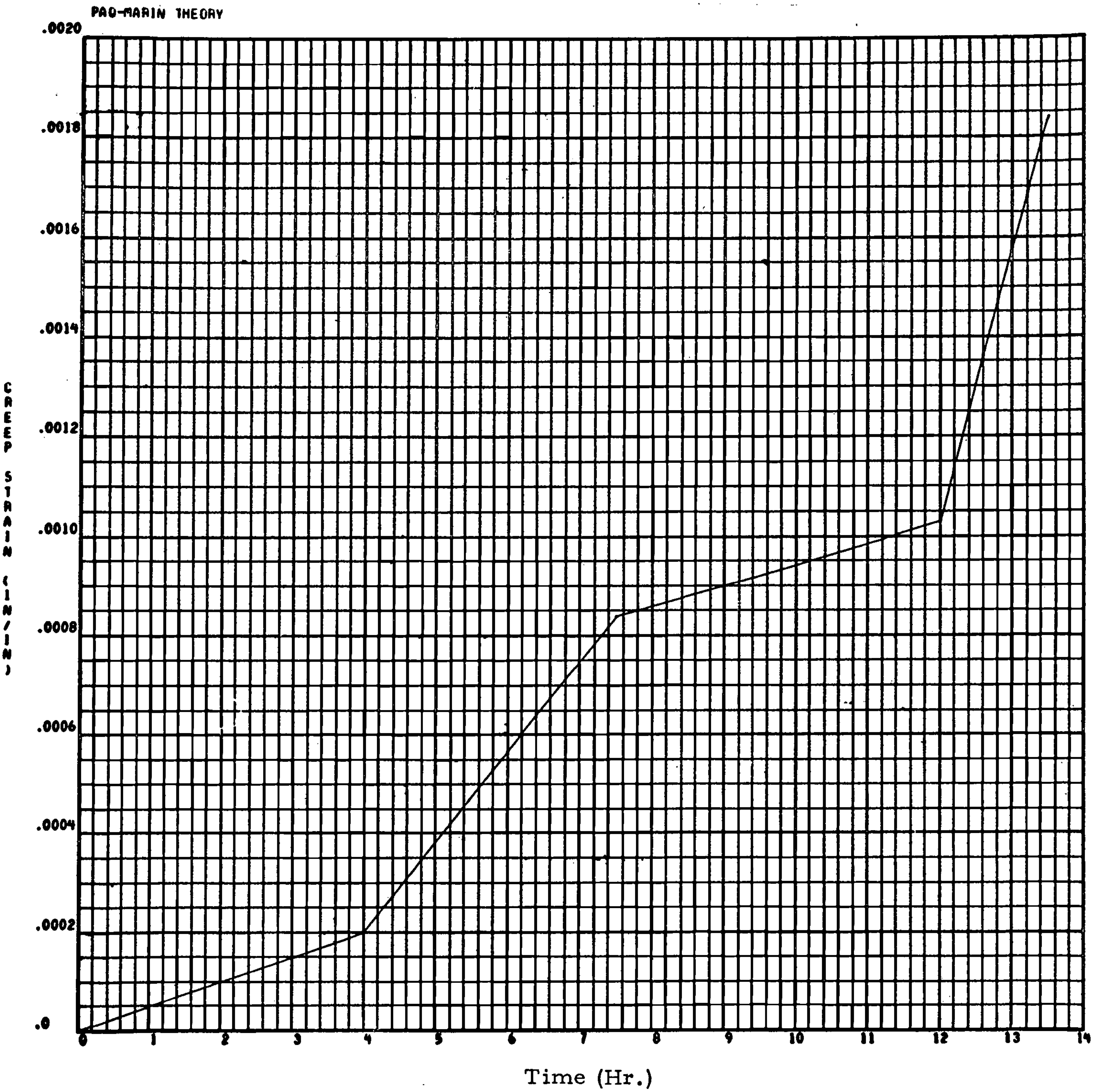

Fig. B-4 - Creep Strain, Pao-Marin Theory

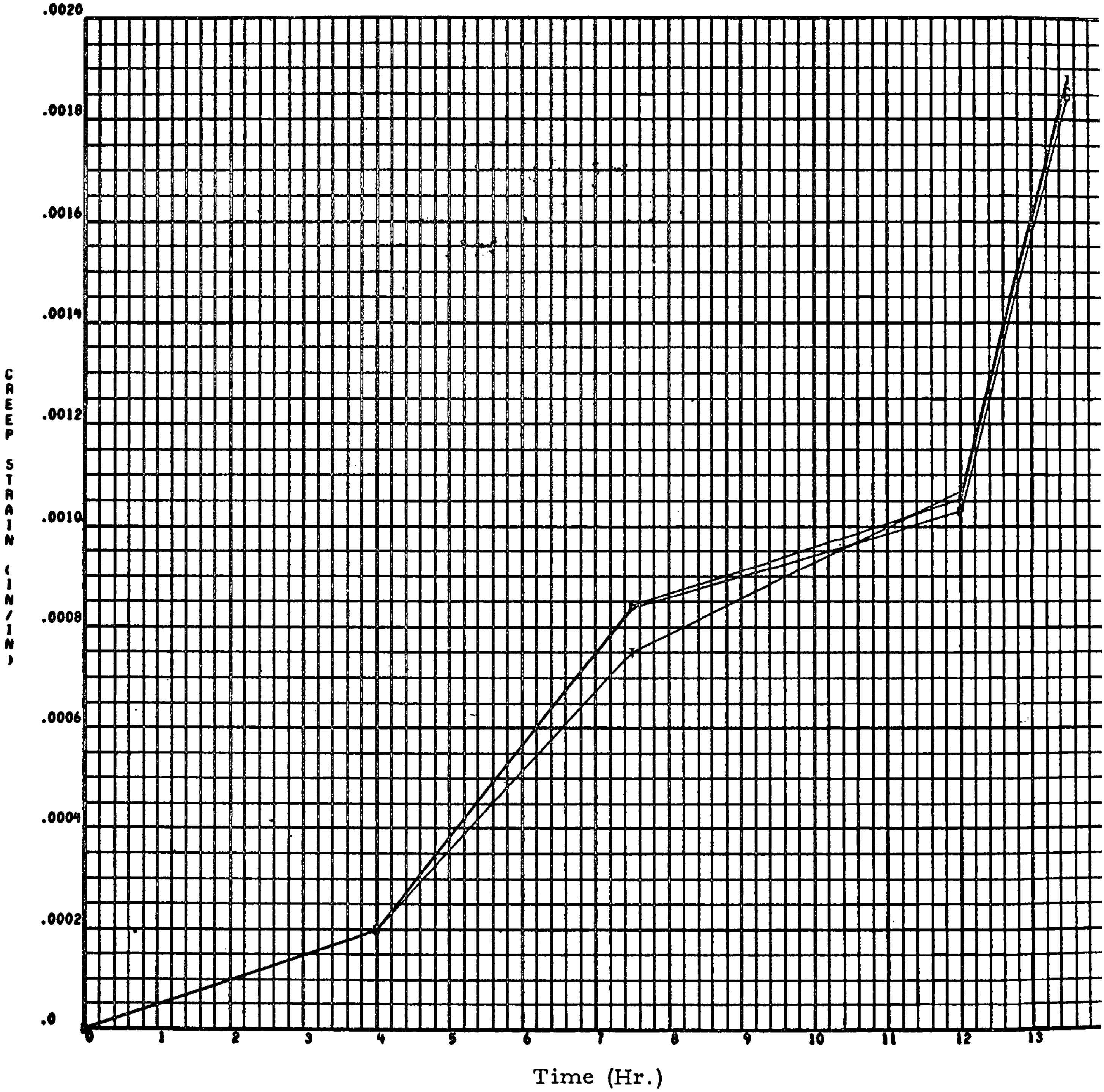

Fig. B-5 - Creep Strain

B.5 REFERENCES

B-1. "Rene' 41," Aerospace Structural Materials Handbook, Vol. II, Air Force Materials Laboratory, Wright-Patterson AFB, Ohio, 1970 edition.

B-2. "Rene' 41," Aerospace Structural Materials Handbook, Vol. II, Air Force Materials Laboratory, Wright-Patterson AFB, Ohio, 1966 edition.

B-3. Gluck, J. B., and J. W. Freeman, "Effect of Creep-Exposure on Mechanical Properties of Rene' 41," ASD TR 61-73, Air Force Materials Laboratory, Wright-Patterson AFB, Ohio, August 1961.